Cellulose derived polymers

Synthesis of functional and degradable polymers from cellulose

---

DISSERTATION

zur Erlangung des akademischen Grades

"doctor rerum naturalium"

(Dr. rer. nat.)

in der Wissenschaftsdisziplin "Polymer Science"

eingereicht an der

Mathematisch-Naturwissenschaftlichen Fakultät

der Universität Potsdam

von

Tapas Debsharma

Potsdam, December 2019

Published online at the
Institutional Repository of the University of Potsdam:
https://doi.org/10.25932/publishup-44131
https://nbn-resolving.org/urn:nbn:de:kobv:517-opus4-441312

Declaration

The enclosed research was conducted in the Institute of Chemistry at the University of Potsdam, under the supervision of Prof. Dr. Helmut Schlaad between August 2016 and August 2019. This thesis has not been submitted for any other qualifications at this or any other institution. This dissertation is the original work of the author and does not include any research that is the outcome of work done in collaboration with others, except where specifically indicated in the text and acknowledgments.

Eidesstattliche Erklärung

Die vorliegende Arbeit wurde in der Zeit von August 2016 bis August 2019 an der Universität Potsdam im Institut für Chemie unter der Leitung von Prof. Dr. Helmut Schlaad angefertigt. Die Arbeit ist bisher an keiner anderen Hochschule eingereicht worden und wurde zudem selbständig und ausschließlich mit den angegebenen Mitteln angefertigt. Hiermit erkläre ich an Eides statt, dass ich die vorliegende Arbeit selbstständig verfasst und nur unter Zuhilfenahme der ausgewiesenen Quellen und Hilfsmittel angefertigt habe. Beiträge von Kooperationspartnern wurden explizit gekennzeichnet.

Potsdam, den _____ **_____**
(Tapas Debsharma)

Supervisors

1. Prof. Dr. Helmut Schlaad (first supervisor)
2. Prof. Dr. Bernd Schmidt (second supervisor)

Referees

3. Prof. Dr. Helmut Schlaad (University of Potsdam)
4. Prof. Dr. Bernd Schmidt (University of Potsdam)
5. Prof. Dr. Andreas Kilbinger (University of Fribourg)

Abstract

Plastics, such as polyethylene, polypropylene, and polyethylene terephthalate are part of our everyday lives in the form of packaging, household goods, electrical insulation, etc. These polymers are non-degradable and create many environmental problems and public health concerns. Additionally, these polymers are produced from finite fossils resources. With the continuous utilization of these limited resources, it is important to look towards renewable sources along with biodegradation of the produced polymers, ideally. Although many bio-based polymers are known, such as polylactic acid, polybutylene succinate adipate or polybutylene succinate, none have yet shown the promise of replacing conventional polymers like polyethylene, polypropylene and polyethylene terephthalate. Cellulose is one of the most abundant renewable resources produced in nature. It can be transformed into various small molecules, such as sugars, furans, and levoglucosenone. The aim of this research is to use the cellulose derived molecules for the synthesis of polymers.

Acid-treated cellulose was subjected to thermal pyrolysis to obtain levoglucosenone, which was reduced to levoglucosenol. Levoglucosenol was polymerized, for the first time, by ring-opening metathesis polymerization (ROMP) yielding high molar mass polymers of up to ~150 kg/mol. The poly(levoglucosenol) is thermally stable up to ~220 °C, amorphous, and is exhibiting a relatively high glass transition temperature of ~100 °C. The poly(levoglucosenol) can be converted to a transparent film, resembling common plastic, and was found to degrade in a moist acidic environment. This means that poly(levoglucosenol) may find its use as an alternative to conventional plastic, for instance, polystyrene.

Levoglucosenol was also converted into levoglucosenyl methyl ether, which was polymerized by cationic ring-opening metathesis polymerization (CROP). Polymers were obtained with molar masses up to ~36 kg/mol. These polymers are thermally stable up to ~220 °C and are semi-crystalline thermoplastics, having a glass transition temperature of ~35 °C and melting transition of 70-100 °C. Additionally, the polymers underwent cross-linking, hydrogenation and thiol-ene click chemistry.

Zusammenfassung

Kunststoffe wie Polyethylen, Polypropylen und Polyethylenterephthalat sind ein großer Bestandteil unseres Alltags und finden Verwendung unter anderem als Verpackungsmaterialien, Haushaltswaren und Elektroisolierungen. Diese Polymere werden aus fossilen Ressourcen hergestellt, sind nicht abbaubar und verursachen nicht nur viele Umweltprobleme sondern können auch zu Gesundheitsschäden führen. Aufgrund dessen muss die Verwendung von erneuerbaren Ressourcen geachtet werden, wobei die hergestellten Polymere im Idealfall komplett biologisch abbaubar sind. Obwohl viele biobasierte Polymere, wie Polymilchsäure, Polybutylensuccinatadipat oder Polybutylensuccinat, bekannt sind, hat noch keines das Potential gezeigt, herkömmliche Polymere zu ersetzen. Cellulose ist einer der am häufigsten in der Natur produzierten nachwachsenden Rohstoffe und kann in verschiedene kleine organische Moleküle wie Zucker (Saccharide), Furan und auch Levoglucosenon umgewandelt werden. Ziel dieser Arbeit ist die Verwendung von Levoglucosenon als Monomer für die Synthese von Polymeren.

Säurebehandelte Cellulose wurde einer thermischen Pyrolyse unterzogen, um Levoglucosenon zu erhalten, das dann weiter zu Levoglucosenol reduziert wurde. Das Levoglucosenol wurde zum ersten Mal erfolgreich über eine Ringöffnungsmetathese-Polymerisation (ROMP) polymerisiert. Die Molmassen der hergestellten Polymere erreichten Werte von bis zu ~150 kg/mol. Die thermische Analyse von Poly(levoglucosenol) zeigt, dass es bis zu einer Temperatur von ~220 °C stabil ist, eine Glasübergangstemperatur bei ~100 °C hat und ein amorphes Polymer ist. Weiterhin kann das Poly(levoglucosenol) in feuchter saurer Umgebung in kurzer Zeit abgebaut werden. Aufgrund dieser Eigenschaften kann Poly(levoglucosenol) als Alternative zu konventionellem Kunststoff, wie z.B. Polystyrol, eingesetzt werden kann.

Levoglucosenol wurde weiter in Levoglucosenylmethylether umgewandelt. Levoglucosenylmethylether kann mit kationischer Ringöffnungs-Polymerisation (CROP) polymerisiert werden. Es wurden Polymere mit Molmassen von bis zu ~36 kg/mol hergestellt. Die Polymere weisen eine thermische Stabilität bis zu einer Temperatur von ~220 °C auf. Es handelt sich bei den hergestellten Poly(levoglucosenylmethylethern) um teilkristalline Thermoplaste, deren Glasüberganstemperatur bei ~35 °C und der Schmelzbereich bei 70-100 °C liegt. Die Doppelbindungen des Levoglucosenylmethylethers wurden genutzt um das Polymer zu vernetzen und zu funktionalisieren.

Acknowledgments

First of all, I would like to take this privilege to express my deepest gratitude to my supervisor Prof. Dr. Helmut Schlaad for providing me the opportunity to pursue my doctoral degree in his group. I am very thankful to him for his encouragement to express and explore my ideas while showing faith in me during my doctoral study. I would also like to thank him for his constant support, especially at difficult times that made the whole process seem easy.

I am deeply indebted to Dr. Heike Küchmeister for her strong support, without that I may not have made to it the group of Prof. Schlaad for pursuing my doctoral degree. In this regard, I would also like to thank Prof. Dr. Bernd Schmidt for his contribution, and also for being my second supervisor. I am deeply thankful to Potsdam Graduate School (PoGS) and University of Potsdam for supporting my research financially and providing the infrastructure and nice campus.

I am also thankful to the very helpful people of University of Potsdam that I came in contact with during the past three years of my stay. I would like to especially thank Dr. Matthias Hydenrich and Prof. Dr. Heiko Möller for sharing his knowledge that helped me learn a lot in NMR spectroscopy. I appreciate the support of Angela Krtitschka for her patients, even with my continuous demands to measure lot-of-samples in 500 MHz or 600 MHz. I would like to thank Prof. Dr. André Laschewsky for his support and fruitful discussion from time to time. Further, I would like to thank Sascha Prentzel for his instruction with SEC and general laboratory support, Dr. Dirk Schanzenbach, Stefan Mies, Matthias Schneider for the measurements of DSC/TGA samples, Dr. Ines Starke and Sylvia Fürstenberg for ESI-ToF MS measurements, Stephan Greiff for optical rotation measurements.

I would like to thank people who constantly supported me, emotionally, socially and academically throughout my stay in Potsdam. In this regard, Dr. Chiranjit Mitra, Andreas Hess, Pronay Kumar Biswas, Suchismita Saha, Indrajit Paul, Abir Gowswami, and Sumit Shekhar have been particularly special to me.

I would like to acknowledge the support of Ina Dambowsky, Dr. Aleksandar Matic, Dr. Sebastian Noack for their constant support. I would also like to thank the entire workgroup, Ines Bastian, Sascha Prentzel, Dr. Felix Behrendt, Nils Lüdecke, Dr. Charlotte Vacogne, Dr. Afroditi Doriti, Daniel Rockel, Shuangyan Hu, Scott Kilbride, Matilde Concilio, Adrian Brandt, Susann Baus, Andreas Schwagerus, Boonya Thongrom and Dr. Anna Bogomolova without whom it would certainly not be easy.

I would like to thank all my family members for their care, unconditional love, and support. You made this possible. Thank you all!

-Tapas Debsharma

List of Publications

Ring-Opening Metathesis Polymerization of Biomass-Derived Levoglucosenol

Tapas Debsharma, Felix N. Behrendt, André Laschewsky, and Helmut Schlaad; *Angew. Chem. Int. Ed.* **2019**, *58*, 6718–6721.

Cellulose-derived polyacetal by cationic ring-opening polymerization of levoglucosenyl methyl ether

Tapas Debsharma, Yusuf Yagci, and Helmut Schlaad; *Angew. Chem. Int. Ed.* **2019**, *58*, 18492–18495.

Contents

1. Introduction 1
2. Theoretical foundation 3
2.1 Metathesis 3
2.1.1 Olefin metathesis 3
2.1.2 Ring-opening metathesis polymerization 5
2.2 Cationic ring-opening polymerization 6
2.3 Analytical Methods 8
2.3.1 Nuclear Magnetic Resonance spectroscopy 8
2.3.2 Size Exclusion Chromatography 11
2.3.3 Thermogravimetric Analysis 13
2.3.4 Differential Scanning Calorimetry 14
2.3.5 Electrospray Ionization Time-of-Flight Mass Spectrometry 15
3. Developments and discussions 16
3.1 Synthesis of monomers from cellulose 18
3.1.1 Synthesis of levoglucosenone 18
3.1.2 Synthesis of levoglucosenol 19
3.1.3 Synthesis of levoglucosenyl methyl ether 21
3.1.4 Structural characterization of levoglucosenyl methyl ether 21
3.1.5 Conclusion 25
3.2 Polymerization of levoglucosenol 26
3.2.1 Reaction monitoring 26
3.2.2 Ring-opening metathesis polymerization of levoglucosenol 26
3.2.3 Kinetics and optimization of reaction condition 30
3.2.4 Structural analysis of poly(levoglucosenol) 34
3.2.5 Polymer properties 49
3.2.6 Degradation of poly(levoglucosenol) 50
3.2.7 Conclusion 51
3.3 Polymerization of levoglucosenyl methyl ether 53
3.3.1 Reaction monitoring 53
3.3.2 Cationic ring-opening polymerization of levoglucosenyl methyl ether 54
3.3.3 Optimization of reaction condition and kinetics 57

3.3.4 Structural characterization of poly(levoglucosenyl methyl ether) 60
3.3.5 Physical properties 64
3.3.6 Functionalization 66
3.3.7 Degradation 70
3.3.8 Conclusion 71
4. Summary and outlook 72
5. Experimentals 75
5.1 Chemicals 75
5.2 Analytical instrumentation and methods 76
5.2.1 Nuclear magnetic resonance spectroscopy 76
5.2.2 Electrospray ionization time-of-flight mass spectrometry 76
5.2.3 Size exclusion chromatography 76
5.2.4 Polarized optical microscopy 77
5.2.5 Thermogravimetric analysis 77
5.2.6 Differential scanning calorimetry 77
5.2.7 Melting point 77
5.3 Synthetic procedures and characterization of materials 78
5.3.1 Levoglucosenone 78
5.3.2 Levoglucosenol 79
5.3.3 Synthesis of levoglucosenyl methyl ether 81
5.3.4 Polymerization 84
5.3.5 Hydrogenation 85
6. References 90
7. Appendix 99
7.1 Attempt for the polymerization of levoglucosenone 99
7.2 NMR spectra 100
7.3 Size exclusion chromatograms 103

1. Introduction

Macromolecules play a crucial role in living organisms on Earth. The genetic coding is transferred in form of a natural macromolecule, deoxyribonucleic acid (DNA), and the genetic codes are utilized by another group of natural macromolecules, ribonucleic acids (RNAs), for processing key functions of the living organism.[1] Other groups of macromolecules or polymers are cellulose, lignocellulose, and hemicellulose, which play key structural functions in plants in the form of wood.[2] It is one of the most important construction materials in use. Apart from natural polymers, we are familiar with synthetic polymers (e.g., polyethylene, polyethylene terephthalate) that became an integrated part of our routine lives in form of food packaging, clothing, tires, electrical insulations, body implants, and armor productions, being few to name.[3–6] These polymers are derived mainly from fossil resources. These resources have been exploited since the industrial revolution to fulfill the energy requirements of industries and societies, fuel for transportations, and feedstock chemicals for various applications that made our everyday life more and more comfortable.

The prosperity of the society came at a hidden cost though. The problem starts right from the beginning of the extraction of the fossil resources in crude form by contamination during drilling. The burning of fuels creates sulfur dioxide, nitrogen oxides as toxic gases apart from carbon dioxide.[7] These gases are known to cause global warming, acid rain, haze, smog and many diseases such as asthma, bronchitis, respiratory symptoms and many more.[8–12] The emitted carbon dioxide creates global warming by trapping solar heat on Earth and also increases carbohydrate content in plants, consequently, reducing the elemental concentrations such as nitrogen (protein content), phosphorus and several trace elements.[4,13] The fossil resources are also finite and on the way of global depletion, forcing oil-dependent companies to find offshore reserves, imposing a high risk to the environment.[14]

Apart from the dependency of polymer industry on fossil resources, conventional plastics produced from non-renewable feedstocks generally lack degradability;[15] as a result, these plastics end up flowing into the ocean[16] through the rivers,[17] contaminating aquatic wildlife[18] or get accumulated in landfills.[19] Switching to alternative renewables sources can overcome or minimize many problems associated with polymers. This justifies the need for bio-based polymers,

preferably bio-degradable polymers. Many bio-based polymers are already known.[20–23] Polylactide and polyhydroxyalkanoates are among the most important known biopolymers.[20,23,24] Production of bio-based polymers is, however, tiny in comparison to total polymer productions. Global production of polymers grew from 2 Mt to 380 Mt between 1950 and 2015, whereas the share of bio-based polymers is only about 2 Mt.[25]

To move away from non-renewable sources we need to identify suitable renewable feedstock that does not compete with food.[26] Cellulose is one such raw material that is one of the most abundant biomass on Earth.[27] It has already been utilized in the production of various value-added chemicals such as sugars, ethanol, lactic acid, levulinic acid.[28] Levoglucosan and levoglucosenone (Chart 1) are two compounds produced from cellulose by pyrolysis.[29] Levoglucosan has its application in the production of glucose[30] and it can be polymerized.[31] For levoglucosenone, Circa Ltd. has achieved an energy-neutral process for its production by burning the char generated as a by-product to meet the energy requirement of the process. Circa Ltd. is commercializing the hydrogenated levoglucosenone, Cyrene™, as bio-solvent.[32,33] Levoglucosenone, on the other hand, has been of interest to organic chemists for decades.[34–37] However, to the best of our knowledge, it is yet to find use in polymer synthesis. Its use to synthesize polymerizable monomers and their polymerization is the main focus of this dissertation.

Chart 1. Chemical structure of levoglucosenone and levoglucosan.

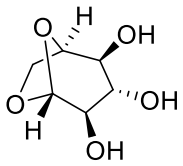

Levoglucosan

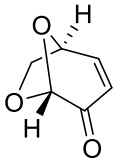

Levoglucosenone

2. Theoretical foundation

2.1 Metathesis

The name *metathesis* originates from the Greek word "μεταθεσιζ" (metátesis) and means transposition or exchange. In general, it means interchange of similar things. In chemistry, interchange of similar ions, groups or functionality can be referred to as metathesis reaction. When such an exchange happens between olefin functionalities, it is termed as olefin metathesis.

2.1.1 Olefin metathesis

The first olefin metathesis reaction was reported in 1931 and the name 'metathesis' was given to these types of reaction by Claderon in 1967.[38] As the name suggests, olefin metathesis is the mixing or shuffling of olefins. The involved mechanism was not understood until Yves Chauvin reported it in 1971.[39] The reaction is a redistribution of alkylidene groups through cleavage and formation of C=C bond by metal alkylidene complex. The metal catalyst binds with olefin via [2+2]-cycloaddition to form metalo-cyclobutane followed by the opening of the ring (retro cycloaddition) to form either precursor or new interchanged olefins (Scheme 1).[40]

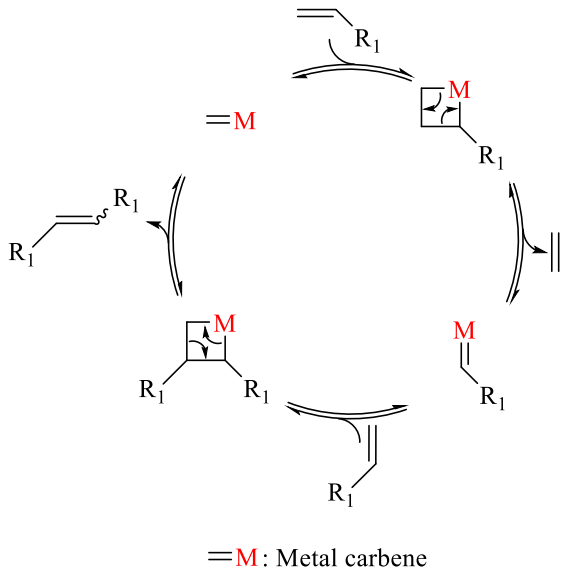

Scheme 1. Reaction mechanism of olefin metathesis.

This topic became mainstream organic and polymer chemistry after the development of molybdenum-based catalysts by Richard R. Schrock in the 1990s.[41] Although the catalyst was highly reactive, it suffered from sensitivity towards oxygen, moisture and various other functional groups making it limited in terms of applicability. Ruthenium-based catalysts developed by Robert H. Grubbs in 1992 overcame these limitations.[42] Further, extensive research produced a library of highly reactive catalysts (Figure 1).[43] This research contribution opened a new path for the utilization of olefin as functionality and the impact was such that the 2005 Nobel Prize in Chemistry was awarded to Yves Chauvin, Richard R. Schrock and Robert H. Grubbs "for the development of the metathesis method in organic synthesis".

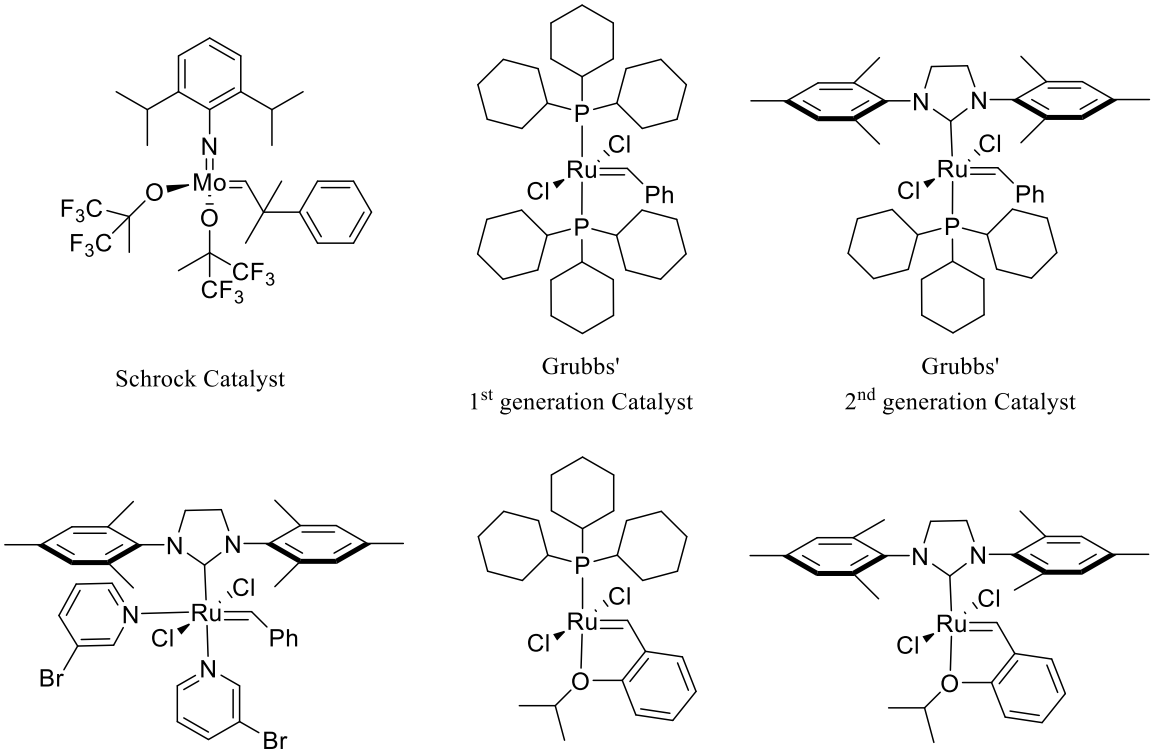

Figure 1. Catalysts for olefin metathesis reactions.

2.1.2 Ring-opening metathesis polymerization

Ring-opening metathesis polymerization (ROMP) is a chain-growth olefin metathesis polymerization. That is, a suitable organic molecule with olefin functionality gets activated by the formation of metalo-cyclobutane. A new monomer is then added to the active chain end by the repetition of the same reaction.[44]

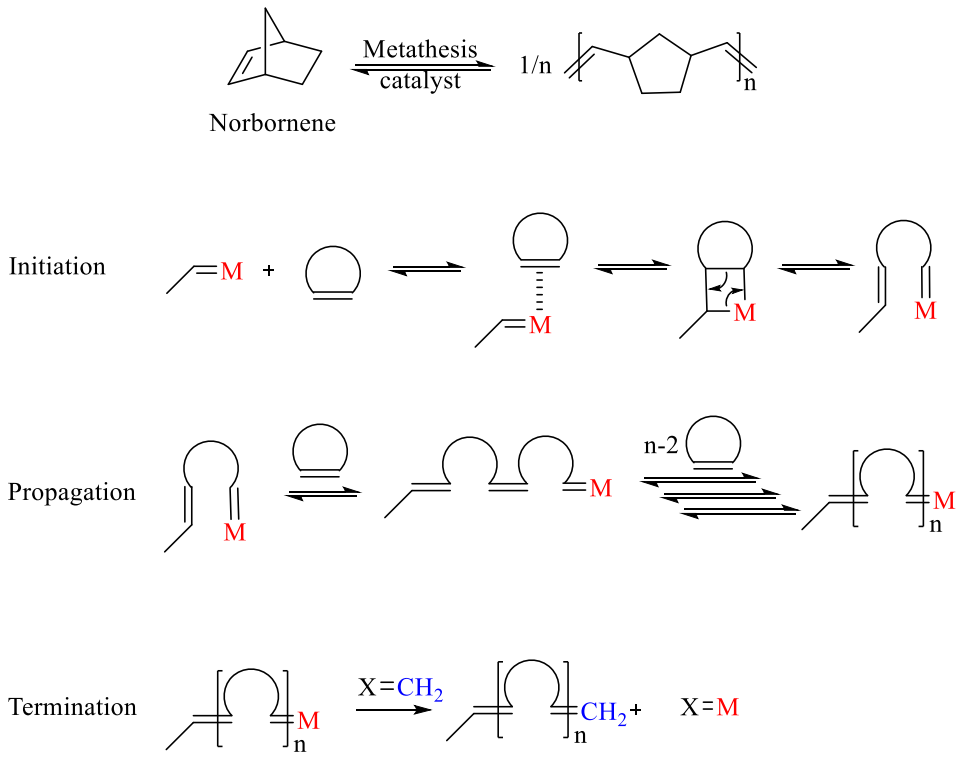

Scheme 2. ROMP of norbornene (top). General mechanism of ROMP (bottom). M is a metal catalyst, usually ruthenium, and X is a moiety that binds irreversibly to the metal catalyst. $X=CH_2$ is generally vinyl ether.

The ROMP of a small organic molecule is enthalpy driven. The polymerization of highly strained small organic molecules is generally very fast and controlled. Most common known substrates are norbornenes, cyclooctenes or similar other strained molecules.

2.2 Cationic ring-opening polymerization

Cationic ring-opening polymerization (CROP) is a class of nucleophilic substitution reactions. This type of polymerization is used for the production of several polymers in industry, such as poly(ethylene oxide), polyacetals, polytetrahydrofurans, poly(2-oxazoline), poly(ethylene imine) and various copolymers.[45–50]

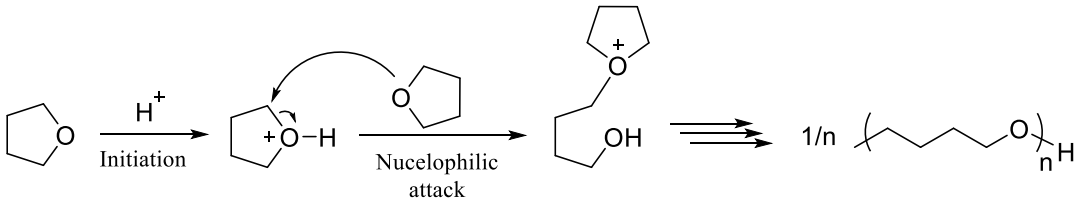

Scheme 3. Acid-catalyzed cationic ring-opening polymerization of tetrahydrofuran.

In these reactions, a strained heterocyclic ring is activated by a cation, and the ring is opened following with the nucleophilic attack by another molecule, as a consequence, the active site is transferred to the newly attached monomer. The iteration of the process leads to a polymer chain (Scheme 3). The nucleophilic substitution can be either S_N1 or S_N2 (nucleophilic unimolecular or bimolecular substitution) pathways depending on the stability of the formed cation.[51,52]

In the case of carbohydrate monomers or monosaccharides, CROP is mainly used to produce polyacetals or polysaccharides.[53] CROP of a carbohydrate monomer is commonly carried out via the activation of the strained heterocyclic ring. The polymerization proceeds through the opening of the strained ring (Scheme 4).[53]

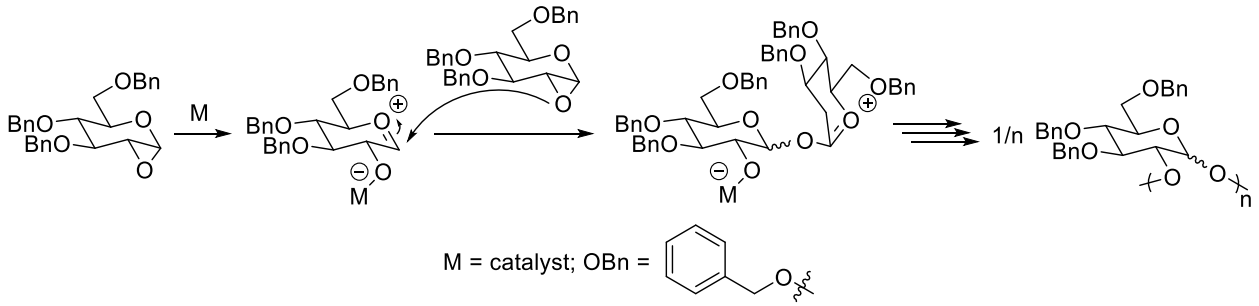

Scheme 4. Schematic presentation of a carbohydrate ring-opening polymerization.

This methodology is applied to epoxides and various bicyclic acetals for the production of linear as well as branched polymers.[54–59]

2.3 Analytical Methods

2.3.1 Nuclear Magnetic Resonance spectroscopy

Nuclear Magnetic Resonance spectroscopy (NMR) is a versatile analytical technique that is used in the structural elucidation of various compounds, quality control, purity determination, and quantification of known compounds in a mixture. It can also be used for the conformational study of various compounds including biomacromolecules. In polymer science, it is used to determine the absolute number average-molar masses by end group analysis in addition to structural characterization.

NMR analysis is generally carried out by the observation of the local magnetic field around nuclei of atoms. The nuclear spin quantum number I is characteristic of nuclei of all atoms. The values of I can be zero, negative, and positive. The nuclei containing even numbers of both protons and neutrons have no spin ($I = 0$) and therefore cannot exhibit NMR, such as ^{12}C. If the number of neutrons plus the number of protons is odd, then the nucleus has a half-integer spin (i.e., $I = 1/2$, 3/2…) such as ^{1}H, ^{13}C. If the number of neutrons and the number of protons both are odd, then the nucleus has an integer spin (i.e., $I = 1, 2\ldots$) such as ^{2}H, ^{14}N. The spinning nuclei possess angular momentum P, and magnetic moment μ, such that, $\mu = \gamma P$, where γ is the magnetogyric ratio and it is constant for any given nuclide.

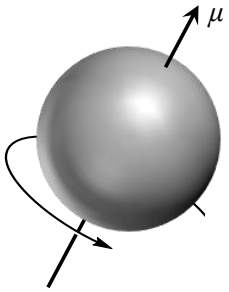

Figure 2. Depiction of the nuclear magnetic moment of a spinning nucleus.

Both the angular momentum and magnetic moment have magnitude and directions, i.e., these are vector quantities. In presence of an external and static magnetic field, the microscopic magnetic moments align themselves relative to the applied field in a certain number of orientations. These orientations depend on $2I + 1$ according to quantum mechanics. For example, a nucleus with

I = 1/2, will have two possible orientations. In the absence of an external magnetic field, the possible orientations are of equal energies.

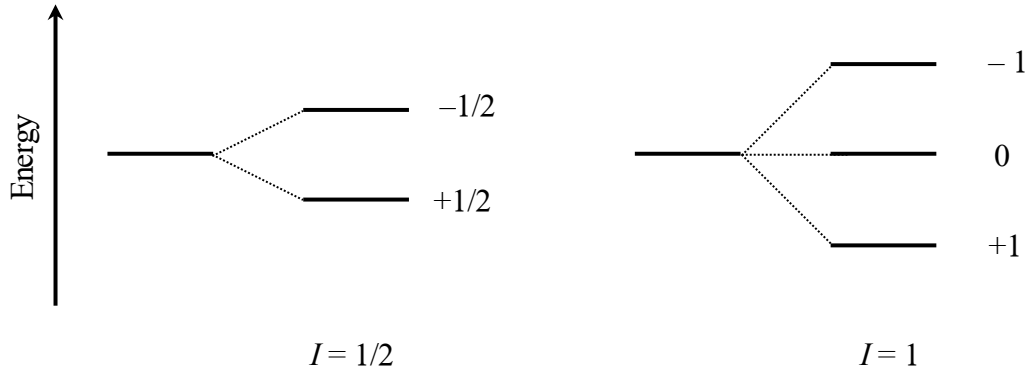

Figure 3. Energy levels of a nucleus with the spin quantum numbers I = ½ and I = 1.

The different isotopes of elements have different resonance wavelength, therefore, NMR of a given isotope can be measured in the presence of other isotopes. Further, the electron density of an atom provides a shielding effect from the external magnetic field. This effect produces chemical shifts, which allows the distinction of two similar NMR active atoms based on a neighboring atom in a given molecule. Additionally, the energy levels of nuclei can be influenced by the same neighboring nuclei due to spin-spin coupling, producing 'multiplet' peaks. The chemical shift is reported in ppm unit, abbreviated as δ and the multiplet distance is measured in Hertz (Hz). The chemical shift and multiplet pattern play a crucial role in determination, distinction, and identification of different functional groups and different protons in organic molecules. The area under the peak provides the information on the relative abundance of the atoms. NMR spectroscopy of any nuclei is measured with respect to a certain reference compound, for instance, tetramethylsilane as a reference compound for ^{1}H NMR spectroscopy.

For further understanding, exemplary ^{1}H NMR and ^{1}H-^{13}C HSQC NMR spectra of ethanol are shown (Figure 4 and Figure 5).

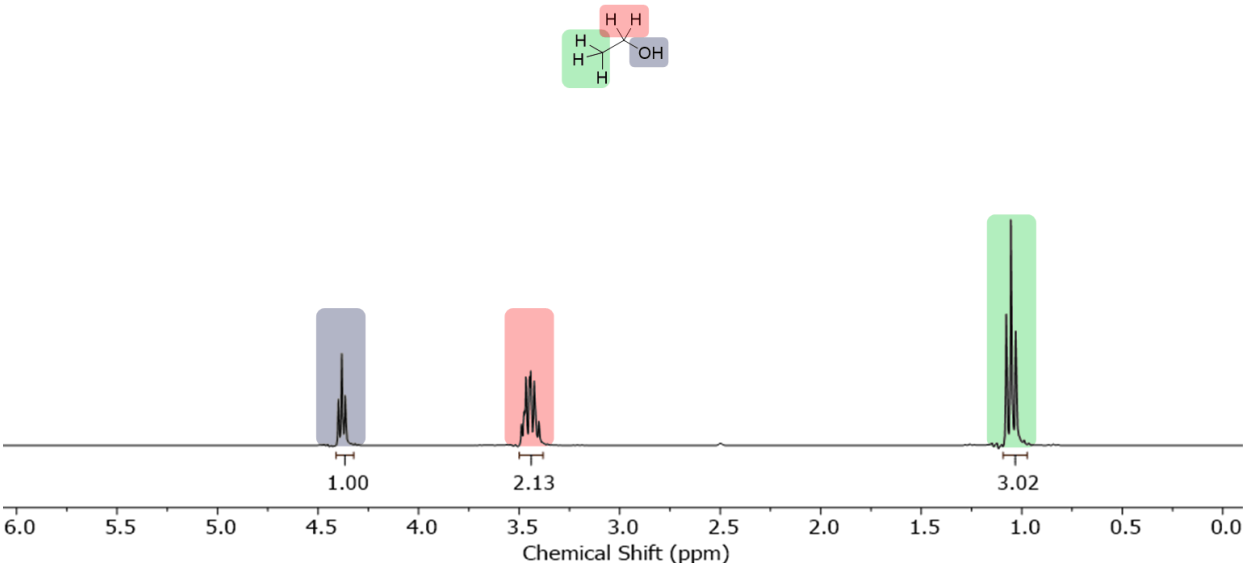

Figure 4. ^{1}H NMR (300 MHz; DMSO-d_6) of ethanol. CH_3 (shown in green) as triplet due to adjacent two CH_2 protons ($2I$+1 = 2.(2. ½) +1 = 3) and so on.

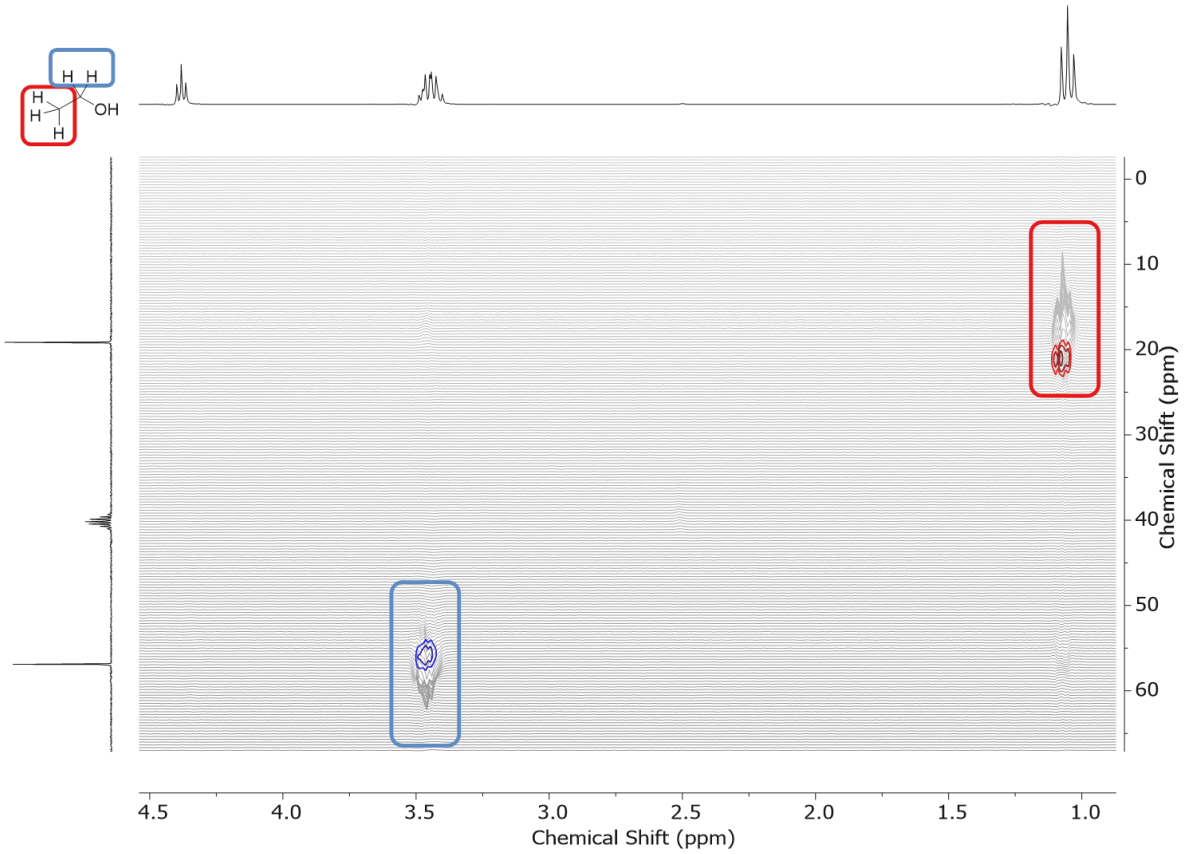

Figure 5. Phase-corrected ^{1}H-^{13}C HSQC NMR (300 MHz, 75 MHz; DMSO- d_6) of ethanol. Negative phase: CH_2, also denoted in blue contour; positive phase: CH_3, also denoted in red contour.

NMR is also useful for the determination of correlations a given atom with neighboring or surrounding atom via 2D NMR measurements such as Correlation Spectroscopy (COSY), Heteronuclear Single Quantum Coherence Spectroscopy or Heteronuclear Single-Quantum Correlation (HSQC), Heteronuclear Multiple Bond Correlation (HMBC). For example, ^{1}H-^{1}H COSY gives information about proton couplings through 2 to 3 bonds. ^{1}H-^{13}C HSQC gives information on the direct correlation between hydrogen to carbon as well as distinguishes the type of protons (such as CH_2 and CH or CH_3; see Figure 5) when the phase is corrected. HMBC provides long-range heteronuclear coupling.

2.3.2 Size Exclusion Chromatography

Size Exclusion Chromatography (SEC), also known as Gel Permeation Chromatography (GPC) is a versatile analytical technique that is used in the analysis and purification of proteins, enzymes, nucleic acids, polymers, and other biological macromolecules. This technique is well suited for macromolecules, especially biomolecules that are sensitive to changes in pH, the concentration of metal ions or other various factors. The SEC technique can also be performed within a wide temperature range. Since SEC analyzes molecules based on the hydrodynamic radius, a calibration is needed to obtain information of apparent molar masses and molar mass distributions of polymers.

SEC constitutes a solid stationary phase and a liquid mobile phase, similar to other chromatographic techniques. The solid phase consists of porous matrices that are chemically and physically stable spherical particles with a minimum tendency of adsorption to avoid molecules sticking to it. These porous matrix resins are packed into a column and a liquid mobile phase is continuously passed through it. The equilibrium of liquid inside and outside of pores of the stationary phase allows separation. The mobile phase can be a buffer or any other solvent depending on the intended use case scenario.

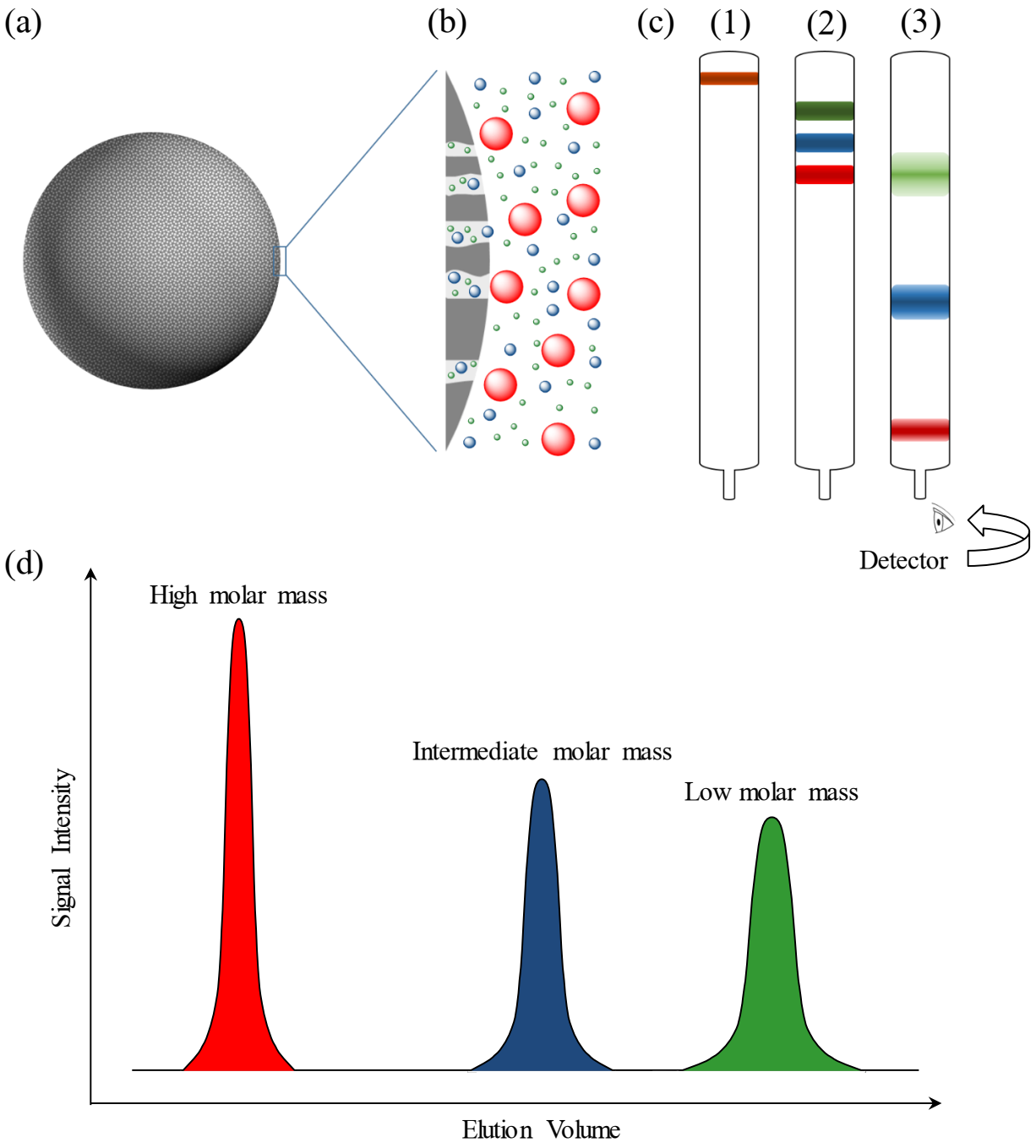

Figure 6. Pictorial representation of the separation process by SEC. (a) Schematic presentation of a porous matrix. (b) Illustration of the separation process.based on the hydrodynamic radius through (c) Illustration of the separation process in an SEC column: (1) the early stage of sample injection followed by stage (2) and stage (3) where the largest molecules are eluted at first. (d) Schematic representation of a typical SEC elugram.

When a compound is subjected to SEC, the molecules larger than the largest pores of the matrix cannot enter into the matrix and thus eluted together with the mobile phase. The molecules

that are small enough to fit into the matrix pores are eluted in their decreasing order of size. The eluted compounds can be detected by various detectors, such as the RI detector (difference in refractive index between eluent and compound with eluent), and, UV (ultraviolet) detector. The separated molecules based on their sizes can further be assigned to molar masses by comparison with a calibration. A calibration curve is obtained usually from SEC measurements of polymer standards (such as polystyrene standards) of various known molar masses and narrow distributions.

2.3.3 Thermogravimetric Analysis

Thermogravimetric analysis (TGA) is a technique to monitor the change of mass of a sample during heating in a controlled atmosphere. A sample is placed in the desired instrument which has a precision balance that resides in a furnace. An inert or reactive gas flows over the sample and the furnace is heated or cooled during an experiment. TGA measures the sample weight during heating or cooling. These measurements monitor the loss of water, solvent, and monitor decarboxylation, pyrolysis, etc. The obtained data can be used to obtain information such as absorption, adsorption, chemisorption, thermal decomposition, and solid-gas reactions. The change of mass (Y-axis) of the sample is typically plotted against temperature or time(X-axis). This is known as the TGA plot. The temperature range is usually between ambient temperature and 1000 °C. The sudden drop of the mass indicates the decomposition of the sample (Figure 7).

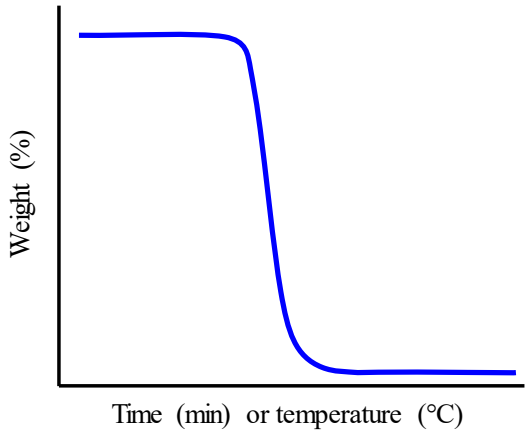

Figure 7. Pictorial representation of a typical TGA curve.

2.3.4 Differential Scanning Calorimetry

Differential Scanning Calorimetry (DSC) is a thermoanalytical technique that is used in the analysis of the thermal behavior of a sample. It measures the difference amount of heat required to increase the same temperature of both the sample and reference compound. The reference is a substance that has well-defined heat capacity over the range of temperature of an experiment. This information can identify the physical transformation of the experimental substance. The basic principle is that the difference amount of heat required for changing the same range of temperature is due to the additional phase transition of the experimental substance. For instance, an endothermic shift is observed in DSC, is an indication of a glass transition (T_g), for amorphous material. A substance is soft and rubbery above the T_g, having higher degrees of freedom than its brittle form (below T_g), thus, results in higher heat capacity. It is also possible to observe crystallization (T_c), polymers align themselves into ordered crystalline domain and heat is released, consequently, giving rise to an exothermic peak in the thermogram. For melting temperature (T_m), additional heat is required to overcome interactions due to crystallization. Therefore, an endothermic peak is observed. These are shown pictorially in (Figure 8).

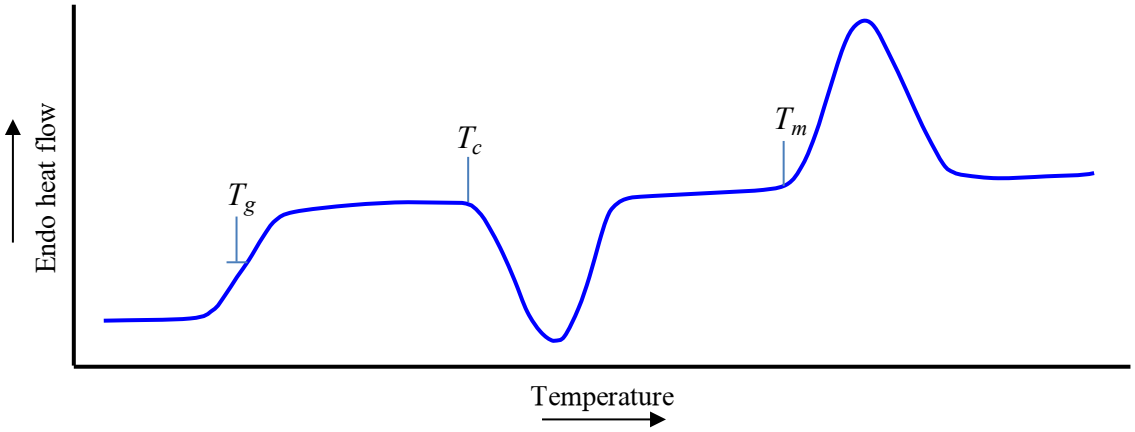

Figure 8. Schematic illustration of a DSC thermogram.

2.3.5 Electrospray Ionization Time-of-Flight Mass Spectrometry

Electrospray ionization time-of-flight mass spectroscopy (ESI-MS) is an analytical technique used for the mass analysis of compounds. This technique produces ions of molecules that pass through an electric potential. For the ions with identical charge, lighter ions will get accelerated faster than the heavier ones, resulting in a shorter time to reach the detector than a heavy-ion. Therefore, ions can be differentiated based on the different time required by these to reach the detector (Figure 9). This technique is "softer" than electron ionization and produces fewer fragments.

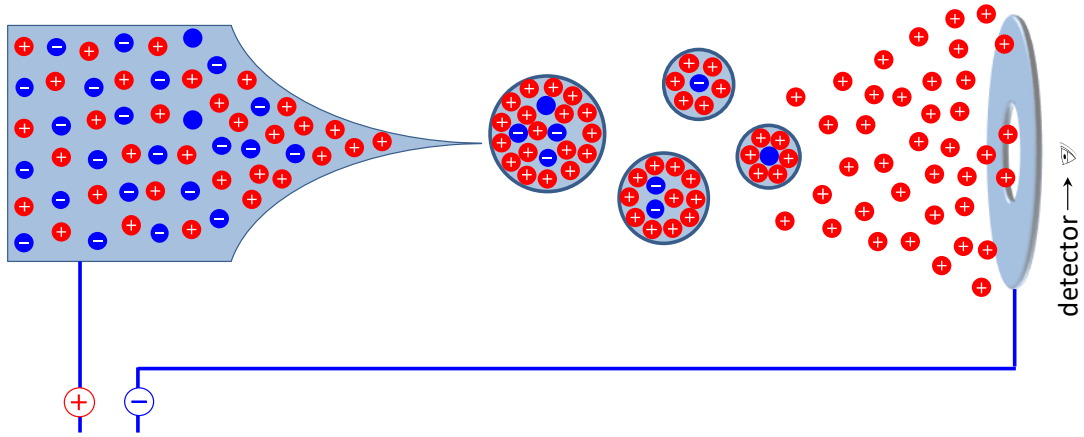

Figure 9. A pictorial illustration of the ESI process. Ionization of sample, evaporation, and explosion to ions that go to the detector.

For analysis, a compound is dissolved in a solvent and a high voltage is applied at the tip of a thin tube. As a consequence, the liquid jet emits through the apex of the tube resulting in a fine aerosol. The fine droplets further lose their size due to solvent evaporation resulting in concentrated ions of the same charge that readily explodes due to Coulomb repulsion. These ions then travel to the detector and are further analyzed.

3. Developments and discussions

Levoglucosenone (**1**) is an unsaturated, bicyclic organic compound derived from cellulose by acid-catalyzed pyrolysis (Scheme 5).[60]

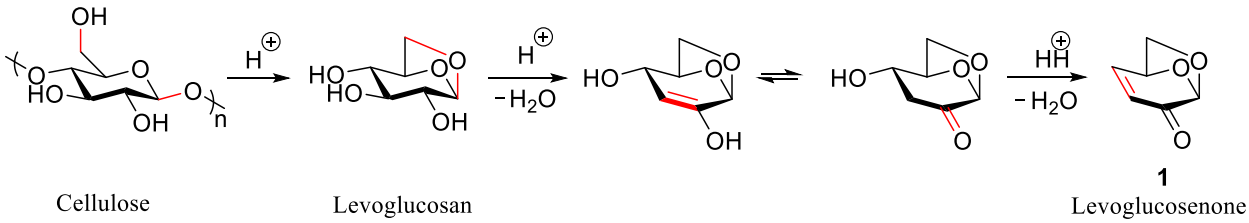

Scheme 5. Dehydration of cellulose to levoglucosenone via levoglucosan.

Cellulose, under acid-catalyzed pyrolysis, undergoes dehydration to form bicyclic molecule levoglucosan.[60] Levoglucosan is well known for the synthesis of glucose when treated with acidic water. The absence of water under acidic conditions, however, produces an *en-ol* compound, which further undergoes tautomerism to form the characteristic keto group of levoglucosenone. Further, dehydration of this molecule leads to the formation of α, β-unsaturated bicyclic ketone, levoglucosenone.

Common carbohydrate molecules (e.g. glucose, mannose, and galactose), require extensive protection-deprotection group chemistry[61] to be useful in polymer applications. The involvement of extensive chemistry makes the overall process very atom inefficient and laborious, thus limits the usability of the traditionally available carbohydrate molecules.

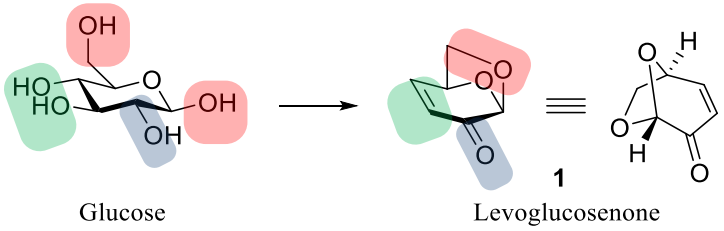

Scheme 6. Functionality comparison of levoglucosenone with its parent carbohydrate, glucose.

Unlike the conventional carbohydrate molecules, **1** is structurally very interesting. The interesting feature of the **1** is that the molecule has no hydroxyl group. The hydroxyl groups are present in the protected form (Scheme 6). The bicyclic acetal ring formed from two-hydroxyl

groups (indicated in red). The unsaturation is the protected form of another two-hydroxyl group (indicated in green). Finally, the remaining keto group is an oxidized form of a hydroxyl group (indicated in blue). The self-protection moiety or functionalities are chemically independent. Olefin moiety, for example, is prone to radical reactions, whereas the keto group is interesting for reduction and the acetal group is acid sensitive. Such independent functionalities make the molecule versatile. In polymer chemistry, such nature brings opportunities for post-polymerization functionalization, thiol-ene click chemistry, for instance.

The presence of double bonds is interesting for the direct polymerization of **1**. It is, however, reluctant towards polymerization. Attempted polymerization of **1** with AIBN could only produce oligomeric materials (see section 7.1), and other attempts with sec-BuLi or $BF_3 \cdot Et_2O$ (ring-opening polymerization of cyclic ether ring) failed to produce any polymer or oligomer. Therefore, it was necessary to modify **1** for polymerization. One of the simplest modifications is the reduction of the 'keto' group to alcohol, which would produce levoglucosenol (**2**). We could reduce **1** with $NaBH_4$ to produce **2** in high yield. Compound **2** can be polymerized by ring-opening metathesis polymerization (see section 3.2).

As mentioned earlier, the multi-functionality of this molecule possesses the potential for different ways for its polymerization. We can modify **2** by methylation of the hydroxyl group to produce levoglucosenyl methyl ether (**3**) with high yield. The compound **3** can be polymerized by cationic ring-opening polymerization (see section 3.3)

3.1 Synthesis of monomers from cellulose

3.1.1 Synthesis of levoglucosenone

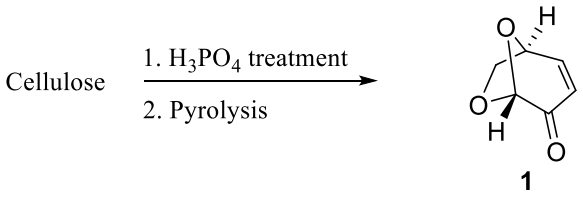

Scheme 7. Synthesis of levoglucosenone (**1**) from cellulose.

Compound **1** is known for decades. It was first reported by Broido in 1972, synthesized by acid-catalyzed pyrolysis of cellulose. Although many routes have been established,[62–64] the pyrolysis of cellulose remained the pioneer method for its synthesis.[65] It can be produced with a yield of up to 51% by thermal pyrolysis in an autoclave.[37] A simple way for small scale synthesis of **1** is to use cellulose, treated with 1% H_3PO_4 and pyrolysis in a kitchen microwave.[66] The drawback of this method is that the freshly produced **1** stays in the same flask of pyrolysis, which causes further degradation (overall yield 1-2 wt%). The thermal pyrolysis of the same acid-treated cellulose in a kugelrohr distillation apparatus under vacuum is rather convenient as it separates the produced **1** out of the pyrolysis flask. Moreover, **1** cloud be produced with somewhat better yield (4-5 wt% after purification by redistillation) as compared to the microwave method. This method is also advantageous to the previous method because of its relative scalability. The purification of **1** is established using column chromatography.[67] However, the combined crude liquid produced from batches of pyrolysis can be passed through solid $NaHCO_3$, followed by distillation of the concentrated liquid in kugelrohr distillation apparatus The resultant yellowish liquid **1** appeared to be of high purity as per the ^1H NMR analysis (Figure 10) A complete characterization of the **1** is provided in the experimental section, and all the spectral data are in agreement with literature reports.

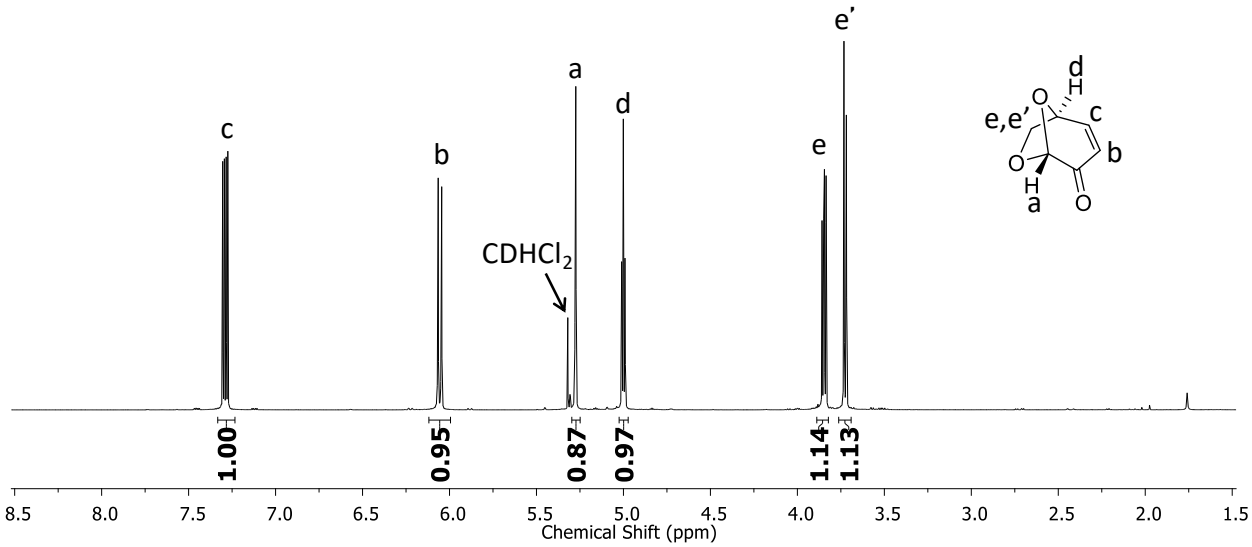

Figure 10. ^{1}H NMR (500 MHz, CD_2Cl_2) spectrum of levoglucosenone (**1**).

3.1.2 Synthesis of levoglucosenol

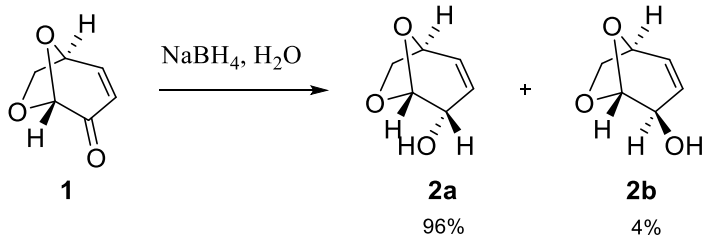

Scheme 8. Synthesis of levoglucosenol (**2**: a mixture of two diastereomers, **2a** and **2b**)

Levoglucosenol **(2)** can be produced by a reduction of **1** using $NaBH_4$ in water. It is a quick (5-10 min) and easy process. The reaction is quenched by the slow addition of acetone while keeping the reaction flask in an ice-bath. The compound **2** was then extracted from water using ethyl acetate. The combined organic portion is then concentrated under reduced pressure. The concentrate upon standing readily crystallizes but compound **2** could not be purified by recrystallization. The purification of **2** by column chromatography is an established method.[68] However, **2** was noticed to sublimate under reduced pressure. Attempt to purify **2** by sublimation leads to high yield. This purification method is advantageous over the column chromatographic technique as no waste solvent is produced. The overall yield was 90%. Compound **2** is a mixture

of diastereomers with *de* of 92%. The diastereomeric excess is due to the structural configuration of **1**. The exact configuration of the major isomer could not be determined by ^{1}H NMR. It is due to the non-trivial pattern of peaks of H_c, possibly due to complicated couplings arising from the allylic conjugation. A recent study showed to isolate the isomers via protection group chemistry and obtained crystal structure of isolated major isomer, showing previous claims of **2a** as major isomer is in agreement.[69] The mixture of the two isomers required acetylation followed by chromatographic separation, and finally deacetylation to obtain each isomer in pure form. The report states that the major isomer is solid with a melting point of 67-68 ^{o}C and the other isomer is liquid at room temperature. Compound **2** (a mixture of **2a** and **2b**), purified by sublimation, also has the same melting feature but it is slightly sticky at room temperature. It is likely due to the presence of minor isomer that is liquid. The ratio of the two isomers, however, is different from the reported literature. It is possible because of the method of preparation. The same report (for crystal structure),[67] and others[67,69] used the 'Luche reduction' condition ($NaBH_4$, $CeCl_3$ in methanol, 2.5 h or higher), which yields **2a**:**2b** with the ration of 11:1, whereas using $NaBH_4$, in water over 10 minutes gave a selectivity of 24:1 (**2a**:**2b**). The reason behind the different selectivity could be a solvent effect or the added $CeCl_3$. The mixture of the isomers **2** was used in polymerization by ROMP without further purification.

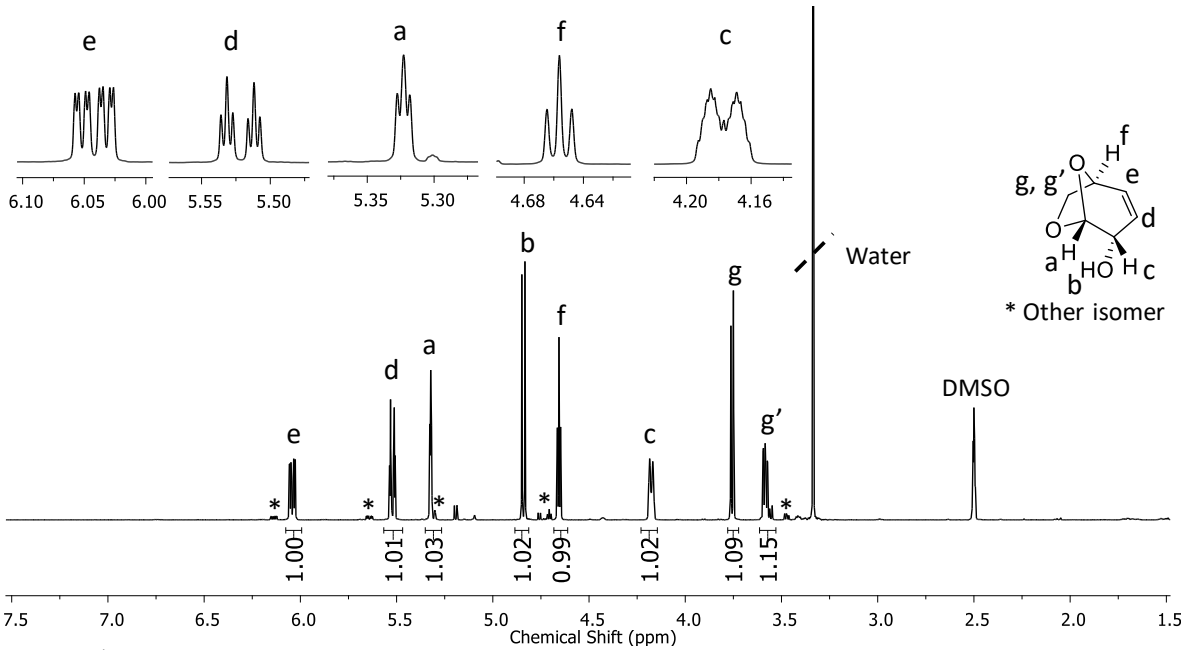

Figure 11. ^{1}H NMR (500 MHz, DMSO) spectrum of levoglucosenol (**2**).

3.1.3 Synthesis of levoglucosenyl methyl ether

Levoglucosenol (**2**) can be polymerized by ROMP but failed to polymerize by CROP (see 3.3) possibly due to allylic alcohol moiety. A modification on the allylic group was required. Therefore, it was converted to levoglucosenyl methyl ether (**3**) following Williamson ether synthesis to obtain a suitable monomer for cationic ring-opening polymerization (see polymerization in 3.3).

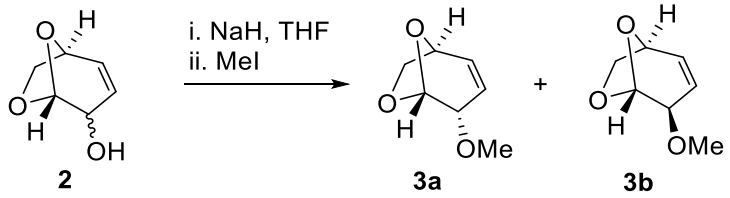

Scheme 9. Synthesis of the levoglucosenyl methyl ether (**3)** (a mixture of two diastereomers **3a** and **3b**) from levoglucosenol, **2**.

The methyl ether of compound **2** can be synthesized by deprotonation of the hydroxyl group using NaH followed by methylation with methyl iodide in tetrahydrofuran. The reaction was allowed to stir at room temperature until TLC (Thin Layer Chromatography) of the reaction mixture showed complete consumption of the starting material (about a couple of hours). The excess sodium hydride was quenched with ice-water and compound **3** was extracted from the crude reaction mixture with dichloromethane (DCM). The DCM portions were combined and concentrated under reduced pressure. The crude material was purified by distillation under reduced pressure (0.1 mbar) in a kugelrohr distillation apparatus with the overall yield of 90% starting from **2**. This compound was characterized with the help of ^{1}H, ^{13}C, ^{1}H-^{1}H COSY, and ^{1}H-^{13}C HSQC NMR spectroscopy and by ESI-MS (Figure 12). This purification process appeared to be quick and greener in comparison to column chromatography.

3.1.4 Structural characterization of levoglucosenyl methyl ether

The ESI-HRMS spectrum (Figure 12) of **3** reveled an *m/z* peak at 143.070 Da that is in agreement with the calculated mass of 143.070 Da. The ^{1}H NMR spectrum (Figure 13) shows the

presence of all the characteristic protons and ^{13}C NMR spectrum (Figure 15) confirms the presence of all characteristic carbon atoms. The ^{1}H-^{13}C HSQC NMR spectrum (Figure 14) gave information on protons H_f, $H_{f'}$ and H_a. Negative cross-peaks (CH_2 peaks appear as negative contours and are indicated by blue) in the ^{1}H-^{13}C HSQC NMR spectrum at 3.96-71.9 ppm and 3.80-71.9 ppm suggest that these protons are H_f and $H_{f'}$, as **3** has single CH_2 group. The cross peak at 5.66-100.6 ppm corresponds to the very characteristic acetal proton (H_a). The ^{1}H-^{1}H COSY NMR spectrum (Figure 16) enabled the assignment of the remaining protons. The proton $H_{f'}$ has a cross-peak at 4.66-3.80 ppm, indicating it as H_e. The acetal proton (H_a) also shows correlation at 5.66-4.11 ppm suggesting that the other proton (at 4.11 ppm) is H_b. The cross-peak corresponding to proton H_e at 6.14-4.66 ppm indicates the olefinic proton at 6.14 ppm is H_d. It means that the reaming proton (at 5.77 ppm) is indeed the olefinic proton H_c. The coupling constant between H_a and H_b is crucial for the determination of the correct isomeric configuration, but could not be determined due to additional unresolvable couplings arising, possibly from allylic moiety. However, we can safely assume that the configuration of **2** is retained in **3**. This is because, in Williamson's synthesis, the hydroxyl group is deprotonated by the base and the resulting alkoxide ion attacks methyl iodide. Thus, chirality is untouched.

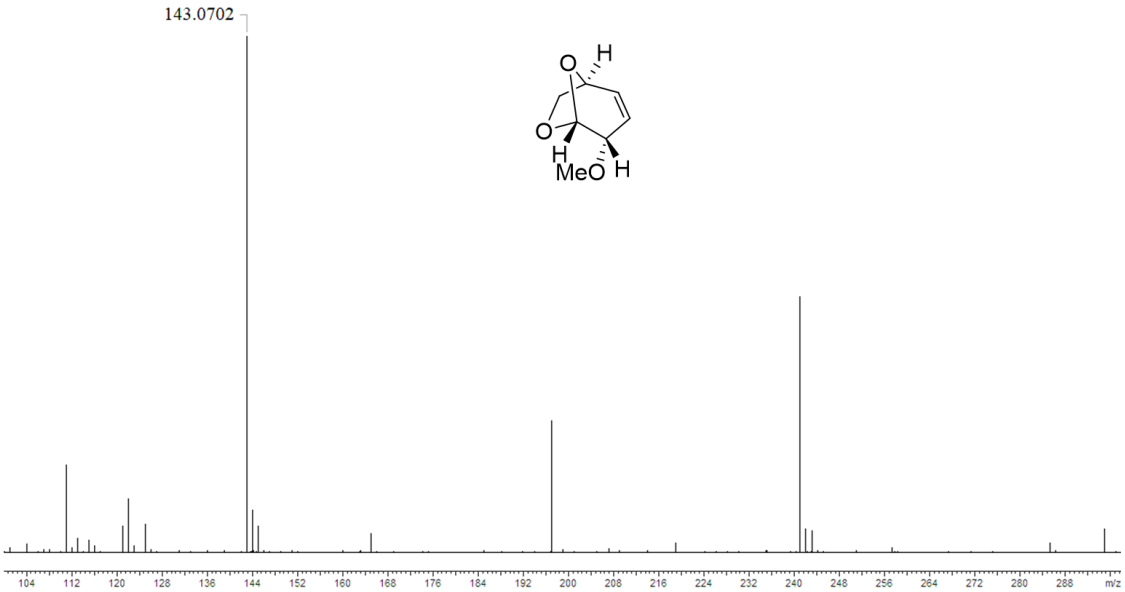

Figure 12. High-resolution mass spectrum of levoglucosenyl methyl ether (**3**).

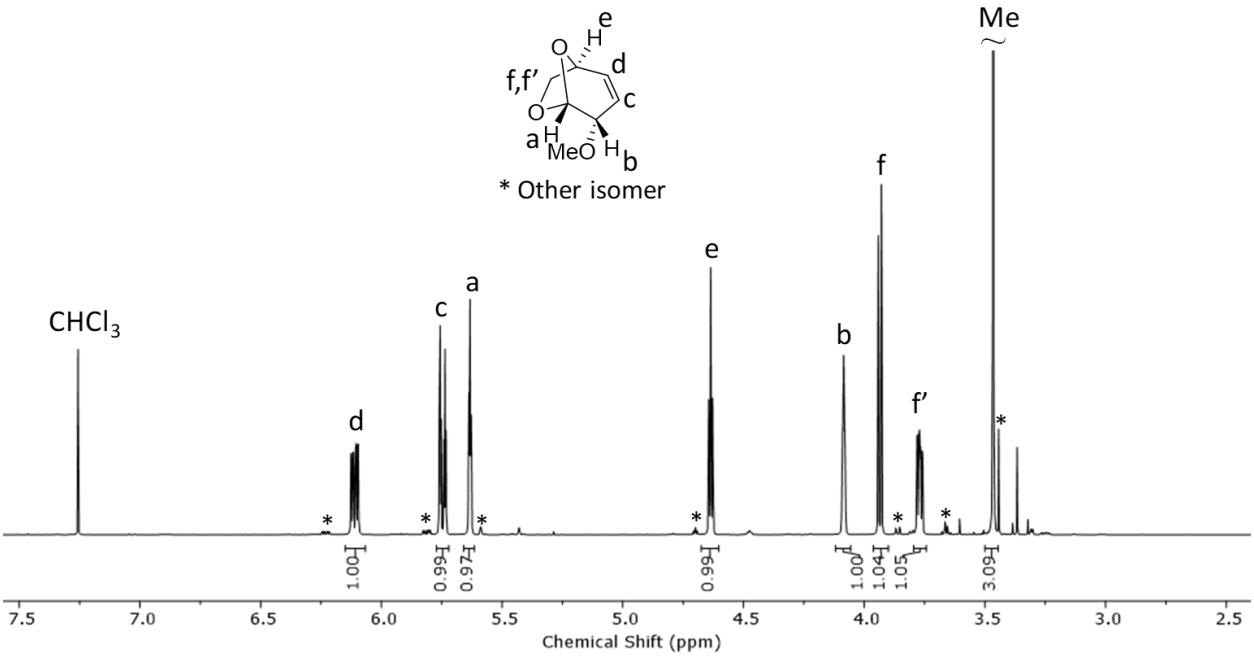

Figure 13. ^{1}H NMR (500 MHz, $CDCl_3$) spectrum of levoglucosenyl methyl ether (**3**).

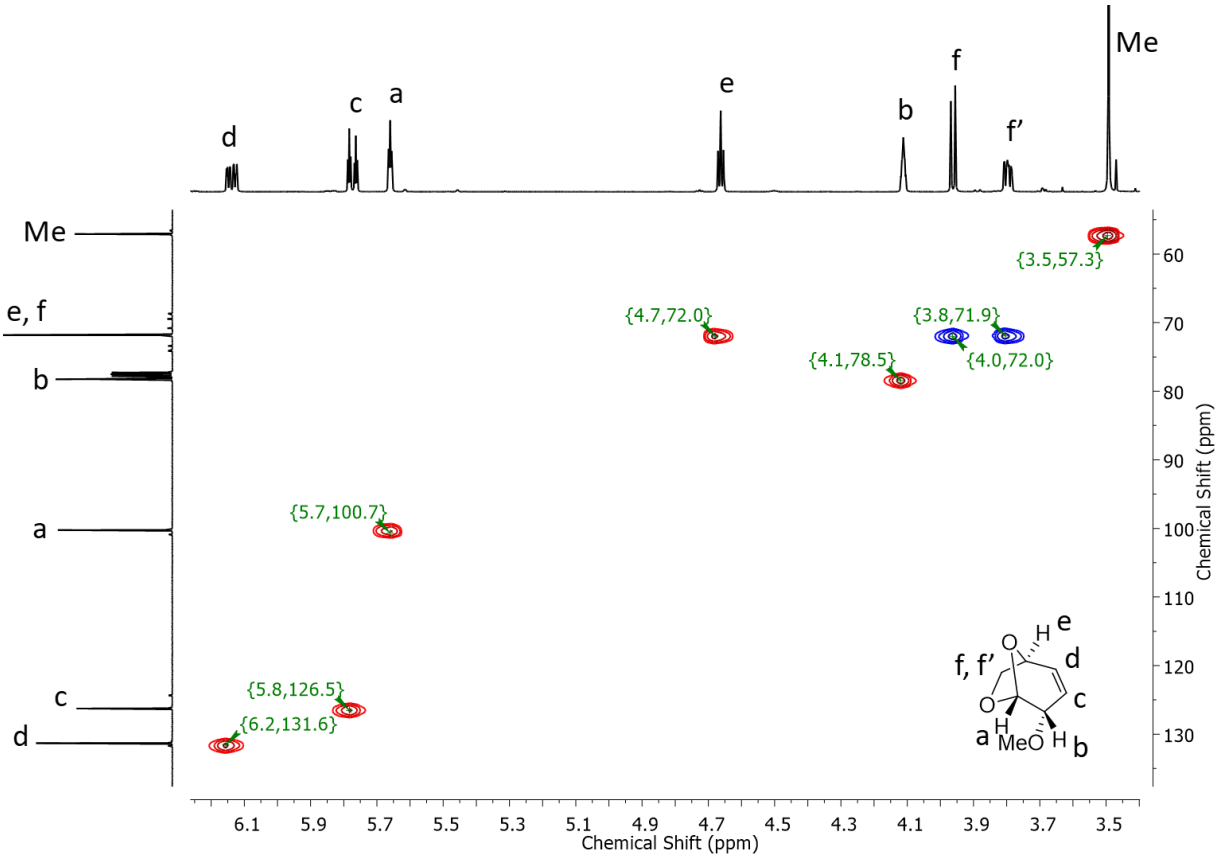

Figure 14. ^{1}H-^{13}C HSQC (500 MHz, 125 MHz, $CDCl_3$) NMR spectrum of levoglucosenyl methyl ether (**3**) (Red: positive contours, CH, CH_3; blue: negative contours, CH_2).

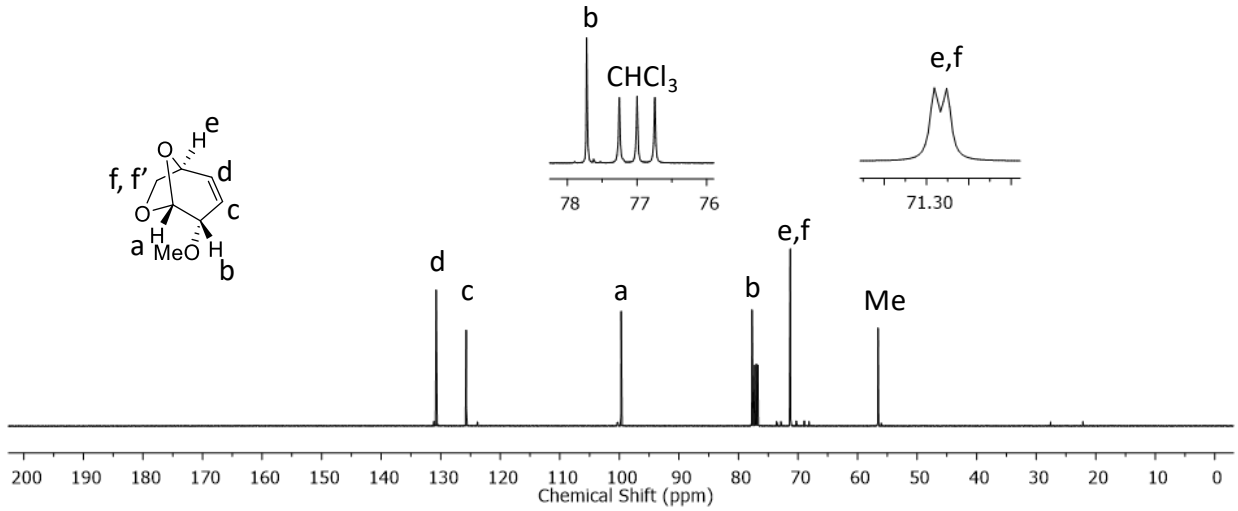

Figure 15. ^{13}C NMR (125 MHz, $CDCl_3$) spectrum of levoglucosenyl methyl ether (**3**).

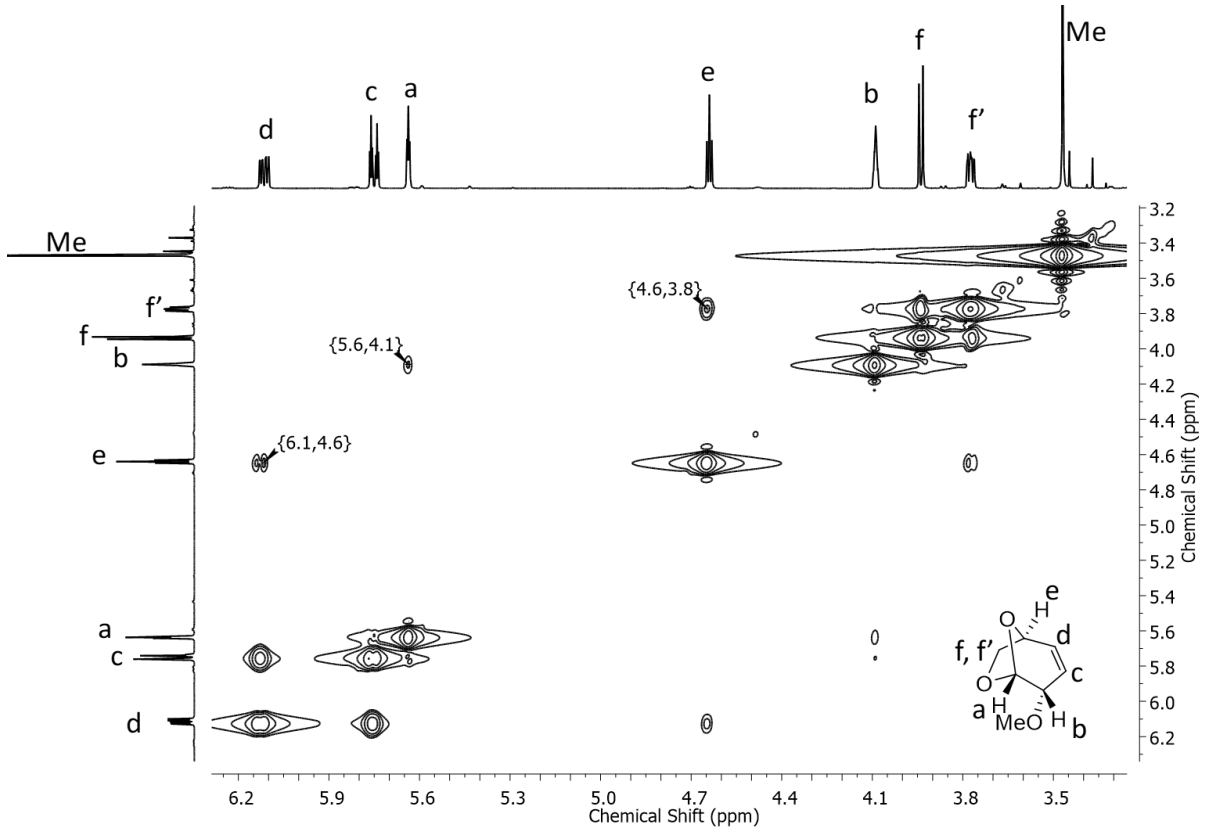

Figure 16. ^{1}H-^{1}H COSY (500 MHz, $CDCl_3$) NMR spectrum of compound (**3**).

3.1.5 Conclusion

Levoglucosenone (**1**) was synthesized by pyrolysis of cellulose following a literature method and was converted into levoglucosenol (**2**) and a new molecule levoglucosenol methyl ether (**3**). Both the synthesis and purification methods of **2** and **3** are simple and high yield processes. The method for the synthesis of levoglucosenol is adapted from the literature. The structural characterization for the molecules is carried out using NMR and ESI-MS analyses.

3.2 Polymerization of levoglucosenol

3.2.1 Reaction monitoring

Polymerization of levoglucosenol (**2**) by ring-opening metathesis polymerization was monitored for conversion (by ^{1}H NMR) and molar mass distribution (by SEC) with time. SEC could not be used to monitoring the monomer conversion since the monomer was iso-refractive with the SEC eluent (N-Methyl-2-pyrrolidone: NMP).

Monitoring the conversion

Monomer conversion of the crude polymerization mixture was determined by ^{1}H NMR spectroscopy in DMSO-d_6. Crude samples of the reaction mixtures were taken at different time intervals, quenched with ethyl vinyl ether, and were subjected to ^{1}H NMR measurements. The olefinic protons of the monomer and of the polymer were used for the determination of monomer conversion.

Monitoring the molar mass

Crude samples of the reaction mixtures were taken at different time intervals, quenched, evaporated at room temperature, redissolved in NMP (eluent) and used for the SEC measurements.

3.2.2 Ring-opening metathesis polymerization of levoglucosenol

We already discussed in section 2.1.2, that the ROMP of small molecules is enthalpy driven, that means the molecule releases strain upon converting to a polymer. Conventional ROMP substrates are aliphatic olefins (Figure 17), such as norbornene and its derivatives or bicyclo[2.2.2]octene and its derivatives. These molecules are very active for ROMP due to high ring strain that can be released during polymerization. Other known substrates also share similar characteristic chemical structures. This limits the application of ROMP for the bio-derived

molecules. There are some examples, that use entropy-driven ROMP.[70,71] However, it is still limited to non-carbohydrate molecules.

Norbornene Bicyclo[2.2.2]octene

Figure 17. Common aliphatic olefins as a substrate for ROMP.

Carbohydrate molecules are generally not strained. The most common olefinic carbohydrates are glycals (Figure 18). The closest aliphatic analog of glycals would be cyclohexene that produces oligomers at best at –60 °C or below.[72] It is due to a lack of enthalpy gain during polymerization.

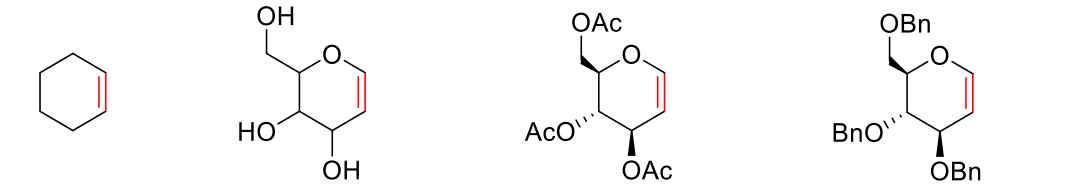

Cyclohexene Glycal 3,4,6-tri-O-acetyl-D-glucal 3,4,6-tri-O-benzyl-D-glucal

Figure 18. Cyclohexane, general glycal structure and its structural analog to cyclohexene.

This has very recently been overcome by en-yne metathesis. Choi reported cascade metathesis polymerization (Scheme 10) of carbohydrate molecules via the introduction of terminal alkyne functionality.[73] Moreover, the attempts for the polymerization of 3,4,6-tri-*O*-benzyl-D-glucal and 3,4,6-tri-*O*-benzyl-D-glucal (Figure 18) with **C6** (Figure 19) produced no oligomeric or polymeric material at room temperature.

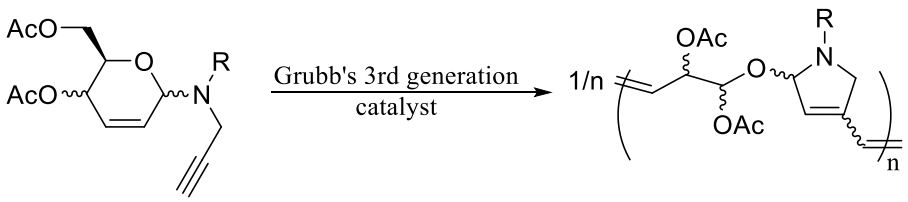

R = Ts (tosyl), TPS (2,4,6-triisopropylbenzenesulfonyl)

Scheme 10. Polymerization of carbohydrate molecule via metathesis.

Compound **2,** having a bicyclic structure and strain, could undergo ROMP. The polymerization attempts of **2** (a mixture of the isomers) with Grubbs 1st, 2nd and 3rd generation catalysts (**C1-C3**), as well as Hoveyda-Grubbs 1st and 2nd generation catalysts (C4-C5) (Figure 19) in DCM solution, failed to produce any oligomeric or polymeric material. A possible reason could be the steric demand of the monomer **2**. Hence, a less steric demanding catalyst, **C6** may become suitable for its polymerization.

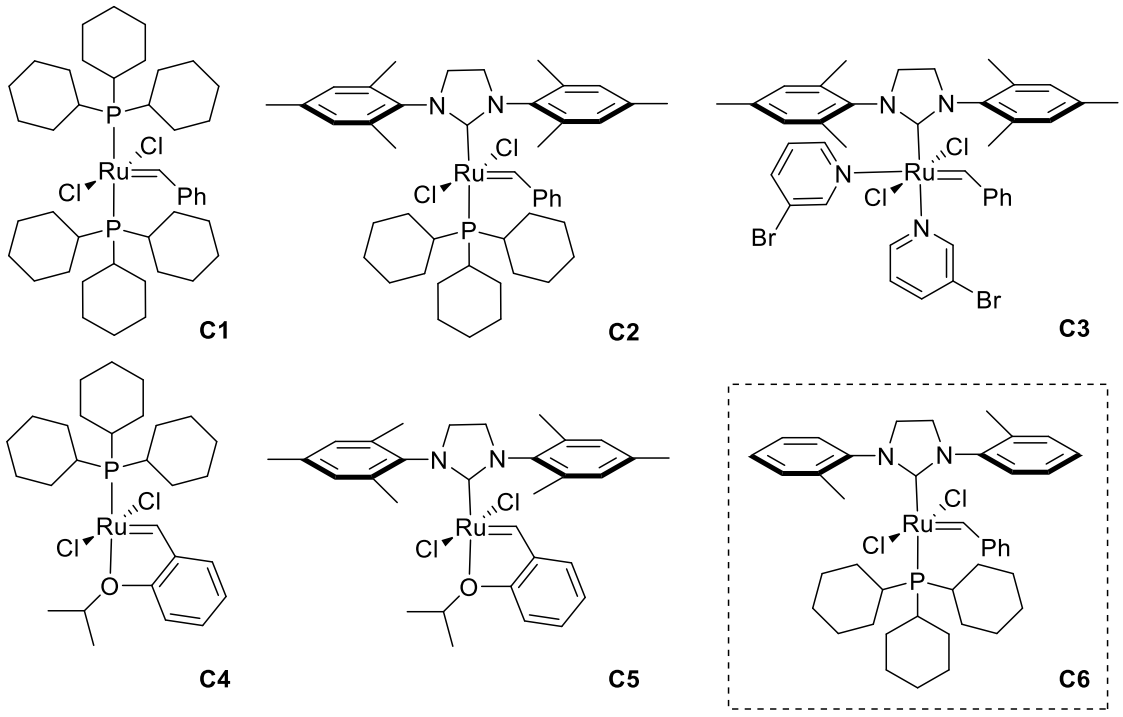

Figure 19. Screened catalysts for the polymerization of **2**.

Catalyst **C6** is similar to **C2**, but the former is having relatively less steric demanding NHC ligand than later. The polymerization of **2** was carried out in DCM ($[\mathbf{2}]_0$ = 4 M, $[\mathbf{2}]_0/[\mathbf{C6}]$ = 100) at room temperature for 24 h. Interestingly, this produced a sticky material at the bottom of the reaction flask indicating a potentially insoluble fraction of poly(levoglucosenol) **4**. After quenching the reaction with ethyl vinyl ether, it was dissolved in 1,4-dioxane, precipitated into diethyl ether, and analyzed by SEC (Figure 20).

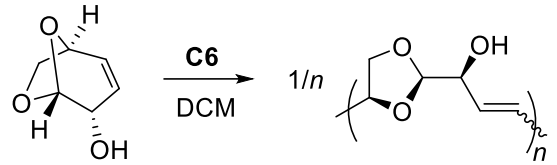

2 **4**

Scheme 11. Ring-opening metathesis polymerization of levoglucosenol (**2**) to yield poly(levoglucosenol) **4**. (Mixture of **2a** and **2b** was used for polymerization, but the structure of **2a** only is drawn here to indicate preservation of stereocenters after polymerization.)

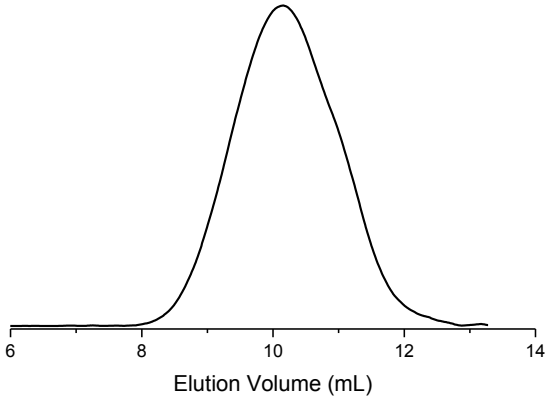

Figure 20. SEC-RI trace (eluent: NMP) of poly(levoglucosenol) (**4**) after precipitation. (M_w^{app} = 66.4 kg/mol, $Đ$ = 2.2)

The SEC-RI trace of the isolated compound is bimodal. The smaller peak at 11 mL could be the formation of new polymer chains due to the insolubility of the bigger precipitated chains during the reaction. The insolubility of the polymer **4** in DCM led to choose alternative solvent for the polymerization. As we already found 1,4-dioxane as a suitable solvent to dissolve **4**, it was chosen as a solvent for further polymerizations.

The monomer **2** was then subjected to polymerization at room temperature with the different monomer to catalyst loadings ([**2**]$_0$/[**C6**] = 66-1000) over 24 h; results are summarized (Table 1). The monomer conversion reached up to 60% (determined by ^{1}H NMR) and polymers with weight-average molar masses (M_w^{app}) of 29-100 kg/mol were produced. Although the different monomer-to-catalyst ratios produced polymers with different molar masses, these do not reflect the targeted molar mass.

Table 1. Polymerization of **2** ($[\mathbf{2}]_0$ = 4 M) with catalyst **C6** in 1,4-dioxane solution at room temperature for 24 h.

Run	$[\mathbf{2}]_0/[\mathbf{C6}]$	x_p [a] (%)	M_w^{app} [b] (kg/mol)	$Đ$ [c]
1	66	60	29	1.8
2	100	59	37	2.0
3	200	59	47	2.2
4	1000	50	100	2.9

[a]Monomer conversion, determined by ^{1}H NMR spectrum. [b]Apparent weight-average molar mass, determined by SEC. [c]Dispersity index, determined by the SEC.

The isolated polymers of Table 1 (Figure 21) are monomodal, thus it is more controlled than the initial attempt (Figure 20). These polymers exhibited color (Figure 21), and the polymer produced with the least amount of catalyst (run-4, Table 1), appears virtually colorless, indicating that the residual catalyst traces are responsible for the color.

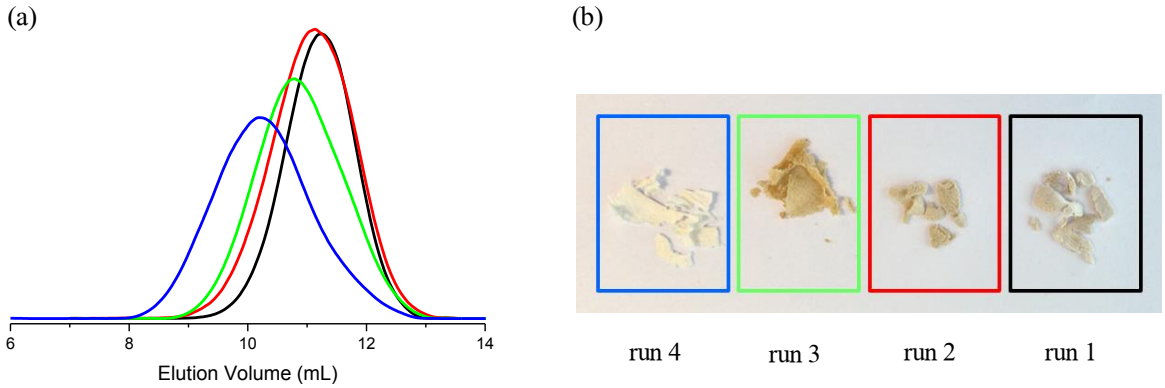

Figure 21. (a) SEC-RI traces (eluent: NMP) of poly(levoglucosenol) **4** prepared by ROMP at different monomer to catalyst ratios, $[\mathbf{2}]_0/[\mathbf{C6}]$ = 66 (black, run 1), 100 (red, run 2), 200 (green, run 3), and 1000 (blue, run 4), corresponding to samples no. 1-4 in Table 1. (b) Optical appearances of poly(levoglucosenol) samples no. 1-4; samples 1-3 are colored indicating residual catalyst traces, sample 4 (blue), prepared with the lowest catalyst loading is virtually colorless.

3.2.3 Kinetics and optimization of reaction condition

The low monomer conversion is an indication of termination reaction(s). Such phenomena could be due to catalyst deactivation. Moreover, the polymerization solution blackened over time and can be attributed to the deactivation of catalyst or active chain ends. The pseudo-first-order time-conversion plot could be fitted with a model of unimolecular termination (Figure 24).

Additionally, the apparent weight-average molar masses do not increase linearly and are much higher than the calculated molar masses from the monomer-to-catalyst ratio. Polymers having high molar mass formed in the early stages of reaction (conversion <20%) and chains grew shorter with increasing consumption of monomer, a typical observation for non-living processes. Furthermore, **4** exhibits a Schulz-Flory type molar mass distribution with $Đ \sim 2$.

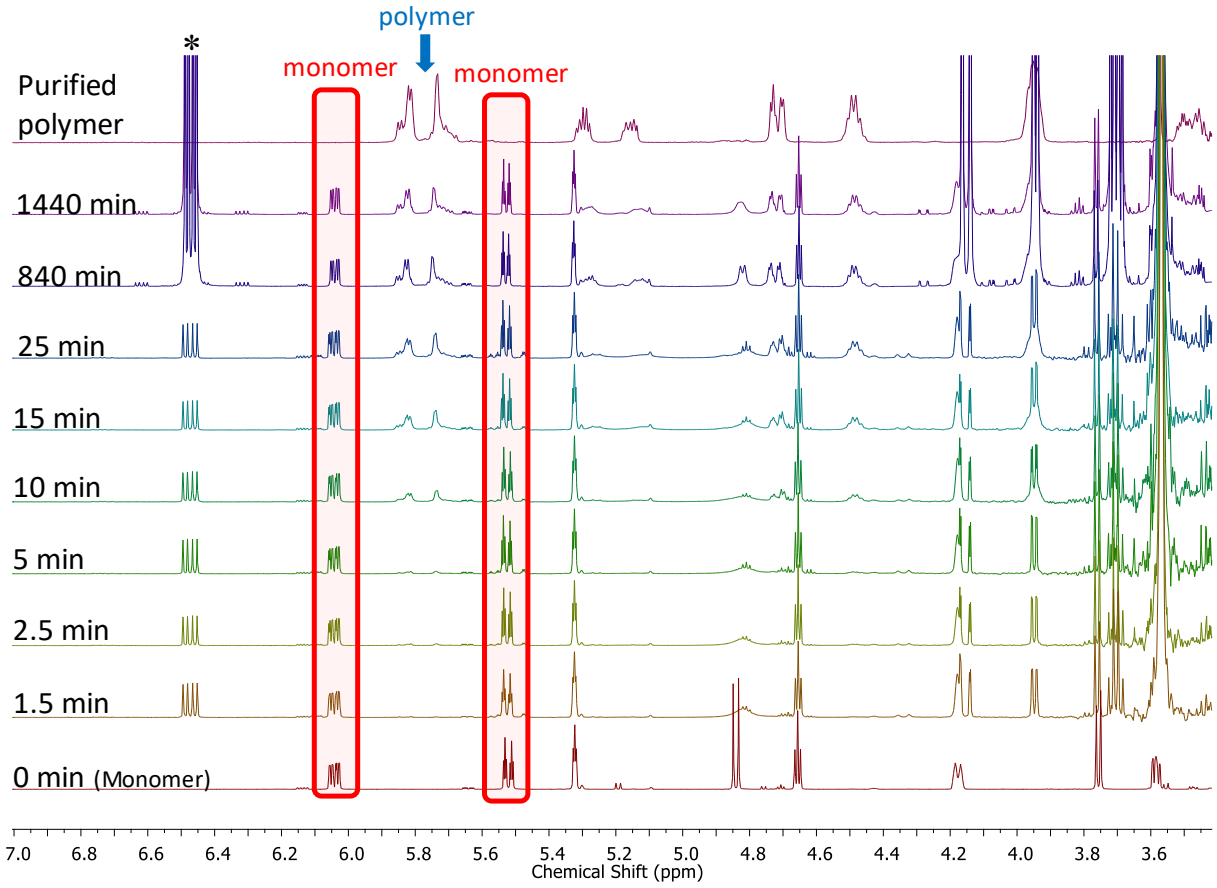

Figure 22. ^{1}H NMR (500 MHz, DMSO-d_6) spectra of crude polymerization mixtures ([**2**]$_0$/[**C6**] = 100, 28 °C) at different reaction times: 1.5-1440 min (bottom to top). The olefinic protons of monomer **2** and poly(levoglucosenol) (**4**) were used for determining monomer conversions; * = quenching agent.

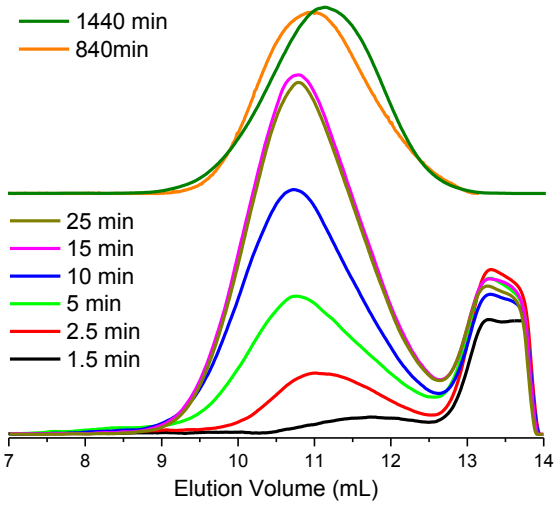

Figure 23. SEC-RI traces (eluent: NMP) of crude polymerization mixtures ([**2**]$_0$/[**C6**] = 100, 28 °C) at different reaction times: 1.5-1440 min. The peak at the elution volume of ~13.5 mL refers to the quenched catalyst **C6**. Samples at 1440 min and 840 min are precipitated samples.

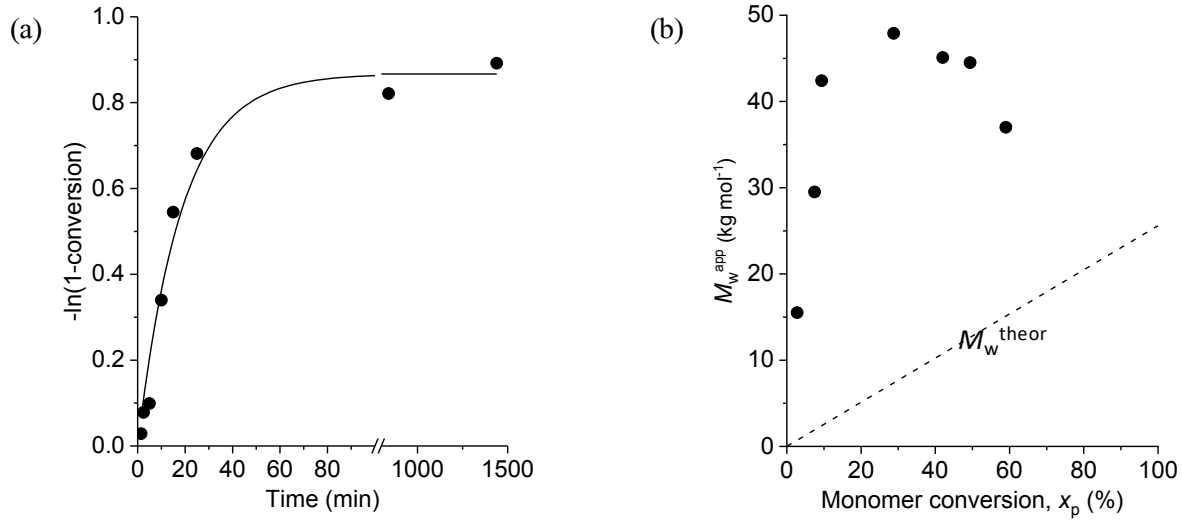

Figure 24. Polymerization of **2** with catalyst **C6** ([**2**]$_0$ = 4 M, [**2**]$_0$/[**C6**]=100) in 1,4-dioxane at room temperature. a) Pseudo-first order time–conversion plot. b) Evolution of weight-average molar mass (M_w^{app}) with conversion (x_p) ($M_w^{theor} = 2(Đ)\cdot[\mathbf{2}]_0/[\mathbf{C6}]\cdot x_p$).

Such nature of reaction kinetics suggests the rate of monomer addition is higher than the rate of initiation step. Active chains grow continuously until irreversible termination or deactivation of the active chain end occurs. Correspondingly, prolonged reaction time contributes to chain-length equilibration, via back-biting leading to the reduction of polymer molar mass. In order to have more insight on the chain-length equilibration, the isolated **4** was treated with catalyst **C6** and allowed to react for 6 and 24 hours. The SEC measurements indicate the reduction of chain length with increasing reaction time (Figure 25).

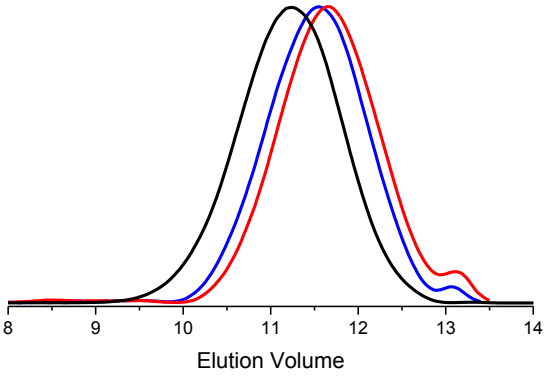

Figure 25. SEC-RI traces (eluent: NMP) of poly(levoglucosenol) **4** before (black) and after treatment with catalyst **C6** for 6 h (blue) and 24 h (red) of equilibration.

Table 2. Polymerization of **2** ($[\mathbf{2}]_0$ = 1-4 M) with catalyst **C6** ($[\mathbf{2}]_0/[\mathbf{C6}]$ = 100) in 1,4-dioxane solution at room temperature for 24 h

Run	$[\mathbf{2}]_0$ (M)	T^a (°C)	x_p [b] (%)	Appearance	M_w^{app} [c] (kg/mol)	$Đ$ [d]
1	4	90	12	Liquid	2	1.6
2	4	60	33	Liquid	18	1.7
3	4	40	49	Liquid	33	1.9
4	4	28	59	Liquid→Gel	35	2.0
5	4	0	62	Liquid→Gel	87	2.2
6	2	60	2	Liquid	-	-
7	2	40	16	Liquid	8	1.9
8	2	28	27	Liquid	13	2.3
9	2	5	74	Liquid→Gel	104	2.0
10	1.8	5	78	Liquid→Gel	150	2.6
11	1	10	9	Liquid	13	1.6

[a]Reaction temperature. [b]Monomer conversion, determined by 1H NMR spectrum. [c]Apparent weight-average molar mass, determined by SEC. [d]Dispersity index, determined by SEC.

Polymerization at different temperatures (0 °C and 28 °C) with the same initial monomer concentration, $[\mathbf{2}]_0$ = 4 M (run 4, 5, Table 2) resulted in very similar conversion; however, apparent molar masses were significantly higher at a lower temperature. The polymerizations at lower temperatures tend to have higher monomer conversions than similar conditions at higher temperatures (Table 2), which is typically observed for monomers having low ring strain. The

highest monomer conversions of 62-78% were obtained at $[\mathbf{2}]_0$ = 4-1.8 M and at 0-5 °C (this is possible due to depression of freezing point of 1,4 dioxane), whereas the highest weight-average molar mass (M_w^{app}) of 150 kg mol^{-1} was achieved at $[\mathbf{2}]_0$ = 1.8 M. In the case of $[\mathbf{2}]_0$ = 4 M, both the (run 4, 5) reactions turned into a gel, thus limiting the polymerization. Further, polymerizations at rather diluted initial monomer concentration ($[\mathbf{2}]_0$ = 2 M) were carried out at 28 °C and 5 °C (reaction mixture was frozen at a temperature lower than 5 °C). Polymerizations with $[\mathbf{2}]_0$ = 2 M (run 8, 9) favored higher monomer conversions at a lower temperature but still turned into gel. Therefore, the reaction mixture was further diluted to $[\mathbf{2}]_0$ = 1.8 M which gave the highest conversion with 78% but still turned into a gel. However, polymerization at any lower initial monomer concentration ($[\mathbf{2}]_0$ = 1 M), drastically decreased both the monomer conversion and molar mass.

These sets of experiments suggest that the polymerization favors lower temperatures for higher conversion and molar mass, possibly because of the low ring strain of the **2**. Higher initial monomer concentration also found to be beneficial for higher conversion except for lower temperatures, where the high viscosity of the polymerization mixture limits the conversion. This temperature profile suggests a limited enthalpy gain for this particular polymerization, hence lowering the temperature might be beneficial for the reaction.

3.2.4 Structural analysis of poly(levoglucosenol)

The structural characterization of the poly(levoglucosenol) (**4**) was carried out with ESI-MS and various NMR experiments. The ESI-MS analysis (Figure 26) of the same revealed peaks having a difference of 128 Da, as expected. Further, ^{1}H, ^{13}C, and 2D correlation NMR experiments allowed assignments of all the protons and carbons of **4**.

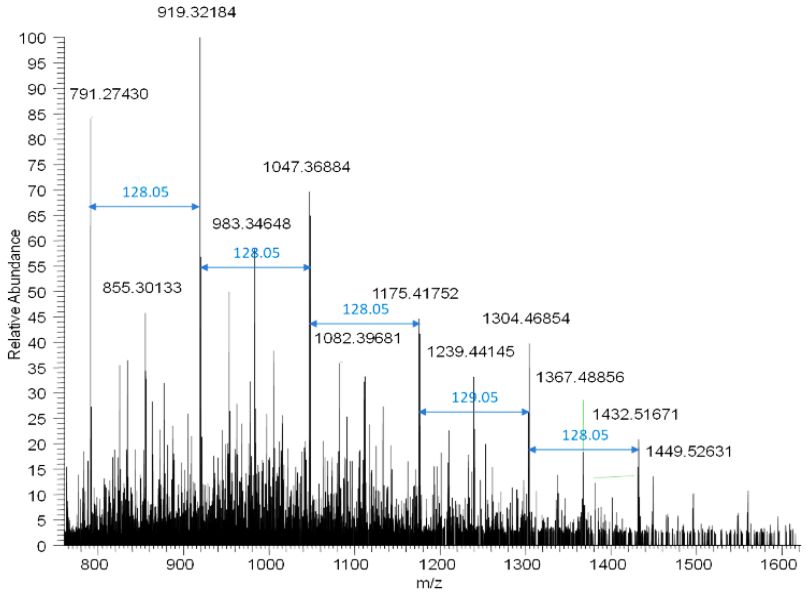

Figure 26. ESI-MS spectrum of poly(levoglucosenol) (**4**). The individual peaks are unknown fragments of polymer chains but the difference between peaks are128 Da.

A total of 8 protons were found in the ^{1}H NMR spectrum (Figure 27), which is in agreement with the expected structure. The signals at 5.90-5.79 ppm and 5.79-5.65 ppm are characteristic of olefinic protons (H_c, H_d). It is interesting to see two multiplets corresponding to half a proton each around 5.37-5.10 ppm. These signals disappeared upon addition of D_2O (Figure 29), indicating hydroxyl protons as hydroxyl protons can exchange with the deuterium (of D_2O). Additionally, these signals show no correlation in the ^{1}H-^{13}C HSQC NMR spectrum (Figure 30), but have cross-peaks, with C_b, C_a, C_c and C_d (carbon assignments are mentioned later in this section, see Figure 28) in the ^{1}H-^{13}C HMBC NMR spectrum (Figure 31). The appearance of these protons as two multiplets indicates the presence of isomeric structures in the polymer chain. The ^{13}C NMR spectrum (Figure 28) shows four singlets with similar intensities at 105.7 ppm, a very characteristic region for acetal carbon and an indication of C_a. The appearance of the C_a as four singlets suggests there are four types or C_a corresponding to four isomeric structures and is discussed later (3.2.4.1).

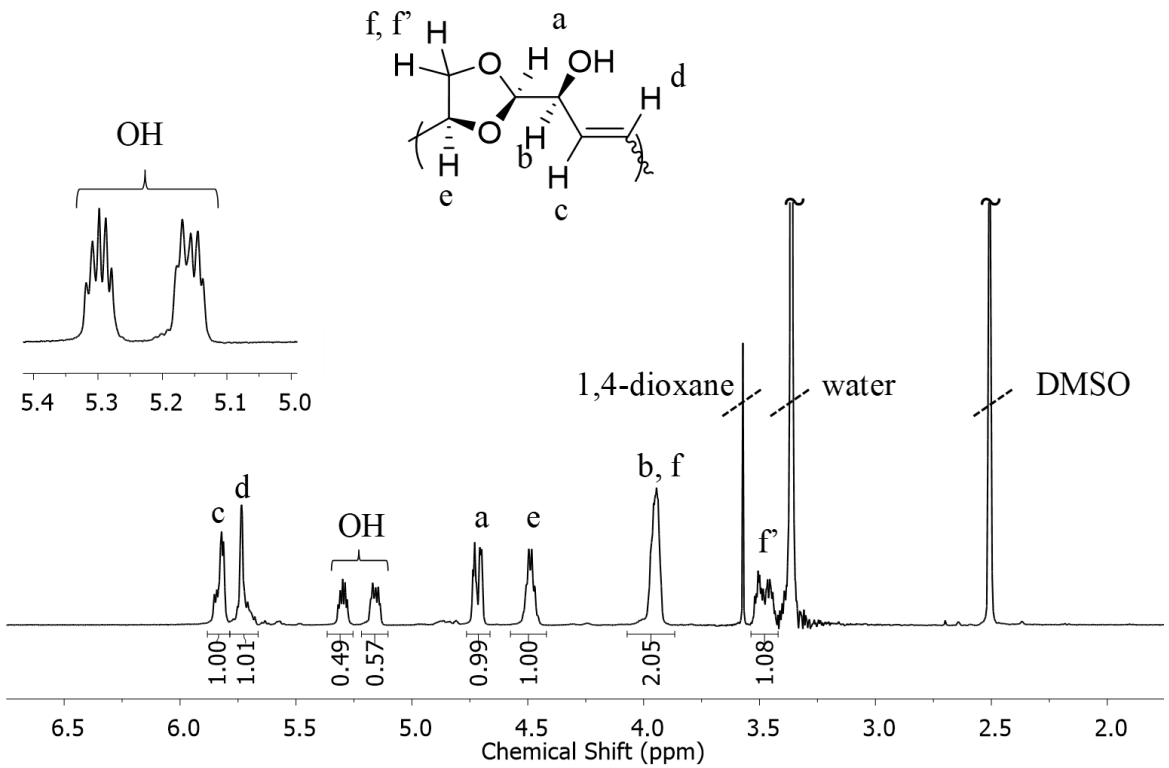

Figure 27. ^{1}H NMR (500 MHz, DMSO-d_6) spectrum of poly(levoglucosenol) (**4**) (run 2).

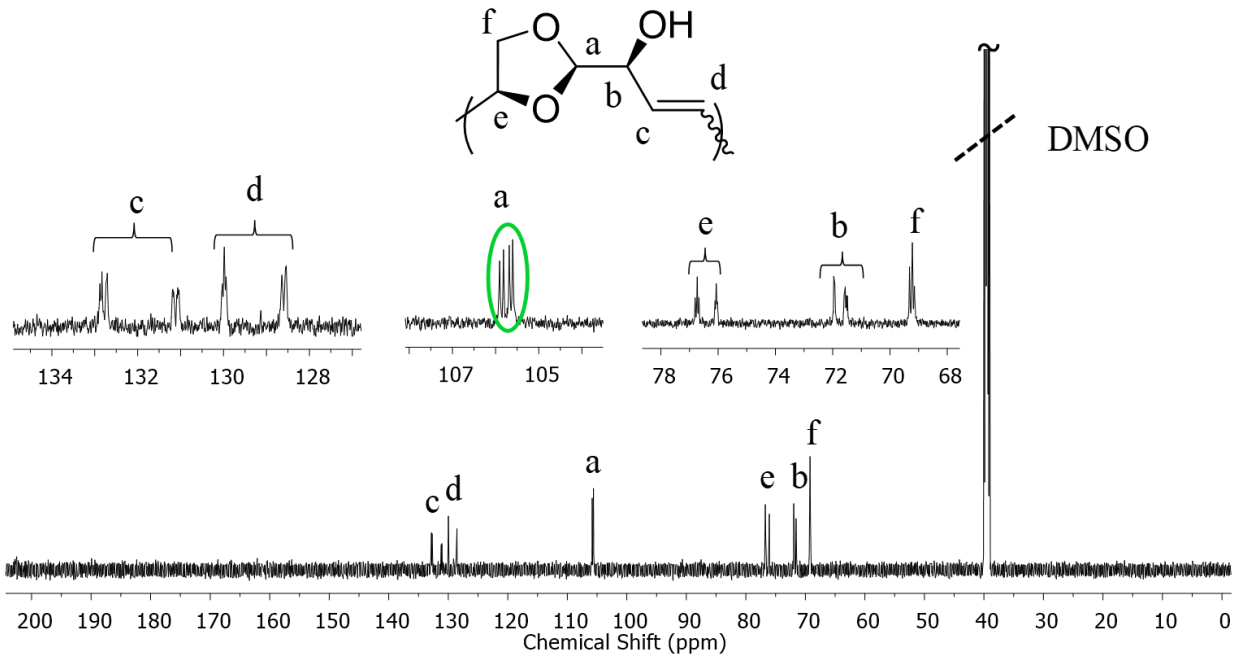

Figure 28. ^{13}C NMR (150 MHz, DMSO-d_6) spectrum of poly(levoglucosenol) (**4**) (run 2).

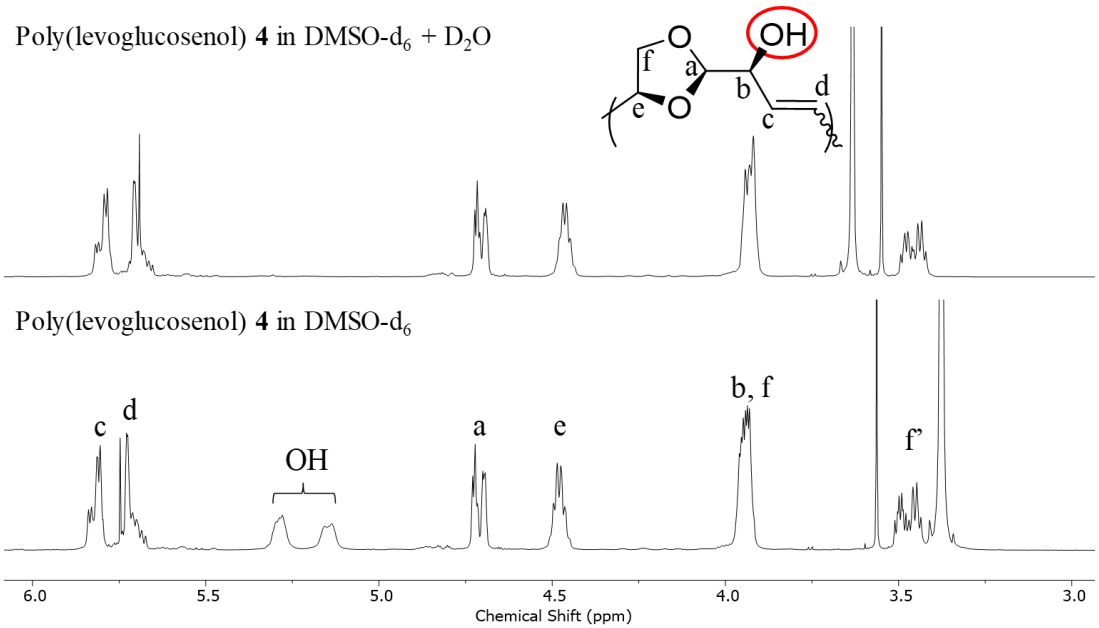

Figure 29. ^{1}H NMR spectrum (500 MHz, DMSO-d_6) of poly(levoglucosenol) (**4**) before (bottom) and after (top) the addition of D_2O.

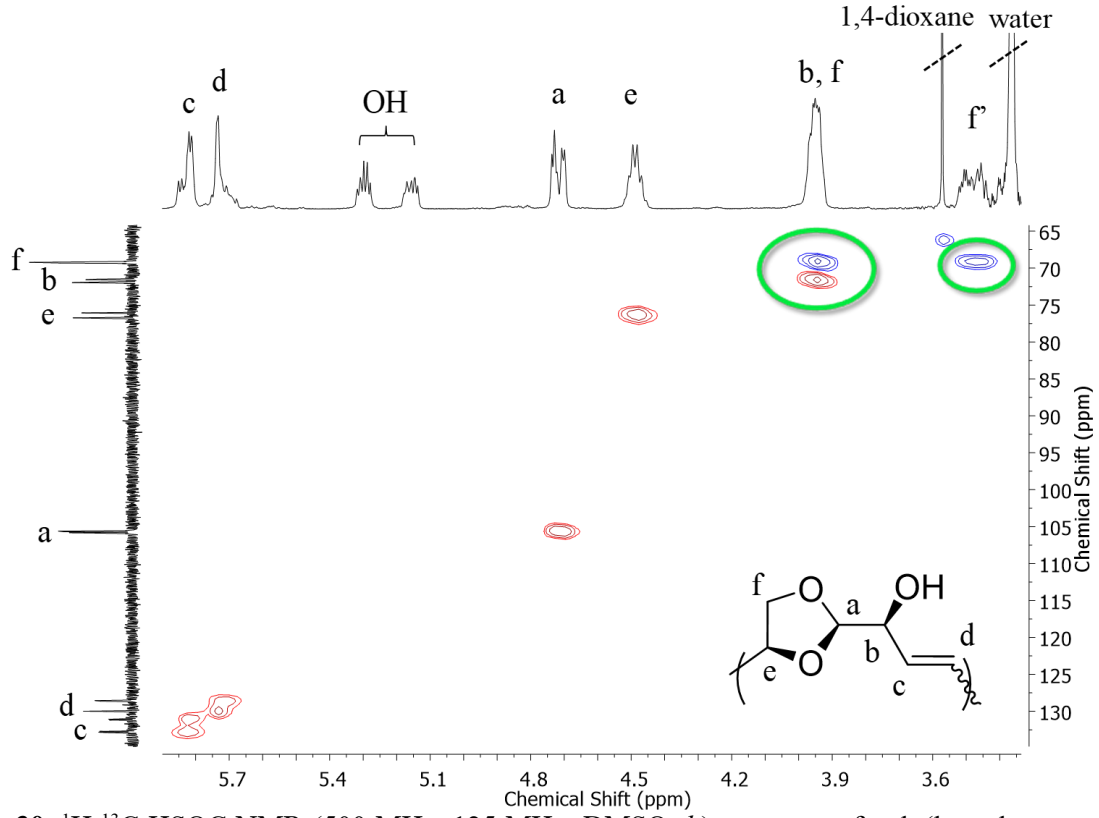

Figure 30. ^{1}H-^{13}C HSQC NMR (500 MHz, 125 MHz; DMSO-d_6) spectrum of poly(levoglucosenol) (**4**). (Red: positive contours, indicates CH, CH_3; Blue: negative contours, indicates CH_2). It shows us the correlation between very characteristic acetal C_a and H_a and the hydroxyl protons show no correlation with any carbon as expected.

The ^{1}H-^{13}C HSQC NMR spectrum shows a cross peak of the proton at 4.78-4.64 ppm with the carbon at 105.7 ppm (C_a), suggests the proton is H_a. This experiment also distinguished the protons (i.e., CH_2 and CH). The two protons ($H_{f,f'}$) corresponding to the only CH_2 group of the structure appear separately (blue colored), one (H_f) of them is overlapped with a CH group at 3.54-3.42 ppm, and another one at 4.05-3.87 ppm ($H_{f'}$). This peak has a correlation with H_a in the ^{1}H-^{1}H COSY NMR spectrum (Figure 32), but has no cross peak with $H_{f'}$, indicates that it is H_b. The proton at 4.58-4.42 ppm in ^{1}H-^{1}H COSY NMR spectrum (Figure 32) has cross-peaks with both the H_f and $H_{f'}$, suggests it is H_e. These assignments of the protons allowed the assignment of the corresponding carbon atoms with the help of the ^{1}H-^{13}C HSQC NMR spectrum.

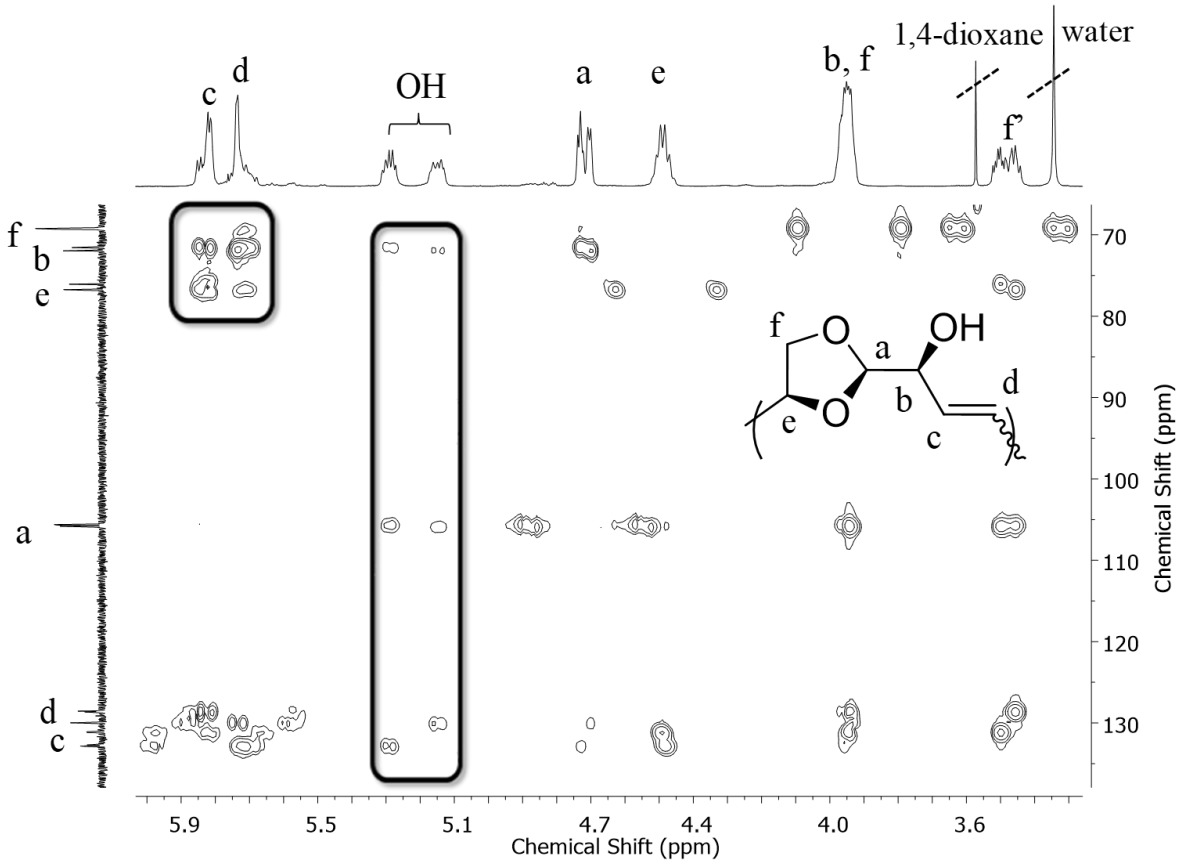

Figure 31. ^{1}H-^{13}C HMBC NMR (500 MHz, 125 MHz; DMSO-d_6) spectrum of poly(levoglucosenol) (**4**). The correlation intensity between C_b and C_e with H_d and H_c respectively distinguished the olefinic protons. The intensity of ^{3}J coupling is higher than ^{2}J coupling in HMBC.

The ^{1}H-^{13}C HMBC NMR spectrum (Figure 31) showed the four cross-peaks with a difference in the intensity of the coupling between the olefinic protons with the neighboring

carbons C_b and C_e. The proton at 5.79-5.65 ppm has a higher intensity correlation with C_b and the proton at 5.90-5.79 ppm with C_e indicates the proton to be H_d and H_c respectively (note: in HMBC, ^3J coupling shows higher intensity cross peak than ^2J coupling). This is further supported by ^{1}H-^{1}H COSY analysis (Figure 32), where H_e has a cross peak with H_d.

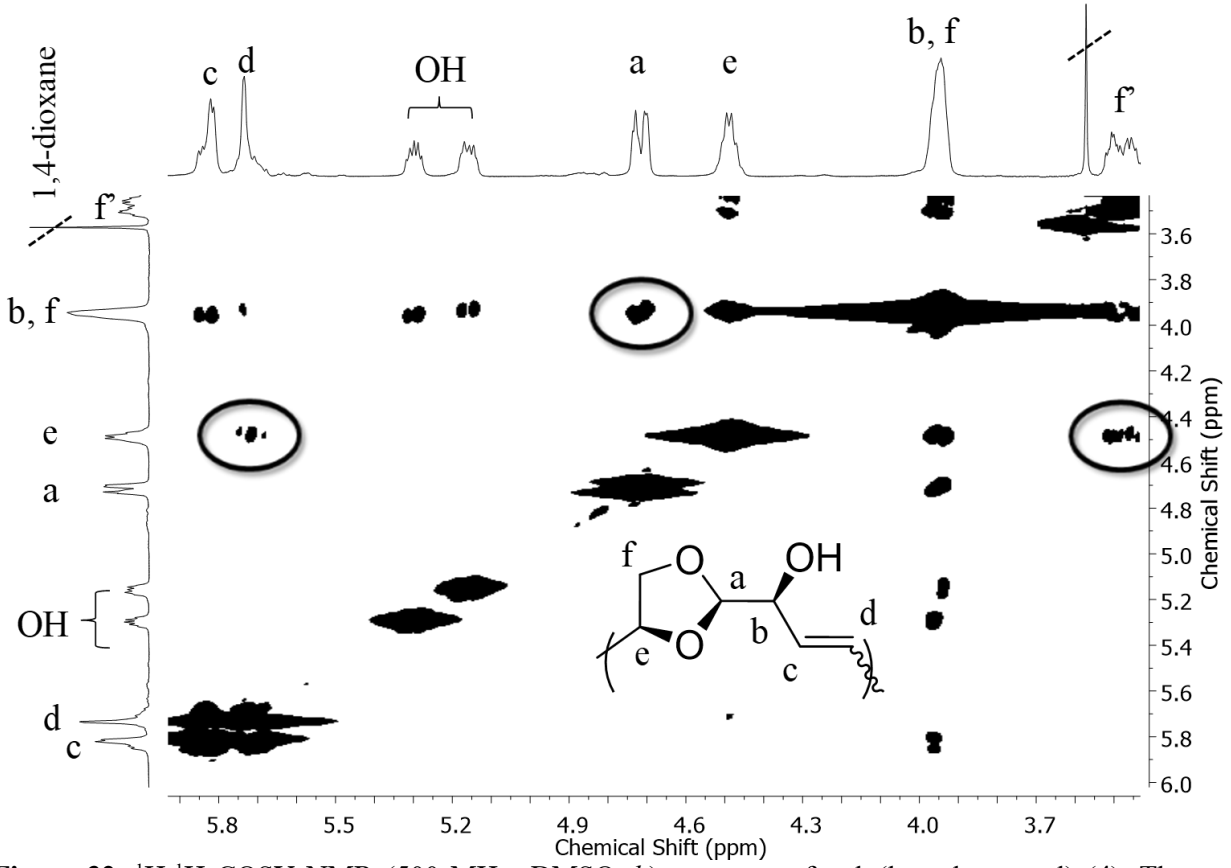

Figure 32. ^{1}H-^{1}H COSY NMR (500 MHz; DMSO-d_6) spectrum of poly(levoglucosenol) (**4**). The two protons appearing together have a distinct correlation with H_a indicates the CH protons (according to ^{1}H-^{13}C HSQC) is H_b and the other highlighted correlation with $H_{f'}$ indicates H_e.

3.2.4.1 Analysis of the isomeric structures

The double bond of the monomer **2** is an asymmetric double bond. This can cause the addition of each monomer in different orientations to the growing polymeric chain, leading to the formation of sequence isomeric structures. Additionally, there is also the possibility of the formation of a *cis-trans* double bond in the main chain. To have more insight of the *cis-trans* isomerism, the **4** was hydrogenated with H_2/Pd-C producing saturated polyacetal **5 (**Scheme 12**)**.

Near quantitative conversion was achieved with seven days of the reduction process, as indicated by the ^{1}H NMR spectrum (Figure 33).

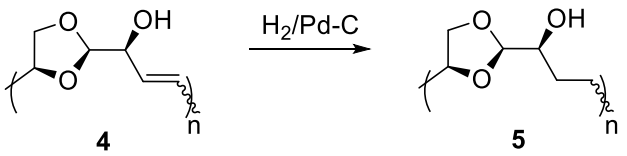

Scheme 12. Hydrogenation of poly(levoglucosenol) (**4**) producing **5**.

The polyacetal **5**, still showed four peaks for the acetal carbon (C_a) in the ^{13}C NMR spectrum (Figure 34), similar to the ^{13}C NMR spectrum (Figure 28) of the **4**. Additionally, the hydroxyl peaks of polyacetal **5** (complete structural characterization of the polyacetal **5** is given in section 5.3.5.1) still appeared as two distinct peaks corresponding to half a proton each. This indicates that the hydrogenation of the olefin moiety did not affect isomeric structures and also of the absence of *cis-trans* isomeric structures. Therefore, we can conclude that either *cis* or *trans* olefinic structures were produced during the polymerization. The coupling constants of the olefinic protons (H_c, H_d) should reveal the configuration of the double bonds. However, the ^{1}H NMR of **4** (Figure 27) is inconclusive for the determination of coupling constants and thus ^{1}H-^{1}H DQF COSY NMR (double quantum filtered COSY) experiment was measured.

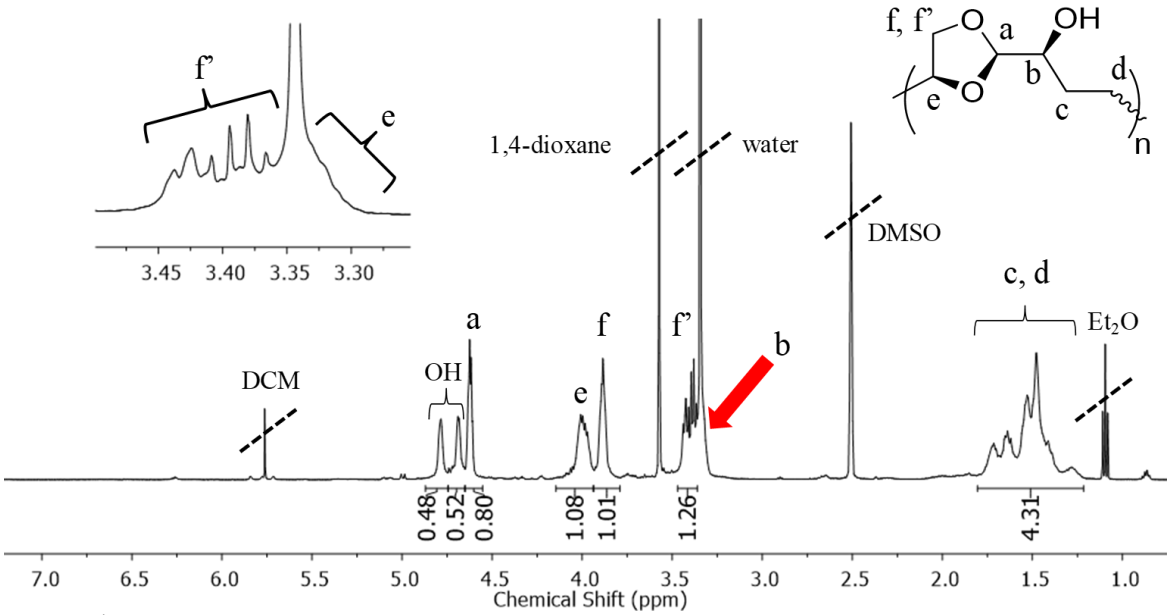

Figure 33. ^{1}H NMR (500 MHz, DMSO-d_6) spectrum of polyacetal **5**. The tiny peaks at ~5.75 ppm are of the remaining (non-hydrogenated) poly(levoglucosenol) (**4**).

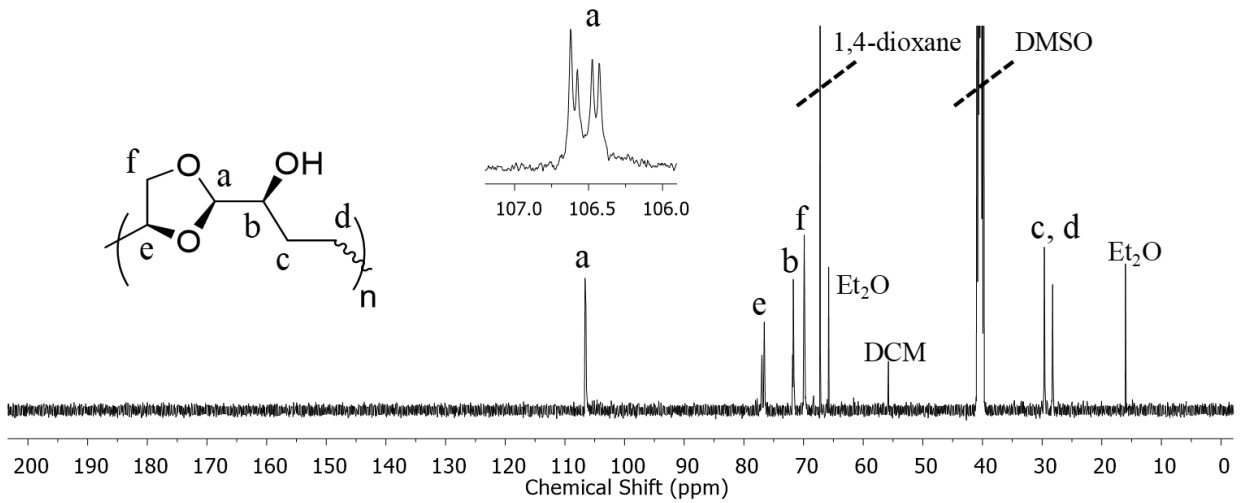

Figure 34. ^{13}C NMR (125 MHz, DMSO-d_6) spectrum of polyacetal **5**,

The further analysis of the polymer structure was carried out in collaboration with Prof. Dr. Heiko Möller.

The ^{1}H-^{1}H DQF COSY NMR experiment (Figure 35) of **4** was carried out in order to measure the coupling constant between the proton H_c and H_d, at the double bond. It is found to be a large coupling of 15.4 Hz (resolution: 0.5 Hz/data point along the x-axis (direct dimension)). The large coupling is indicative of *trans* configuration supported by data from similar structures reported in the literature,[74] thus, only the *trans* isomer is formed during polymerization. Consequently, the isomeric peaks seen in the NMR spectrum of the **4** are arising only due to the sequence of monomer addition in various orientations to the growing polymer chain.

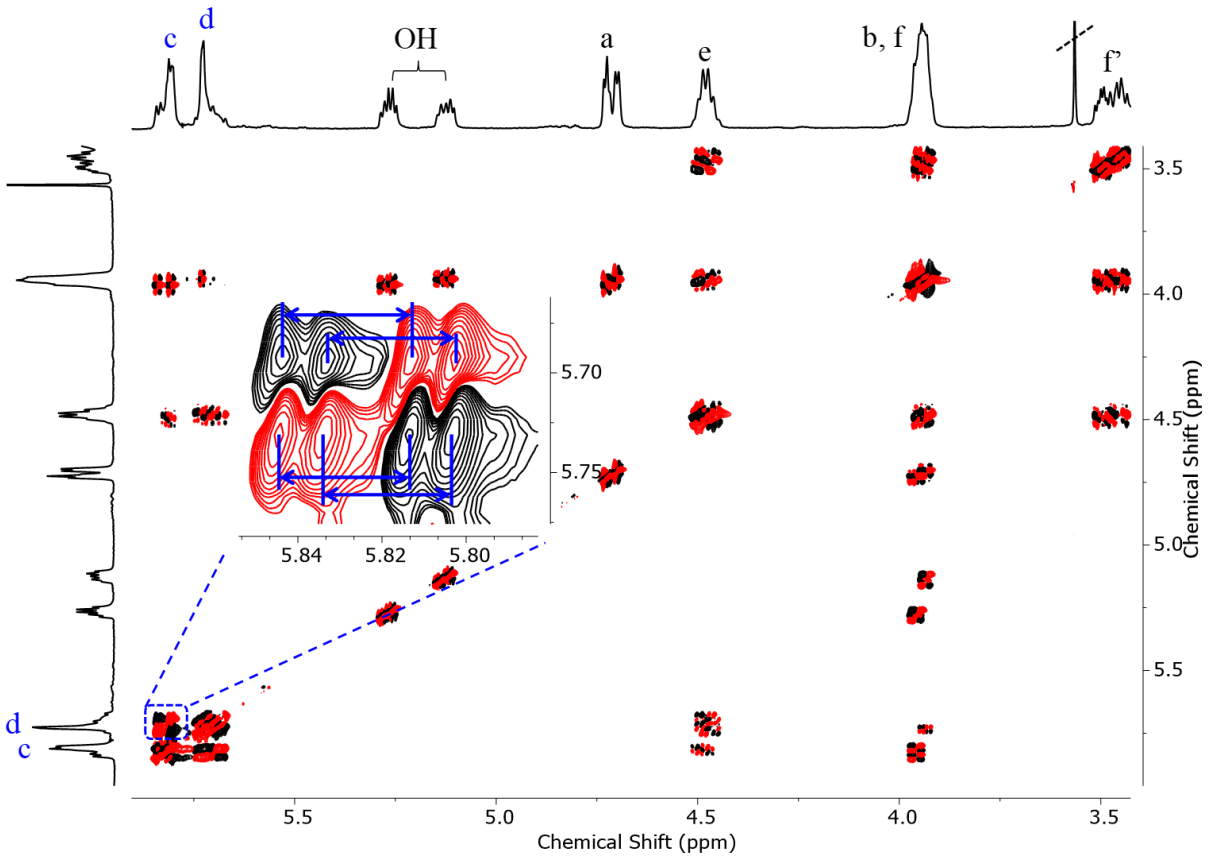

Figure 35. ^{1}H-^{1}H DQF COSY NMR (DMSO-d_6) spectrum of poly(levoglucosenol) **4**. The coupling constant corresponding to the olefinic protons is 15.4 Hz, shown in blue. Only this large couplings of the same value are found, suggesting the presence of only *trans* olefinic configuration in the polymer chain.

Interestingly, the ^{1}H NMR spectrum (Figure 37) of **4** in pyridine resolved the olefinic protons into three categories (with intensity ratios of about 1:2:1), presumably, because of some sort of π-π stacking interaction. These three different olefinic signals are postulated to arise due to different sequences of the monomer (**2**) addition, namely, *head-head* (*HH*), *head-tail* (*HT*), *tail-tail* (*TT*) (Figure 36). The other form of *head-tail* diad would be *tail-head* (*TH*) but both the *head-tail* and *tail-head* are chemically identical, according to symmetry analysis.

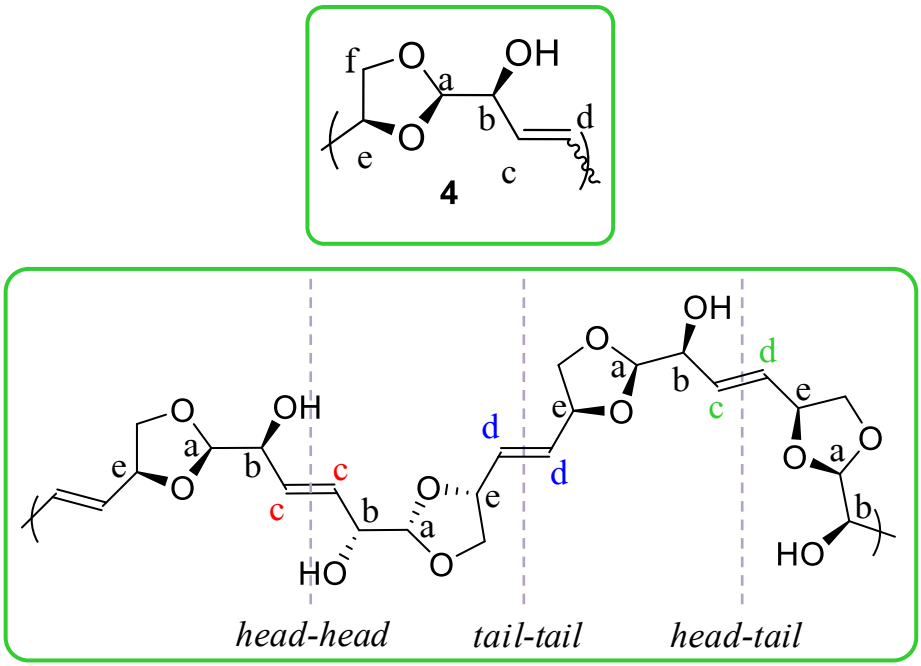

Figure 36. Depiction of *head-head*, *tail-tail*, *head-tail* isomeric structures via the double bond of poly(levoglucosenol) (**4**).

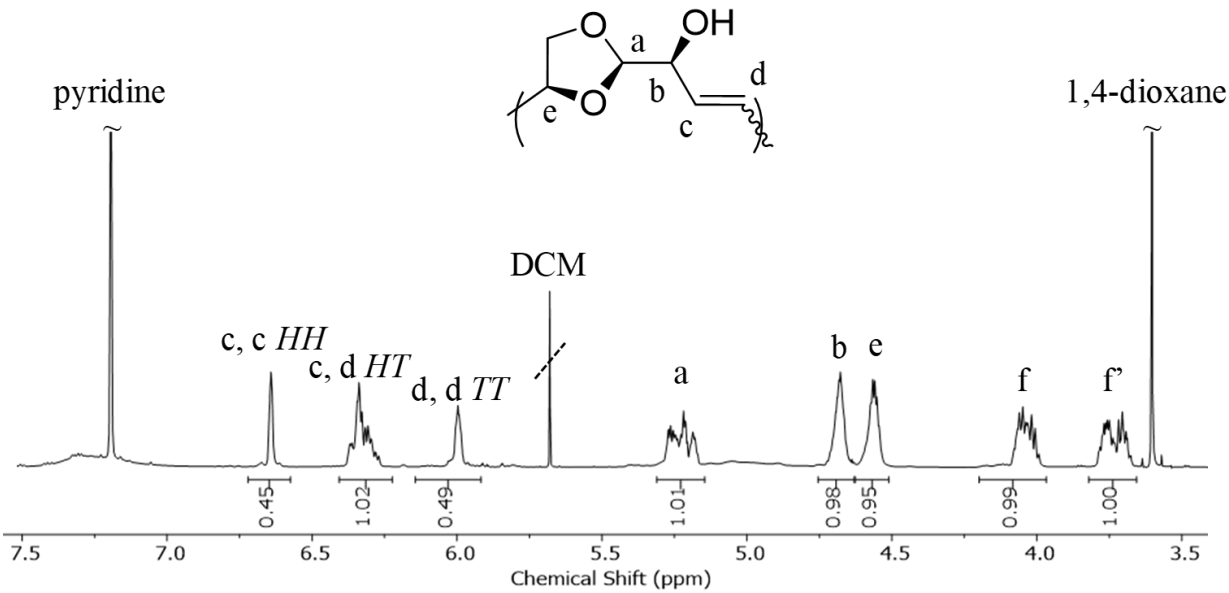

Figure 37. ^{1}H NMR (600 MHz, pyridine-d_5) spectrum of poly(levoglucosenol) (**4**). It resolved the olefinic protons into three categories, *HH/HT/TT*, and is based on ^{1}H-^{1}H TOCSY spectral analysis described later in this section.

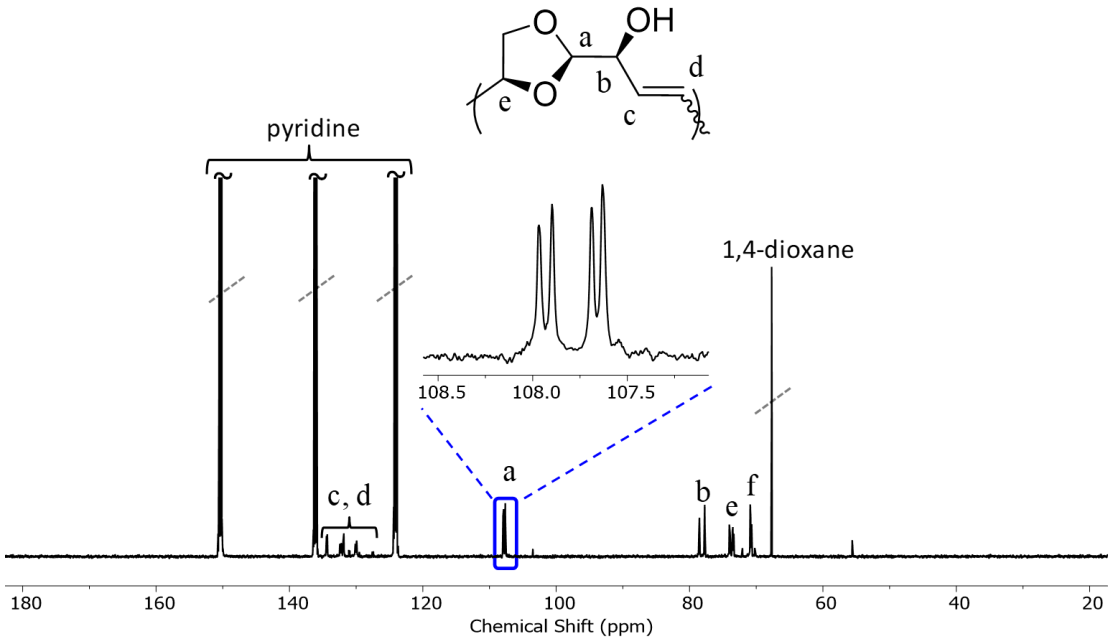

Figure 38. ^{13}C NMR (150 MHz, pyridine-d_5) spectrum of poly(levoglucosenol) (**4**).

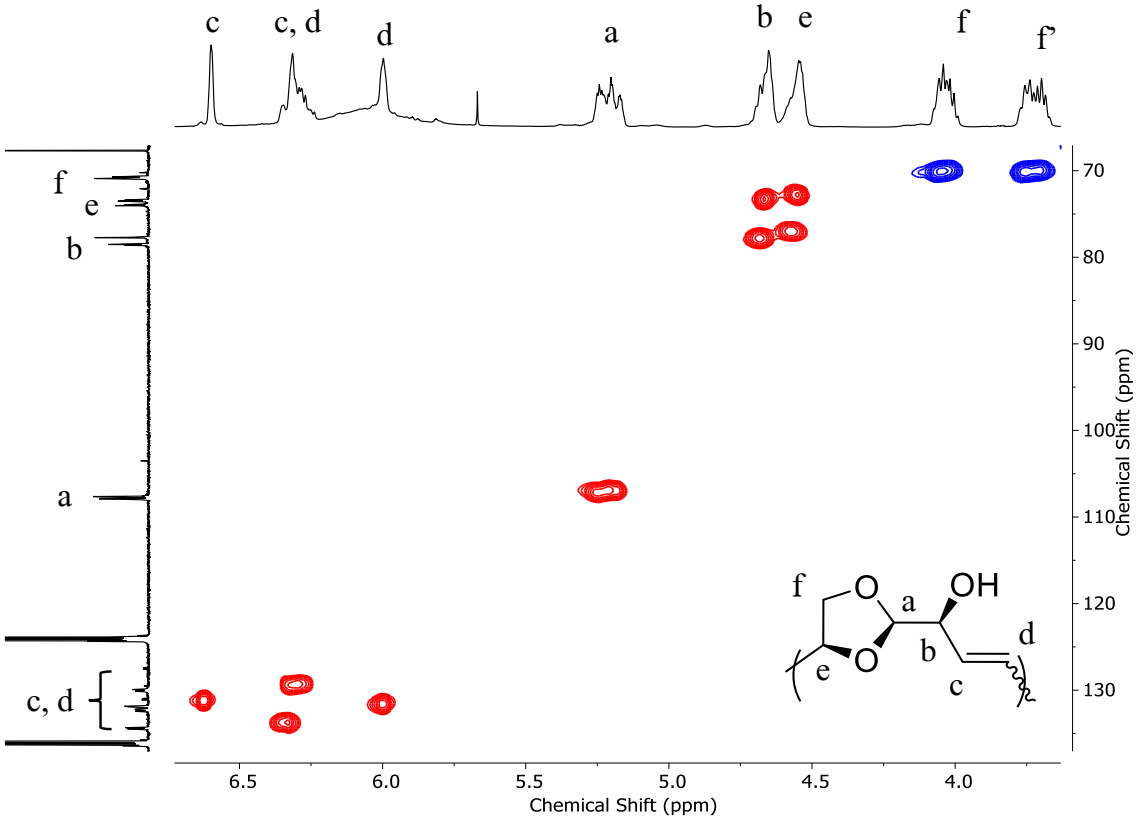

Figure 39. ^{1}H-^{13}C HSQC NMR (600, 150 MHz, pyridine-d_5) spectrum of poly(levoglucosenol) (**4**). (Red: positive contours, CH, CH_3; Blue: negative contours, CH_2). Distinguished CH_2 and CH protons, assigned C_a and H_a, and olefinic protons resolved into four categories.

The ^{13}C NMR spectrum (Figure 38) of **4** in pyridine, however, still showed four signals with similar intensities corresponding to C_a, similar to the ^{13}C NMR spectrum of the same in DMSO (Figure 28), indicating four possible environments around C_a. Additionally, the ^{1}H-^{13}C HSQC spectrum in pyridine (Figure 39) showed the presence of four kinds of olefinic protons. Similar to the earlier case, the ^{1}H-^{13}C HSQC NMR analysis distinguished the CH_2 protons (shown in blue); and H_a through correlation with the very characteristic acetal carbon ~107 ppm. The initial measurements, ^{1}H, ^{13}C, and ^{1}H-^{13}C HSQC NMR analyses could only designate H_a, $H_{f,f'}$ and C_a. For further assignment of the protons, especially for the olefinic protons, ^{1}H-^{1}H TOCSY NMR analysis is required. All the proton and carbon signals assignments are achieved by analyzing ^{1}H-^{13}C HSQC and ^{1}H-^{1}H TOCSY experiments.

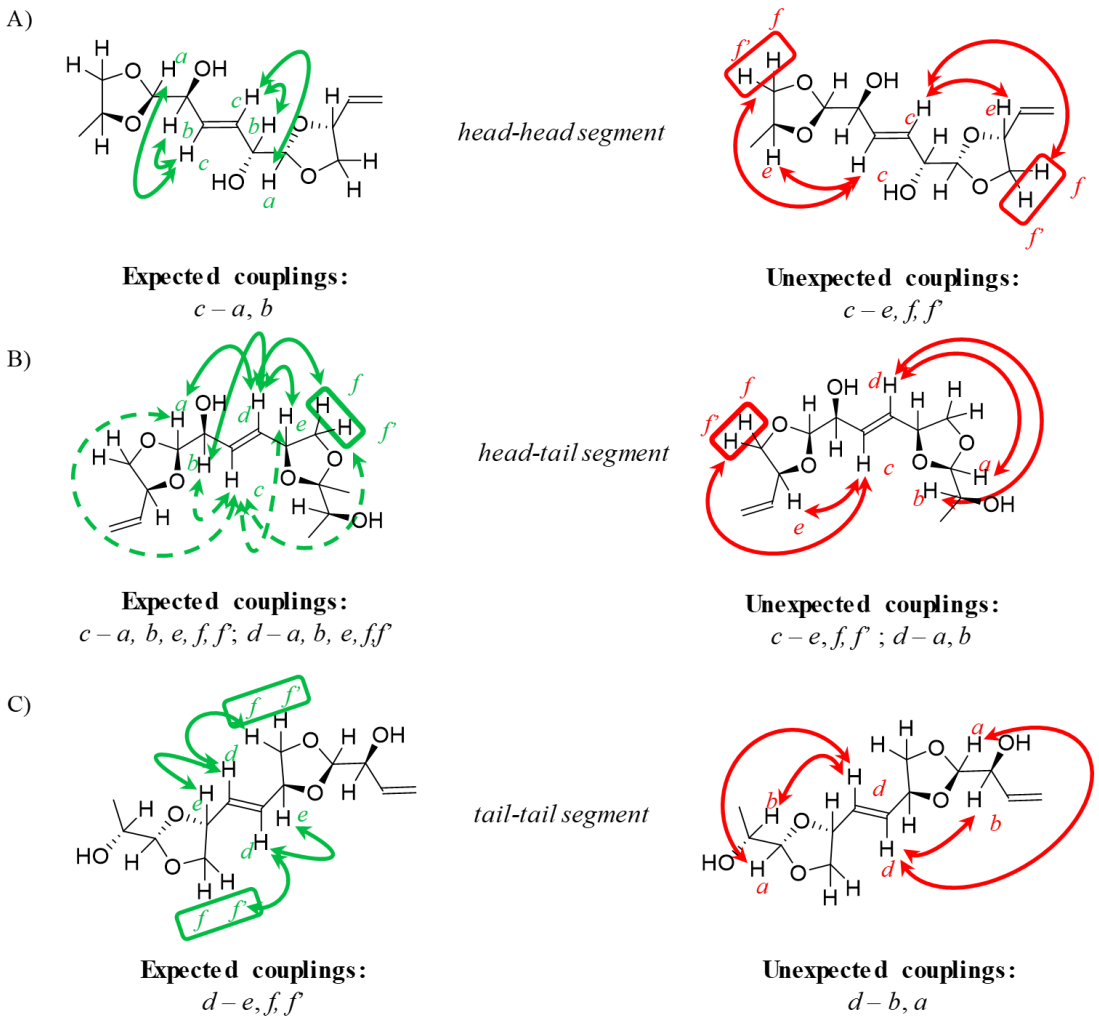

Figure 40. Pictorial representation of the expected and unexpected ^{1}H-^{1}H TOCSY correlations for poly(levoglucosenol) (**4**).

In a typical ^{1}H-^{1}H TOCSY experiment, correlations are expected between nuclei of the same spin system. This means that cross-peaks appear between nuclei, that are connected by a network of not-too-small (i.e., ≥2-3 Hz,) couplings. In the case of **4**, ether linkages contribute to small couplings. Therefore, ^{1}H-^{1}H TOCSY analysis should distinguish *head-head*, *head-tail*, *tail-tail* diads, in principle. The expected couplings for *head-head* diads are H_c with $H_{b,}$ and H_a. The expected couplings for *head-tail* diads are $H_{c,d}$ with H_a, H_b, H_e, and $H_{f,f'}$. Similarly, the expected couplings for *tail-tail* diads are H_d with H_e, and $H_{f,f'}$. The expected couplings for *head-head*, *head-tail,* and *tail-tail* diads are categorized as *A, B,* and *C* (Figure 40).

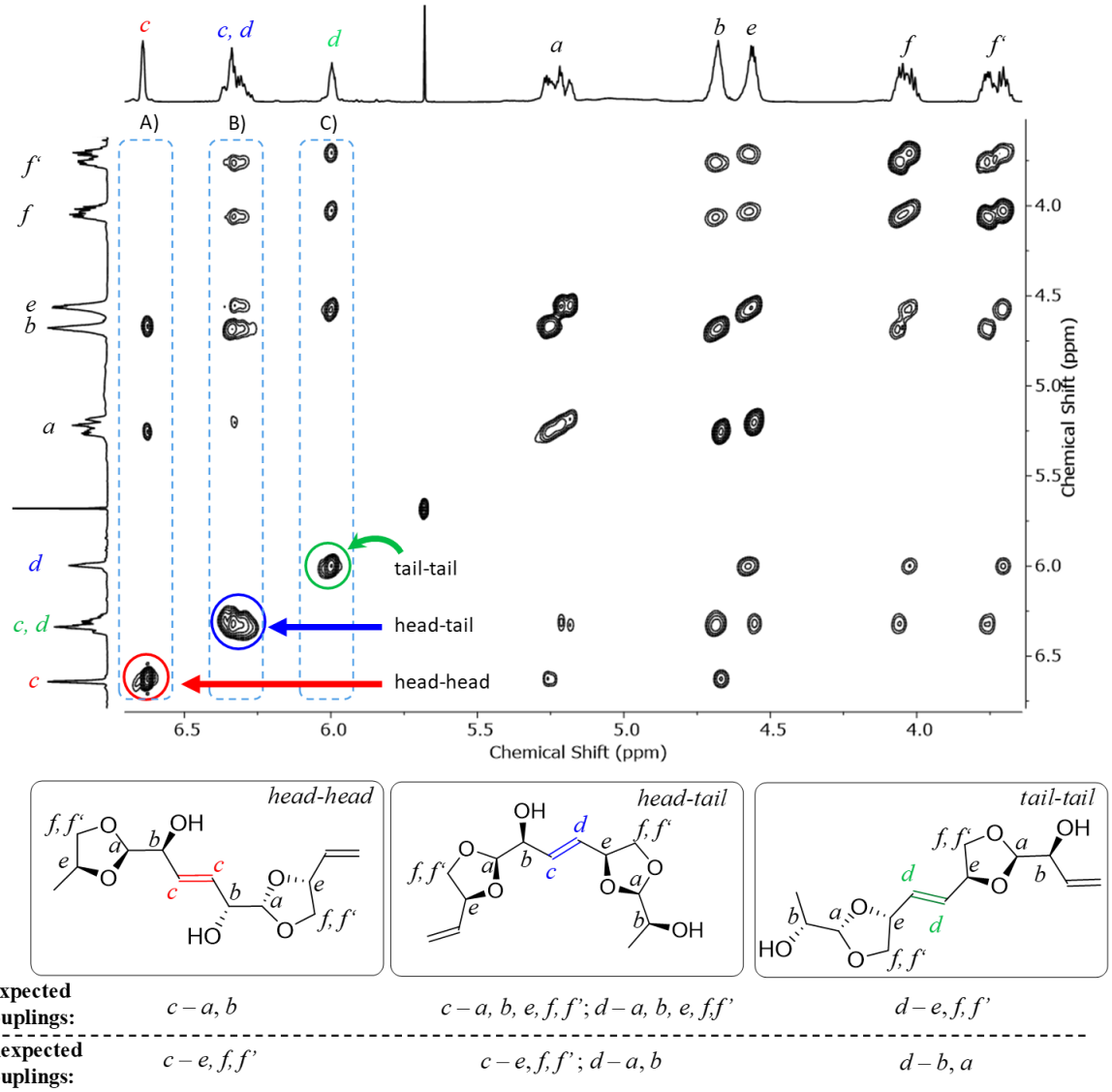

Figure 41. ^{1}H-^{1}H TOCSY (600 MHz, pyridine-d_5) spectrum of poly(levoglucosenol) (**4**). It shows the expected couplings for the possible diad structures, and thus concluded the existence of postulated *head-head, head-tail, tail-tail* structure in the polymer chain.

The ^{1}H-^{1}H TOCSY experiment (Figure 41), indeed, shows the expected couplings. Therefore, we can conclude that the postulated *head-head, head-tail,* and *tail-tail* diads structures are indeed present in the polymer chain. Still, the four signals corresponding to C_a in ^{13}C NMR (Figure 38) needed further investigation. The different environments of C_a give rise to different signals corresponding to C_a. Therefore, triad units are considered (Figure 42). It is important to note that we are avoiding the denotations of chiral centers, as it does not contribute to additional isomerism that is not considered in the *HH*, *HT*, and *TT* notation.

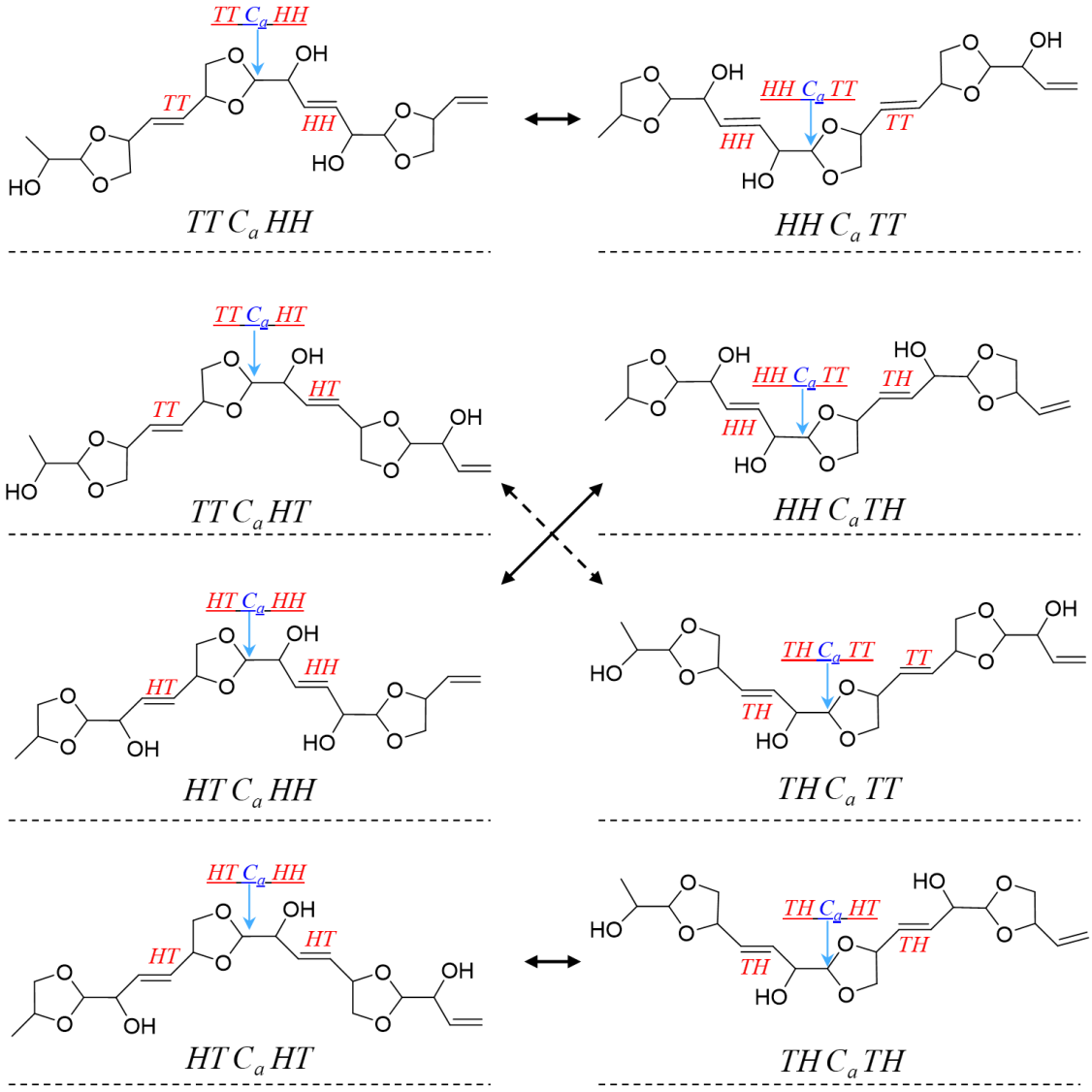

Figure 42. All possible triads of the poly(levoglucosenol) (**4**) in the polymer chain. It also indicates the environment of C_a. Four C_a are possible in total and can be named as *HH–*C_a*–TT*, *HH–*C_a*–TH*, *TT–*C_a*–HT*, *TH–*C_a*–TH*. Each of these is repeating the same number of times. The arrows represent the symmetrically similar counterparts.

We can divide C_a into four categories, namely *HH–C*$_a$*–TT*, *HH–C*$_a$*–TH*, *TT–C*$_a$*–HT*, *TH–C*$_a$*–TH*. Thus, this explains the four singlets corresponding to C_a in the ^{13}C NMR spectrum. Additionally, *HH–C*$_a$*–TT, HH–C*$_a$*–TH*, *TT–C*$_a$*–HT*, and *TH–C*$_a$*–TH* combinations are found in 1:1:1:1 ratio. Interestingly, the C_a peaks of **4** appear as four singlets with similar intensities in ^{13}C NMR of in both pyridine and DMSO (Figure 43).

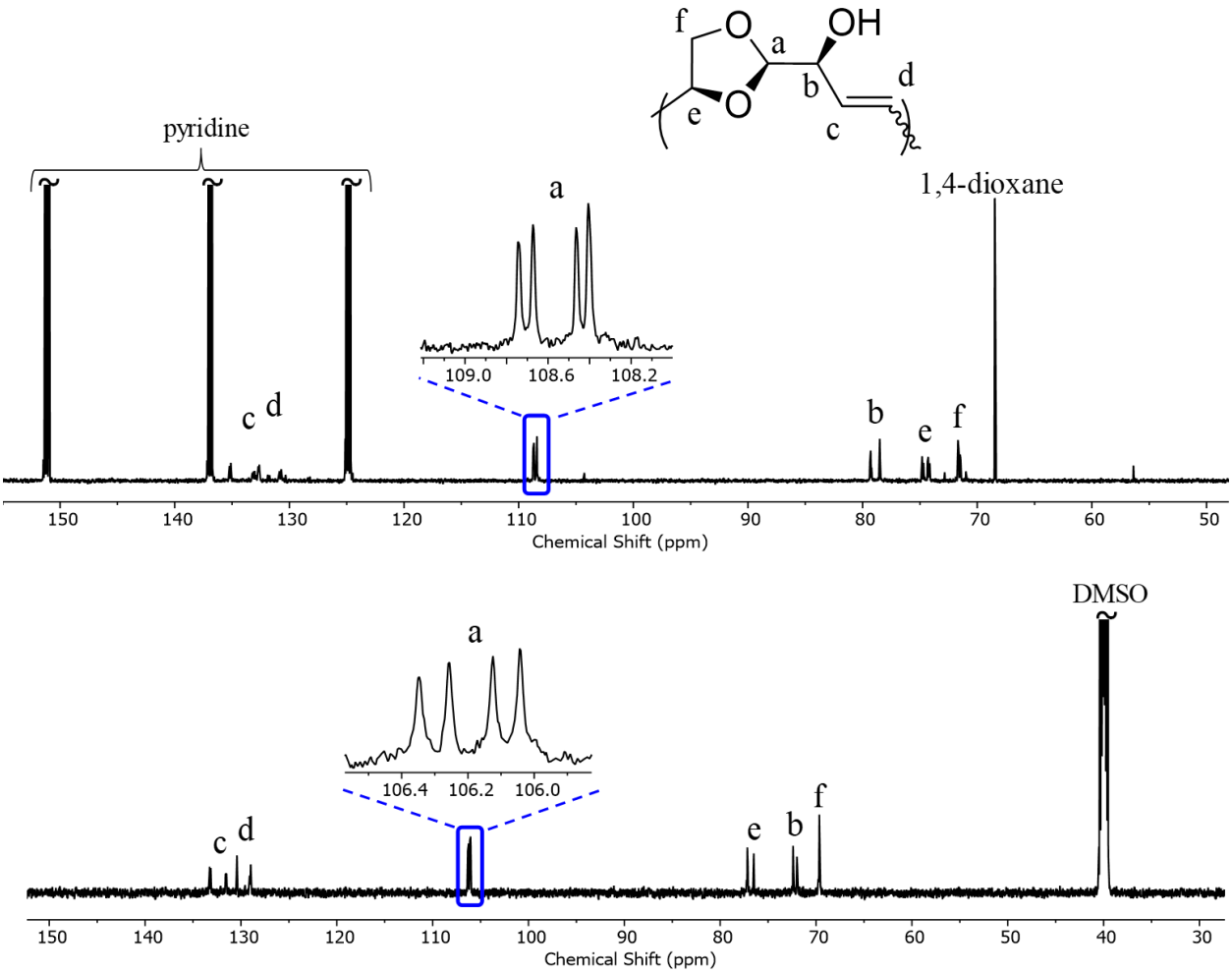

Figure 43. ^{13}C NMR (150 MHz; pyridine-d_5 (top), DMSO-d_6 (bottom)) of poly(levoglucosenol) (**4**).

In conclusion, we can explain the sequence isomerism in the polymer chain by sophisticated NMR analysis. There are *head-head* (*HH*), *tail-tail* (*TT*), *head-tail* (*HT*) sequence isomers in the polymer chain that gave rise to the various multiplets in the NMR.

3.2.5 Polymer properties

The poly(levoglucosenol) **4** is insoluble in THF, dimethyl carbonate, alcohols or water and soluble in 1,4-dioxane, pyridine, DMF, NMP, DMSO, and sulfolane. Additionally, it is also soluble in a mixture of methanol and DCM in various proportions. Among these solvents, 1,4-dioxane was chosen as solvent for polymerization.

Table 3. Various molar mass of poly(levoglucosenol) **4** and its glass transitions temperatures.

Run	$[\mathbf{2}]_0/[\mathbf{C6}]$	M_w^{app} [a] (kg/mol)	$Đ$ [b]	T_g [c] (°C)
1	66	29	1.8	100
2	100	37	2.0	100
3	200	47	2.2	92
4	1000	100	2.9	98

[a]Apparent weight-average molar mass, determined by SEC. [b]Dispersity index, determined by SEC. [c]Glass transition temperature, determined by DSC.

According to thermogravimetric analysis (TGA), **4** is thermally stable up to ~220 °C (~5% weight loss) and having a glass transition temperature (T_g) of ~100 °C (determined by DSC) (Figure 44). A transparent polymer film (preparation method: 5.3.4.1.1) could be produced, therefore it might serve as a thermoplastic polymer and for the fabrication of transparent films (Figure 45). The high glass transition temperature could be due to the combined stiffening effect of the dioxolane ring and hydrogen-bonding interactions of the alcohol moieties.

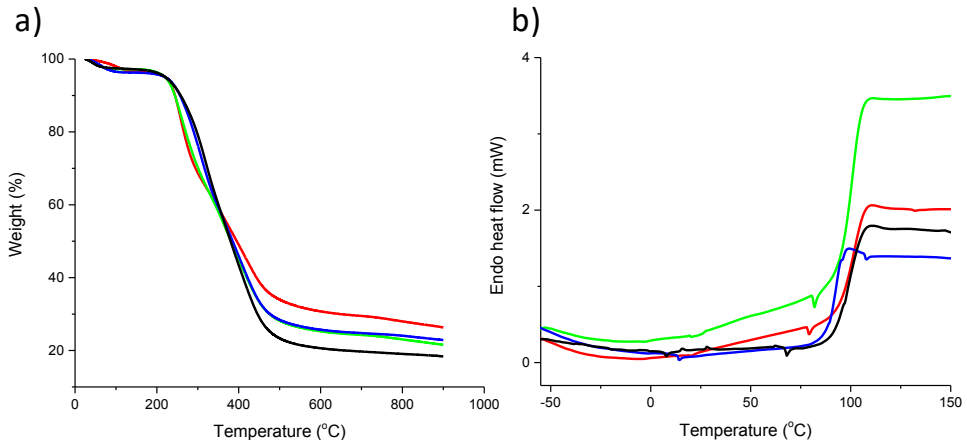

Figure 44. TGA (a) and DSC curves (4th heating cycle) (b) of poly(levoglucosenol) (**4**) of the sample in Table 3. Run 1 (red), run 2 (green), run 3 (blue), run 4 (black).

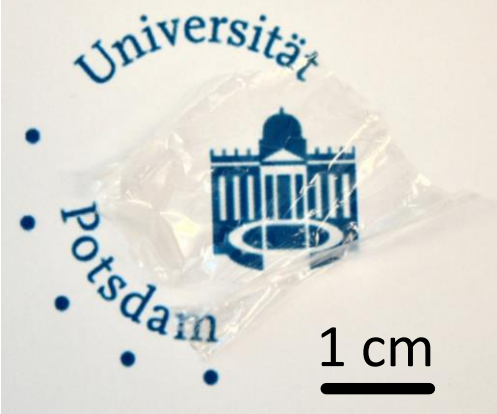

Figure 45. The photograph shows a transparent film produced from poly(levoglucosenol) (**4**) on top of the University of Potsdam logo.

3.2.6 Degradation of poly(levoglucosenol)

Acetal compounds are known to be sensitive towards nucleophiles in the presence of acid. Since the poly(levoglucosenol) **4** is a polyacetal, it is expected to degrade in an acidic environment. To prove that, **4** was dissolved in moist 1,4-dioxane followed by treatment with *p*-toluenesulfonic acid. The reaction was continued at room temperature for 40 days and then subjected to SEC analysis. SEC analysis showed the disappearance of the polymer peak and appearance of a new peak at lower elution volume (Figure 46) confirms the degradation of **4**.

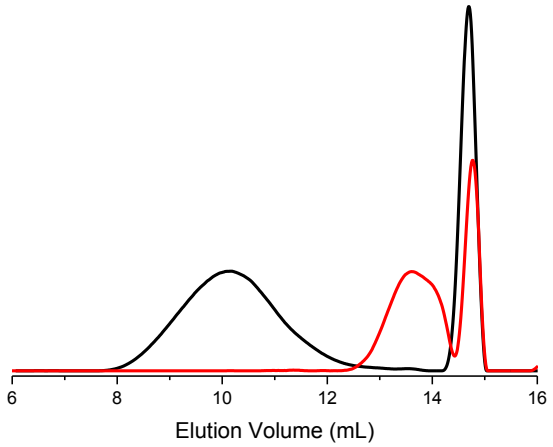

Figure 46. SEC traces (eluent: NMP, detector: RI) of poly(levoglucosenol) (**4**) before (black) and after (red) treatment with p-toluenesulfonic acid/water for 40 days. The peak at the elution volume of ~14.5 mL refers to the internal reference (toluene).

The degradation is expected to happen via the acid-sensitive acetal group. It is thought that the acetal group of **4** gets activated by the protons followed by nucleophilic attack by the water molecules resulting in corresponding diol and aldehyde (**Error! Reference source not found.**).

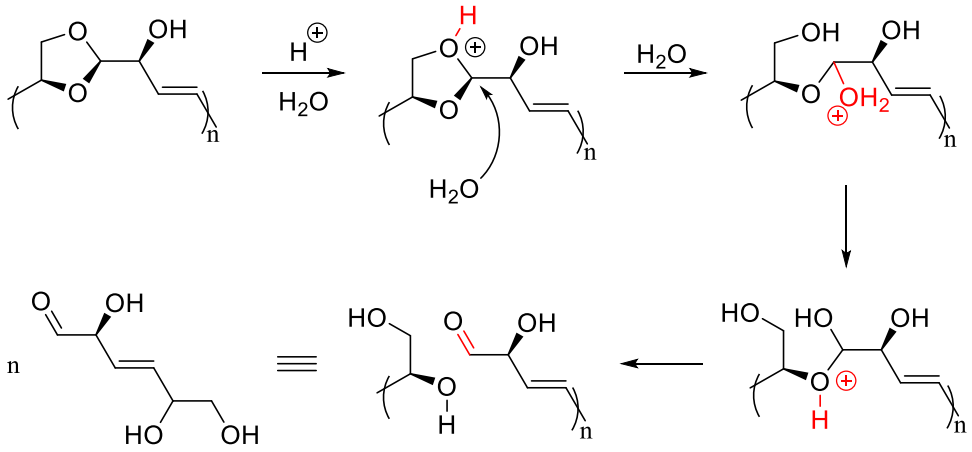

Scheme 13. A plausible mechanism of degradation of poly(levoglucosenol) (**4**) (only *head-tail* sequence isomer is shown here) in an acidic aqueous environment.

3.2.7 Conclusion

Levoglucosenol, a carbohydrate derivative was polymerized via ring-opening metathesis polymerization by a derivative of Grubbs' 2nd generation catalyst. The ROMP of levoglucosenol is slower at a higher temperature and faster at a relatively lower temperature. The polymerization lacks living nature and has little control. This is possibly due to catalyst deactivation and was indicated by the blackening of the reaction mixture. The poly(levoglucosenol) could be obtained with apparent weight-average molar mass up to 150 kg/mol and appeared as colorless, whereas polymers with lower molar mass had brownish color due to higher catalyst contamination.

Structural analysis of the polymer was carried out by NMR, ESI-MS analyses. The NMR analysis revealed most of the information, such as the presence of a different sequence of the repeating unit in the polymer chain. The levoglucosenol possesses an asymmetric double bond that leads to various sequences of isomers. In total, there were three sequence isomers, *head-to-head*

(HH), *head-to-tail (HT)*, and *tail-to-tail (TT)*. A detailed NMR study showed the presence of all three structures in about 1:2:1 ratio. Moreover, signals corresponding to acetal carbon in ^{13}C NMR are different due to different environments of the same, that is, signals arising due to acetal carbon in *HH, HT,* and *TT* segment are non-identical. These segments are connected by double bonds, which can form two isomers, in principle. Hydrogenation of these double bonds does not influence the signal pattern corresponding to the acetal carbon, and the isomeric structures. This indicated the absence of an isomeric mixture of double bonds. The ^{1}H-^{1}H DQF COSY analysis confirmed the polymer to contain *trans* double bonds.

The poly(levoglucosenol) is soluble in 1,4-dioxane, DMSO, DMF, sulfolane, as well as in a various proportioned mixture of methanol and DCM. The polymer, however, is insoluble in DCM and methanol individually as well as in chloroform, THF, diethyl ether, and water. The thermogravimetric analysis revealed that the poly(levoglucosenol) is thermally stable up to ~220 °C and differential scanning calorimetry revealed it is amorphous with a glass transition temperature of ~100 °C. A transparent film could be produced from the polymer that may find use as an alternative to common plastic such as polystyrene. Finally, the polymer degraded under an acidic environment in the presence of water.

3.3 Polymerization of levoglucosenyl methyl ether

The first report of cationic ring-opening polymerization (CROP) of anhydrosugar catalyzed by acid dates back to 1966.[75] The report mentioned the use of Lewis acid for the polymerization of glucopyranose anhydrosugar derivative. So far, the commonly known polymerization of such bicyclic anhydrosugar derivatives generally requires an elaborate and tedious methodology for the preparation of a suitable monomer. Additionally, until the date, the monomers reported for such polymerization contains only hydroxyl group-based (masked with methyl, benzyl, and benzoyl, etc. groups) functionality. This is probably due to additional complications in introducing further functionalities. Consequently, these polymers are limited to further functionalization. The anhydrosugars enriched with unmasked hydroxyl groups when subjected to polymerization resulted in branched polymers.[54] Hence, the protection of the hydroxyl group is an essential part of polymerization.

3.3.1 Reaction monitoring

Monitoring of conversion

The conversion of the polymerization was determined by ^{1}H NMR spectroscopy from the crude reaction mixture in DMSO-d_6. Crude samples of the reaction mixtures were taken at different time intervals, quenched excess triethylamine, and subjected to ^{1}H NMR measurements. The olefinic protons of the monomer and of the polymer were used for the determination of monomer conversion.

Monitoring of molar mass

Reaction samples at different time intervals are quenched with excess trimethylamine and precipitated into methanol to remove the salt of boron trifluoride and trimethylamine. These samples are subjected to SEC (THF) measurements for molar mass determination.

3.3.2 Cationic ring-opening polymerization of levoglucosenyl methyl ether

Levoglucosenyl methyl ether, **3** is an unsaturated bicyclic acetal or 1,6-anhydrosugar. Its synthesis is also simpler than the synthesis of similar molecules in literature.[56,61,76] The two functionalities present in **3** are independent of each other, which means that the reaction of the acetal functionality will not alter the olefin moiety in general. This makes it especially useful for its polymerization in different pathways as well as versatile for polymer functionalization. Similar to levoglucosenol, compound **3** undergoes ROMP (data not shown) via the olefin functionality, however, it also possesses the potential for acid-catalyzed CROP via the acetal functionality, to yield polymer **6.**

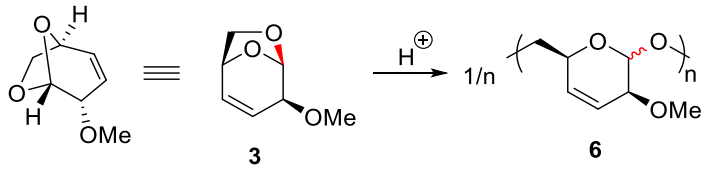

3 **6**

Scheme 14. Cationic ring-opening polymerization (CROP) of compound **3**.

The initial attempts to polymerize **3** involved triflic acid (CF_3SO_3H, TfOH) and boron trifluoride etherate ($BF_3{\cdot}OEt_2$). The polymerizations were carried out in dichloromethane (DCM) solutions, $[\mathbf{3}]_o$ = 4-2 M at room temperature or 0 °C for 24 h. Each reaction was quenched with trimethylamine. The results are summarized (Table 4).

Table 4. CROP of **3** in DCM solution with triflic acid or boron trifluoride etherate as initiator/catalyst (acid) for 24 h to yield polymer **6**.

Run	Acid	$[\mathbf{3}]_o$/[acid]	$[\mathbf{3}]_o$ (M)	T [a] (°C)	x_p [b] (%)	M_n^{app} [c] (kg/mol)	$Đ$ [d]
1	TfOH	200:1	4	25	92	15.1	1.4
2	TfOH	200:1	4	0	92	18.6	1.4
3	$BF_3{\cdot}OEt_2$	200:1	2	25	2	-[e]	-[e]
4	$BF_3{\cdot}OEt_2$	5:1	2	0	84	11.8	1.5

[a]Reaction temperature. [b]Monomer conversion, determined by ^{1}H NMR spectroscopy. [c]Apparent number-average molar mass, determined by SEC with polystyrene calibration. [d]Dispersity index, determined by SEC. [e]Not determined.

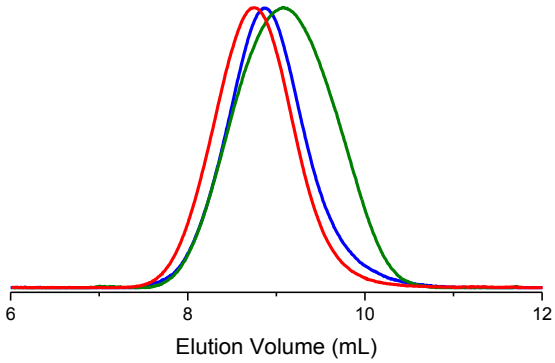

Figure 47. SEC-RI traces of polymer **6** of Table 3. Blue: run 1, red: run 2, green: run 4.

TfOH, in comparison to $BF_3{\cdot}OEt_2$, appeared to be a very efficient initiator for CROP of **3** under the chosen reaction condition. In the case of TfOH-initiated polymerization, the monomer conversion reached >90% and polymer **6** was obtained with relatively higher number-average molar masses (M_n^{app}) of 18.6 kg/ mol, and disparities $Đ$ ~1.4 (by SEC analysis, Figure 47) at a lower temperature. TfOH catalyzed polymerization also produced a relatively narrow distribution of polymer over $BF_3{\cdot}OEt_2$. It is important to mention here that levoglucosenol (**2**) did not produce any polymer under similar conditions (as in Table 4). It could possibly be due to side reaction(s) under the acidic condition of the allylic alcohol moiety.

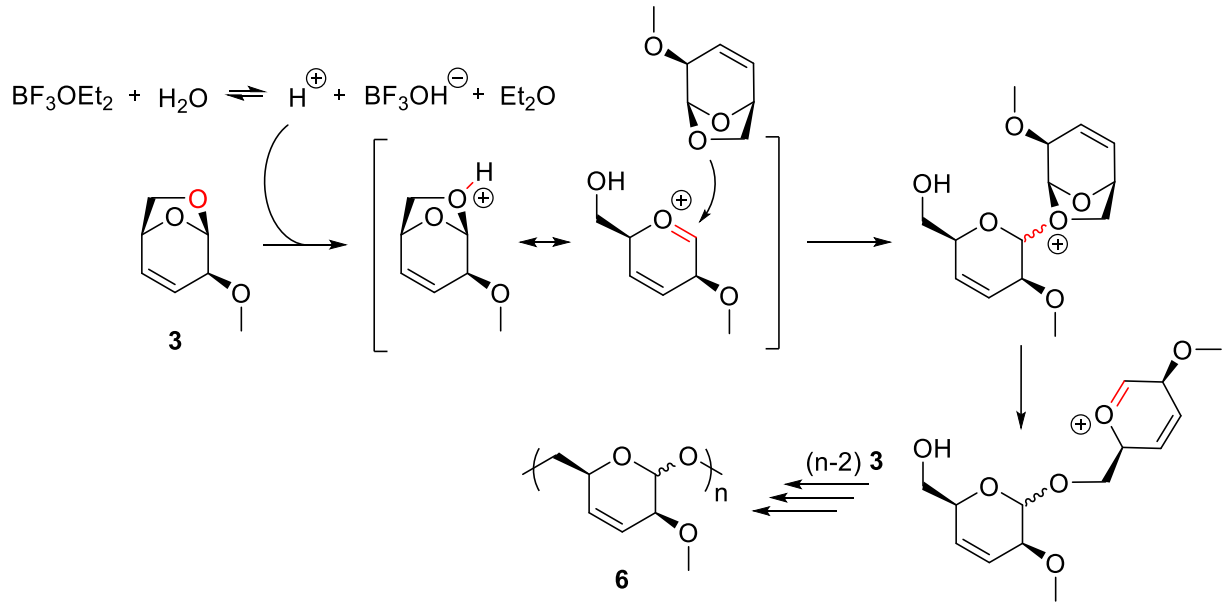

Scheme 15. Equilibrium reaction of $BF_3{\cdot}OEt_2$ with water to release protons and proposed pathways of proton-initiated cationic polymerization of **3**.

The requirement of $BF_3 \cdot OEt_2$ at higher catalyst concentrations can be explained by the fact that a trace amount of water is crucial for the initiation of polymerization (Scheme 15). $BF_3 \cdot OEt_2$ first reacts with water to form protonic species, which initiates the polymerization. This can be supported by the previous study of trioxane polymerization where $BF_3 \cdot OEt_2$ failed to initiate polymerization under rigorous dry conditions.[77] Additionally, the achieved molar mass of the polymer is not linearly related to the number of catalysts used in the polymerization and no polymerization occurred at low catalyst concentration (run 3, Table 4) as well. It is likely due to the equilibrium nature of the reaction between water and $BF_3 \cdot OEt_2$ where a higher amount of $BF_3 \cdot OEt_2$ is required in order to shift the equilibrium (Scheme 15) to the right-hand side for the production of the proton that can initiate polymerization.

The polymerization of **3** is believed to proceed through an oxonium ion by the active chain end mechanism (Scheme 15). The cyclic-acetal ring is activated by acid catalyst leading to the opening of the ring and stabilization of the cation via the formation of oxonium ion. Successive addition of another monomer via higher nucleophilic $–OCH_2–$ than –OCH– leads to the formation of polymer **6**, thermodynamically favoring the six-membered ring structure.

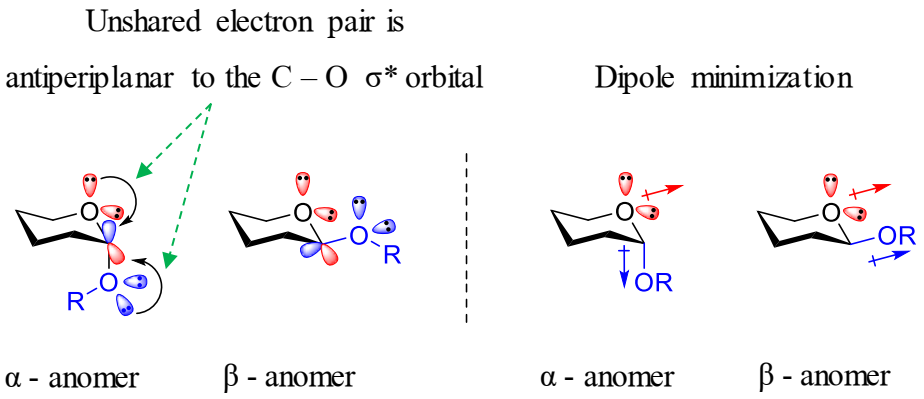

Figure 48. Pictorial representation of anomeric effects in an exemplary pyranose ring form showing stabilization of α-isomer over β-isomer.

The attack on the anomeric center by another monomer can happen from both the α side, assisted by the anomeric effect and β side, assisted by the steric demand of the incoming group. In a non-polar solvent, the anomeric effect is predominant (Figure 48) favoring α substitution. In a polar solvent, such as water, the α substitution will make the system sterically unfavorable via syn-

axial (Figure 49) interaction as the solvated substitution will have a bigger hydrodynamic radius, favoring β substitution.

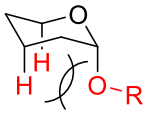

Syn-axial interaction

Figure 49. Pictorial representation of syn-axial interaction in an exemplary pyranose form.

In the particular case of polymerization of **3**, the use of DCM as a solvent may favor the α substitution, but cannot be confirmed without the knowledge of complete structural analysis.

3.3.3 Optimization of reaction condition and kinetics

Although TfOH is proven promising for the polymerization of **3**, its hygroscopic and corrosive nature makes it difficult to handle and therefore, $BF_3{\cdot}OEt_2$ was chosen for further investigations. The $BF_3{\cdot}OEt_2$ catalyzed polymerizations of **3** were conducted at different monomer-to-catalyst ratios (100:1 to 100:3), monomer concentrations (1-4 M), reaction temperatures (–50 to 25 °C) and times (1.5 to 48 h). These results are summarized (Table 5).

Table 5. $BF_3{\cdot}OEt_2$ catalyzed the polymerization of **3** at –50 °C to –20 °C and at different monomer-to-catalyst ratios, monomer concentrations, and reaction times.

Run	$[\mathbf{3}]_o$/ $[BF_3{\cdot}OEt_2]$	$[\mathbf{3}]_o$ (M)	T^a (°C)	t^b (h)	Appearance	x_p [c] (%)	M_n^{app} [d] (kg/mol)	$Đ$ [e]
1	100:10	1	–50	48	Liquid	n.d.[f]	n.d.[f]	n.d.[f]
2	100:10	2	–50	48	Liquid	n.d.[f]	n.d.[f]	n.d.[f]
3	100:10	3	–50	48	Viscous Liquid	3	n.d.[f]	n.d.[f]
4	100:10	4	–50	48	Liquid → Solid[g]	9	18.6	1.33
5	100:10	1	–20	48	Liquid	19	n.d.[f]	n.d.[f]
6	100:10	2	–20	48	Liquid	57	23.2	1.25
7	100:10	3	–20	48	Viscous Liquid	70	23.9	1.29
8	100:10	4	–20	24	Liquid → Solid[g]	74	25.3	1.31

[a]Reaction temperature. [b]Reaction time. [c]Monomer conversion, determined by ^{1}H NMR spectroscopy. [d]Apparent number-average molar mass, determined by SEC with polystyrene calibration. [e]Dispersity index, determined by SEC. [f]Not determined. [g]Solid (frozen), dissolved upon addition of solvent.

A high catalyst loading (30 mol%) resulted in the highest monomer conversion (97%) and polymer molar mass (28.8 kg/mol) at –10 °C in DCM solution (run 8, Table 6). The polymer **6** produced under this condition, exhibited a monomodal molar mass distribution and dispersity of 1.4. The trend is to the production of polymers with higher conversions at higher initial monomer concentrations and at higher temperatures, but higher temperatures produced relatively lower molar masses polymers in comparison to polymerization at lower temperatures under similar conditions.

Table 6. $BF_3{\cdot}OEt_2$ catalyzed the polymerization of **3** with different monomer-to-catalyst ratios, monomer concentrations, temperatures, and reaction times.

Run	$[\mathbf{3}]_o$/ $[BF_3{\cdot}OEt_2]$	$[\mathbf{3}]_o$ (M)	T^a (°C)	t^b (h)	Appearance	x_p [c] (%)	M_n^{app} [d] (kg/mol)	$Đ$ [e]
1	100:10	2	–10	24	Liquid	68	18.6	1.27
2	100:10	3	–10	24	Viscous Liquid	77	19.3	1.33
3	100:10	4	–10	24	Viscous Liquid	87	21.2	1.43
4	100:20	1	–10	24	Liquid	61	13.0	1.47
5	100:20	2	–10	24	Liquid	85	17.6	1.44
6	100:20	3	–10	24	Viscous Liquid	92	20.3	1.44
7	100:20	4	–10	24	Viscous Liquid	94	21.7	1.52
8	100:30	4	–10	24	Viscous Liquid	97	28.8	1.43
9	100:10	2	0	24	Liquid	85	14.6	1.31
10	100:10	3	0	24	Viscous Liquid	90	17.2	1.36
11	100:10	4	0	24	Viscous Liquid	93	19.8	1.39
12	100:20	2	0	2	Liquid	84	11.8	1.46

[a]Reaction temperature. [b]Reaction time. [c]Monomer conversion, determined by ^{1}H NMR spectroscopy. [d]Apparent number-average molar mass, determined by SEC with polystyrene calibration. [e]Dispersity index, determined by SEC.

The polymerization under various conditions shows that polymerization at 0 °C at $[\mathbf{3}]_o = 4$ M gives high conversion and reasonably high molar mass. Therefore, this condition was used for the kinetic study with $[\mathbf{3}]_o/[BF_3{\cdot}OEt_2]$ = 100:10. The crude samples, quenched with excess triethylamine were used to determine the conversion of the polymerization. The olefinic protons

of both polymer and monomer were used to determine conversion by ^{1}H NMR (Figure 51). The crude samples were precipitated into methanol in order to remove the BF_3-triethylamine salt and then subjected to SEC (Figure 50) for apparent molar mass determination.

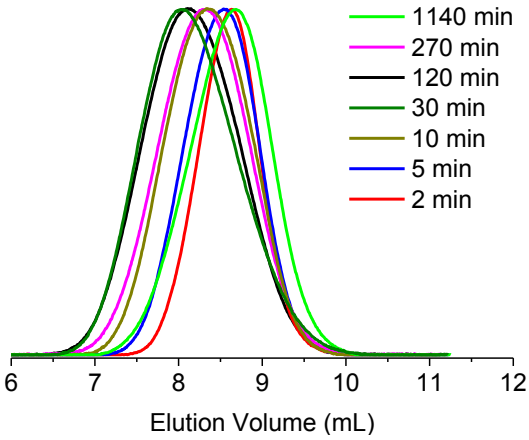

Figure 50. SEC-RI traces (eluent: THF) of crude polymerization mixtures ([**3**]$_0$/[**C6**] = 100, 28 °C) at different reaction times: 2-1440 min.

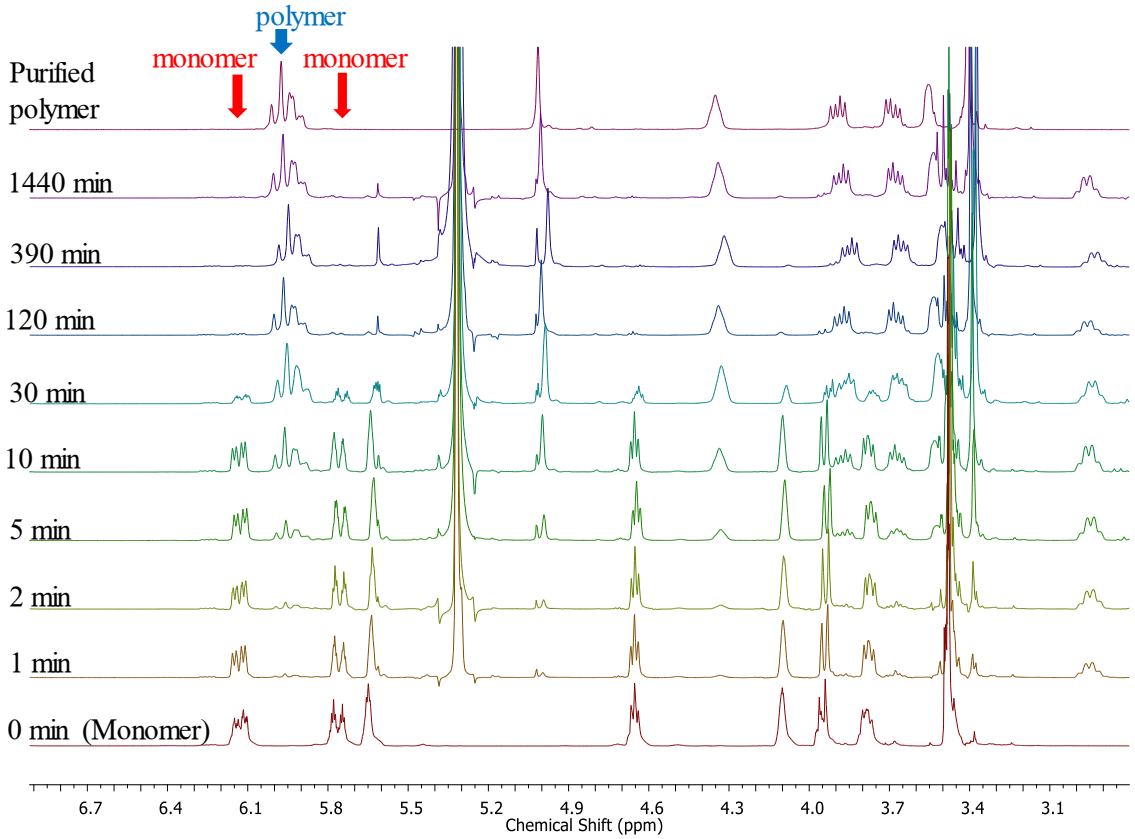

Figure 51. Kinetic study of the polymerization of **3** with $BF_3{\cdot}OEt_2$ at 0 °C by ^{1}H NMR (300 MHz, $CDCl_3$). The separated signals of olefinic protons of monomer (**3**) and polymer (**6**) were used for determining monomer conversions.

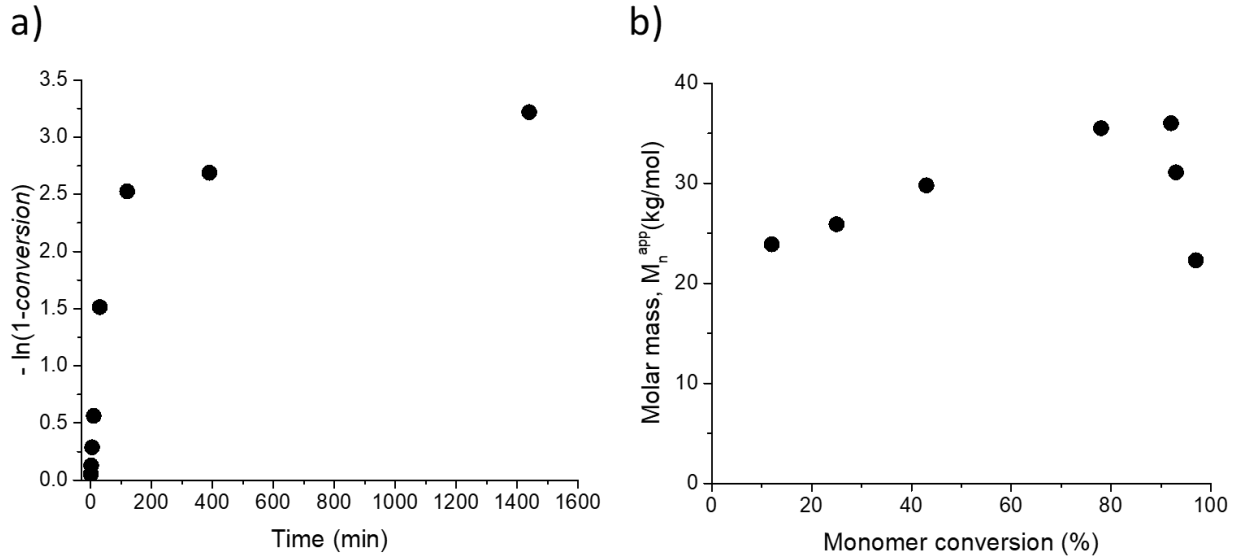

Figure 52. Kinetic investigation of polymerization of compound **3** with $BF_3{\cdot}OEt_2$ ($[\mathbf{3}]_0$ = 4 M, $[\mathbf{3}]_0$:[$BF_3{\cdot}OEt_2$] = 10) in DCM at 0 °C a) First-order time–conversion plot. b) Evolution of number-average molar mass (M_n^{app}) with conversion (x_p).

The kinetic investigation of the polymerization of **3** shows quick consumption of the monomer within one hour (Figure 52), following pseudo-first-order kinetics, but levels off thereafter. The apparent number-average molar masses (M_n^{app}) increases linearly and rapidly to ~36 kg/mol but decreases thereafter at a very high monomer conversion, possibly by back-biting and chain transfer process that is commonly observed in cationic polymerization of cyclic ethers[78].

3.3.4 Structural characterization of poly(levoglucosenyl methyl ether)

The ^1H NMR spectrum (Figure 53) shows the presence of all the characteristic protons. The integral of the area under the peaks confirms methyl proton of poly(levoglucosenol methyl ether) as ~3 H appearing as a singlet at 3.38 ppm. The ^{13}C NMR spectrum also shows the presence of all the characteristic carbons. The assignment of the protons requires ^1H-^{13}C HSQC NMR experiment (Figure 55), which indicates the H_f and $H_{f'}$ as blue (negative phase) or CH_2 protons at 3.92-3.82 ppm as multiplet and ~3.67 ppm as a doublet of doublets. The peak at (4.99, 98.3) ppm

is very characteristic to an acetal peak that suggests H_a. The correlation of the methyl proton (from ^{1}H NMR spectrum) with the signal at (3.38, 56.3) ppm confirms the peak at 56.3 ppm (^{13}C NMR spectrum) as methyl peak. The protons at 5.90 and 5.96 ppm are olefinic and need further investigation for detailed analysis.

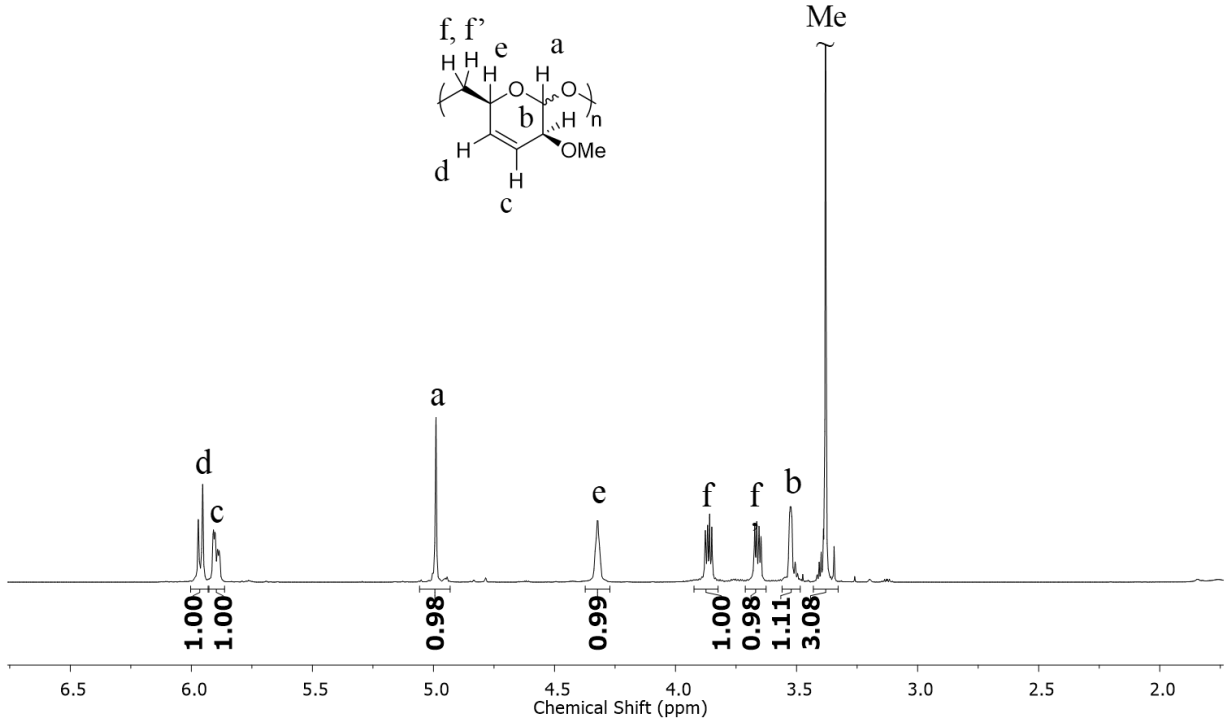

Figure 53. ^{1}H NMR (600 MHz, $CDCl_3$) spectrum of polymer **6**.

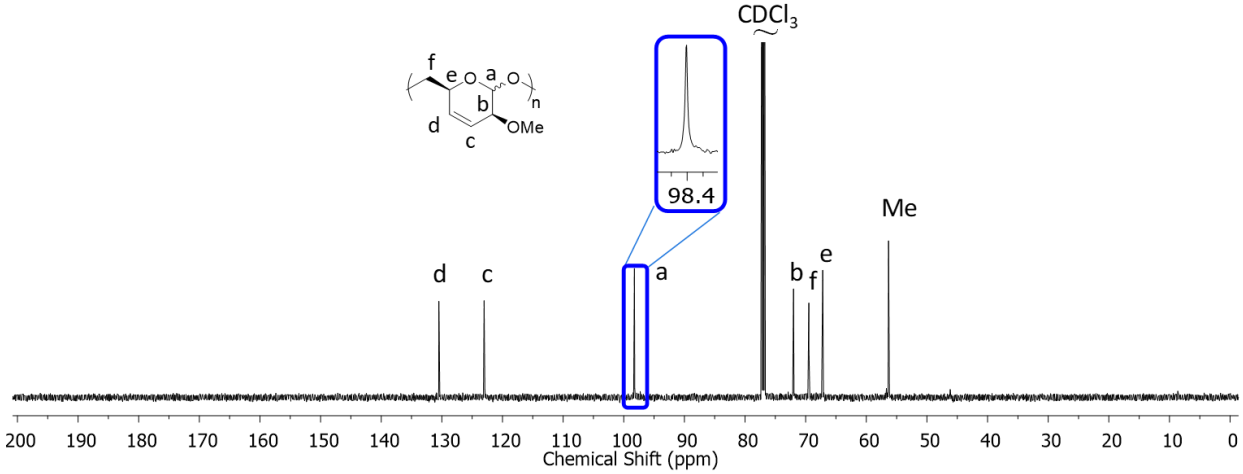

Figure 54. ^{13}C NMR (150 MHz, $CDCl_3$) spectrum of **4** (run 11,Table 6). All peaks appear as singlets.

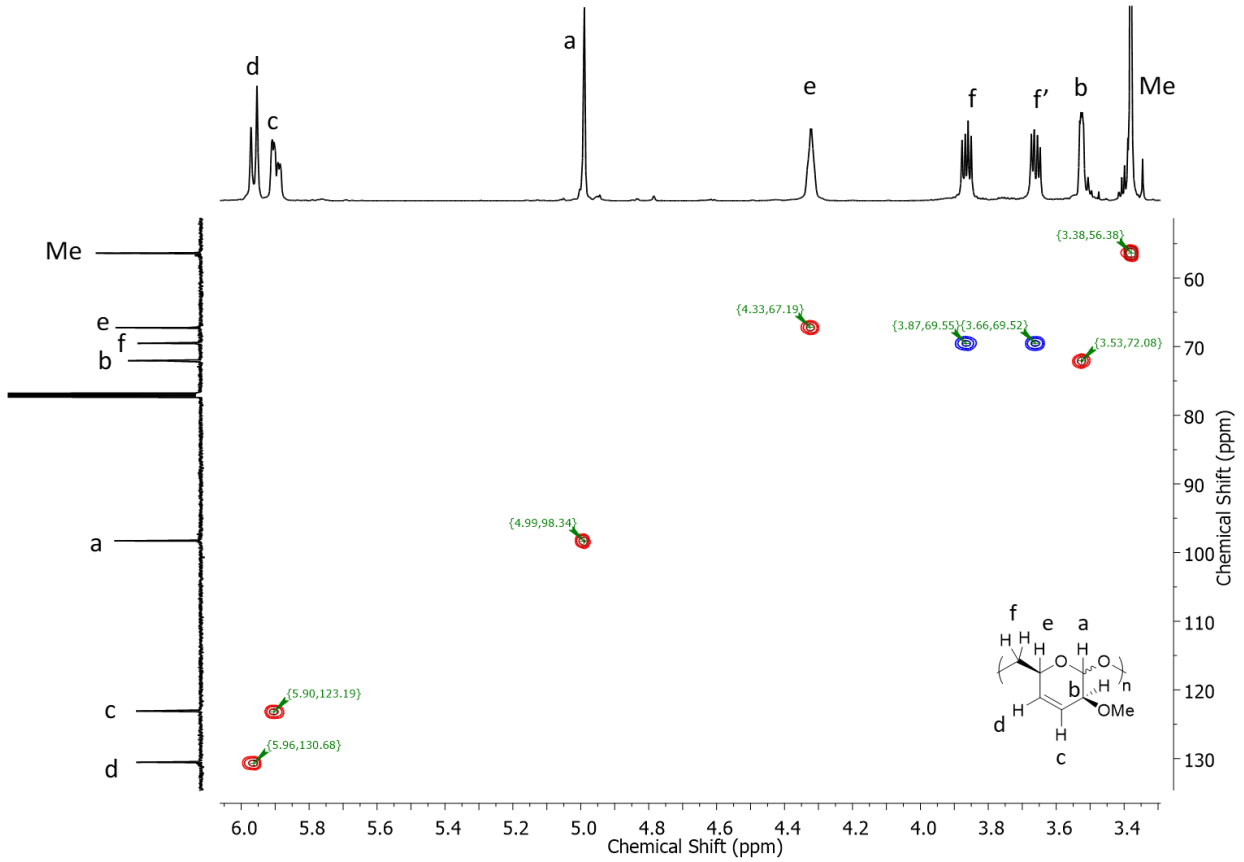

Figure 55. ^{1}H-^{13}C HSQC NMR (600 MHz, 150 MHz, $CDCl_3$) spectrum of polymer **6** (blue: negative contours, CH_2; red: positive contours, CH, CH_3).

The ^{1}H-^{1}H COSY NMR spectrum (Figure 56) was measured for further assignment of the peaks. Correlation at ~(4.31, 3.66) ppm and ~(4.32, 3.86) ppm indicate correlation of the proton at 4.31 ppm with H_f and $H_{f'}$, suggesting it to be H_e. Hence, the remaining aliphatic proton at 3.61-3.50 ppm must be H_b and its correlation with the olefinic proton at (5.89, 3.52) ppm suggests the concerned olefinic proton as H_c. Hence, the other olefinic proton at 5.96 ppm is H_d.

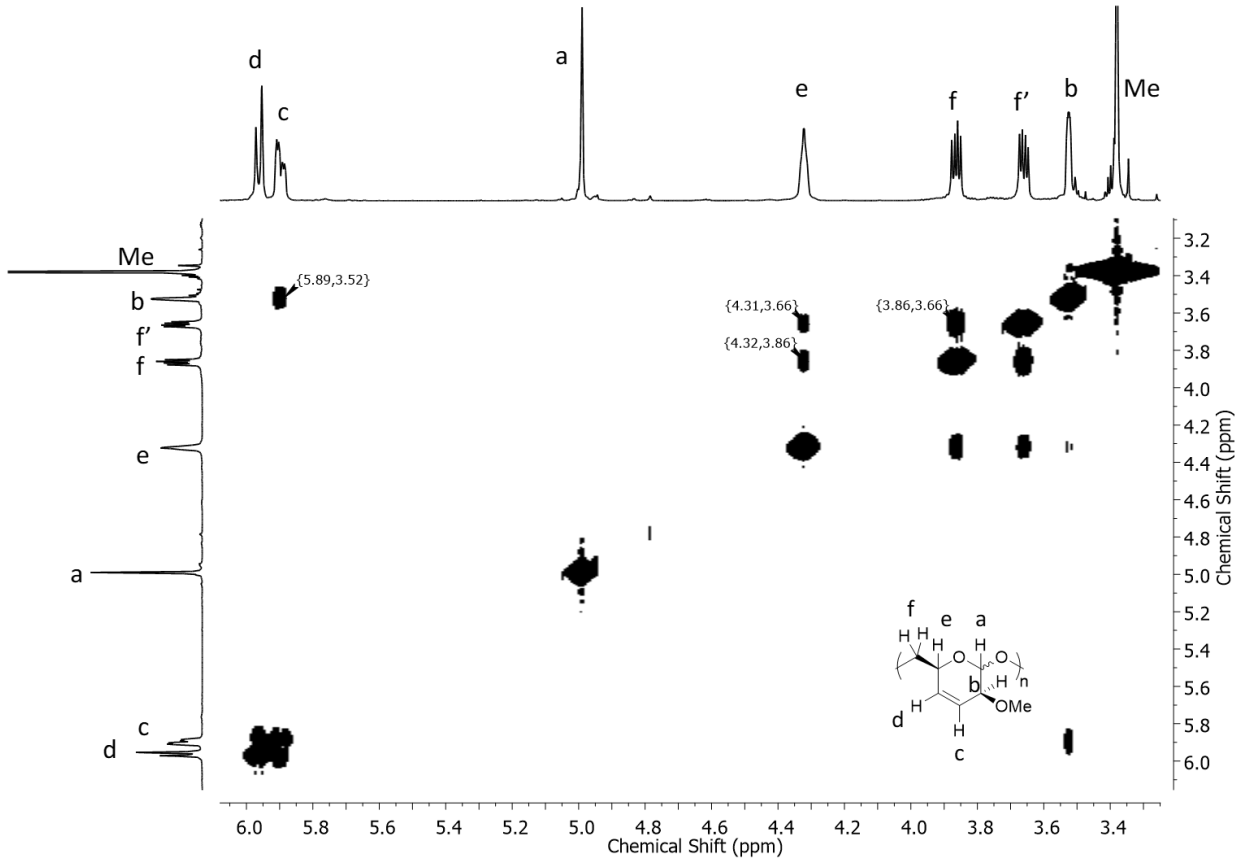

Figure 56. ^{1}H-^{1}H COSY NMR (600 MHz, $CDCl_3$) spectrum of polymer **6**.

With this information, we can conclude that the expected structural protons are present in polymer **6**. The singlets in the ^{13}C NMR spectrum (Figure 54) of polymer **6** and the acetal carbon (C_a) in particular indicates the absence of (at least, not in an amount that is detectable by NMR) any other anomeric structure (isomerism at C_a) in the polymer **6**. This is further confirmed by the ^{1}H-^{1}H DQF COSY (Figure 57) of polymer **6** where only a single coupling between H_a and H_b is visible. The exact conformation of the six-membered ring could not be resolved with the present data and needs further investigation.

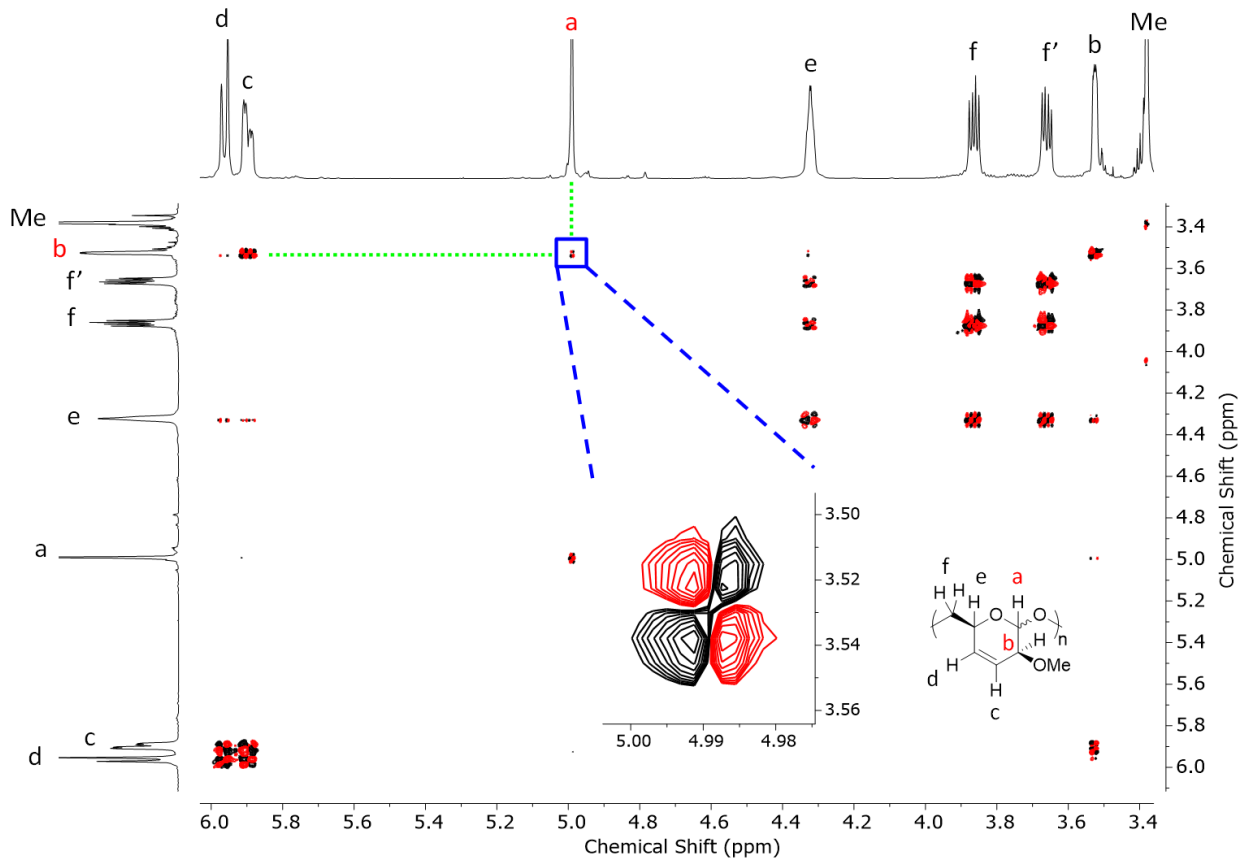

Figure 57. ^{1}H-^{1}H DQF COSY (500 MHz, $CDCl_3$) spectrum of polymer **6**.

In conclusion, we can say that the polymerization of levoglucosenyl methyl ether (**3**) does not induce any isomerism in the repeating unit as well as any sequence isomerism in the polymer chain.

3.3.5 Physical properties

Poly(levoglucosenyl methyl ether) (**6**) is soluble in common organic solvents such as dichloromethane, chloroform, acetonitrile, and tetrahydrofuran. It is insoluble in diethyl ether, water, NMP, DMSO, and methanol.

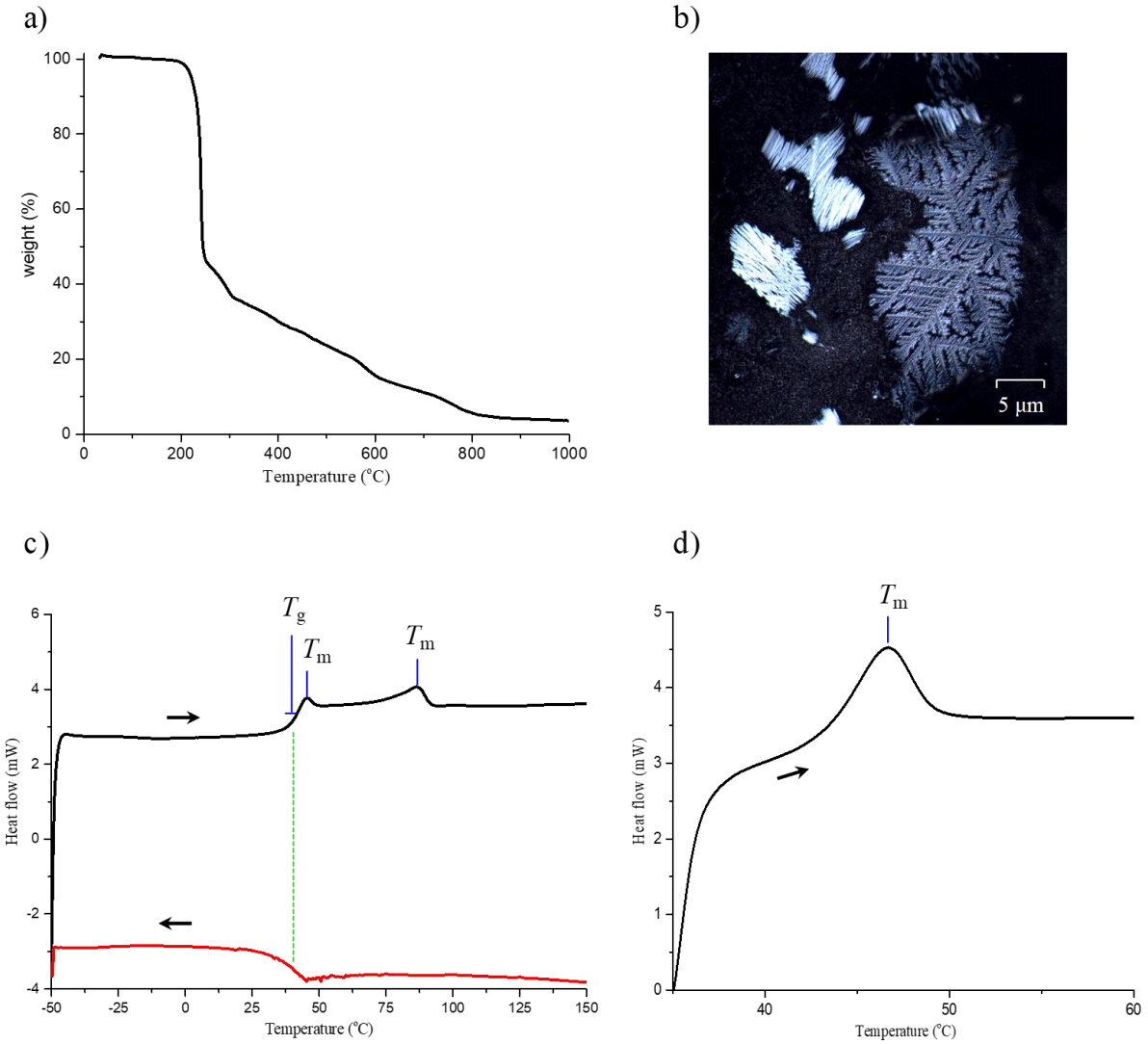

Figure 58. (a) TGA curve of polymer **6**, degradation temperature, T_d ~220 °C (5% weight loss). (b) Plane polarized optical microscope photo of polymer **6.** (c) DSC plot of polymer **6**: heating isotherm (black) and cooling isotherm (red). (d) DSC plot of polymer **6**: heating isotherm of 35-60 °C region. Heating and cooling rates are 30 K/min

The polymer **6** is thermally stable up to ~220 °C according to TGA measurements (Figure 58). In the DSC, the cooling curve shows that the transition at ~35 °C is indeed a glass transition temperature. Further analysis shows the presence of an endothermic (melting) transition near to the glass transition of 42-50 °C and another melting transition in the region of 70-100 °C. Therefore, these polymers are semi-crystalline in nature. The presence of crystalline structures in polymer **6** is seen in polarized optical microscopy image (Figure 58). These polymers contain only one sequence isomer, which is likely to be the reason for crystallinity.

3.3.6 Functionalization

As mentioned earlier, the acid-catalyzed polymerization does not affect the in-ring olefinic functionality. This is interesting for the post-polymerization modification as it opens a wide range of functionalization possibilities. One such possibility is cross-linking. It was observed that the polymer **6** tends to crosslink even when stored at –20°C. It is believed that the crosslinking is promoted by the peroxide formation of allylic ether unit in presence of oxygen.[79] The addition of a radical inhibitor (butylated hydroxytoluene, BHT) was helpful to avoid the cross-linking. The olefin functionality can bring further opportunities for polymer modification. Among a wide range of opportunities, thiol-ene click chemistry was chosen to demonstrate the functional ability of the polymer.

3.3.6.1 Thiol-ene click chemistry

Polymer **6** was treated with excess methyl 3-mercapto propionate with benzophenone and UV irradiation (Scheme 16). The conversion of the polymer **6** into the thiol-ene adduct was quantitative, indicated by the ^{1}H NMR spectra (Figure 59). The addition of 3-mercapto propionate to the 1,2-disubstituted *cis* olefin can occur in four distinct ways due to the (planner) geometry of the olefin. However, only two addition should be predominant over the others due to *syn-axial* interactions (Figure 60). This is evident by the appearance of methyl peak as two separate peaks corresponding to the 3-mercapto propionate. The SEC-RI traces (Figure 61) shows an increase in overall hydrodynamic volumes of the resulting polymer **7**, confirming the successful functionalization of polymer **6**.,

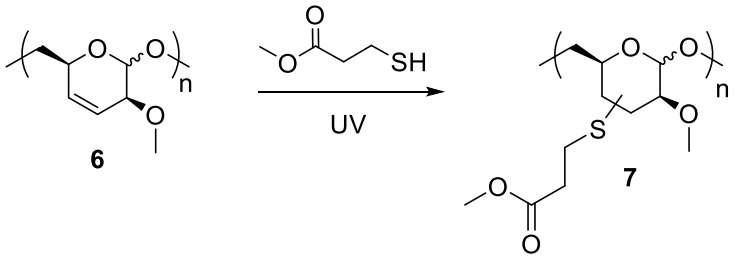

Scheme 16. Chemical modification of polymer **6** by the radical thiol-ene reaction.

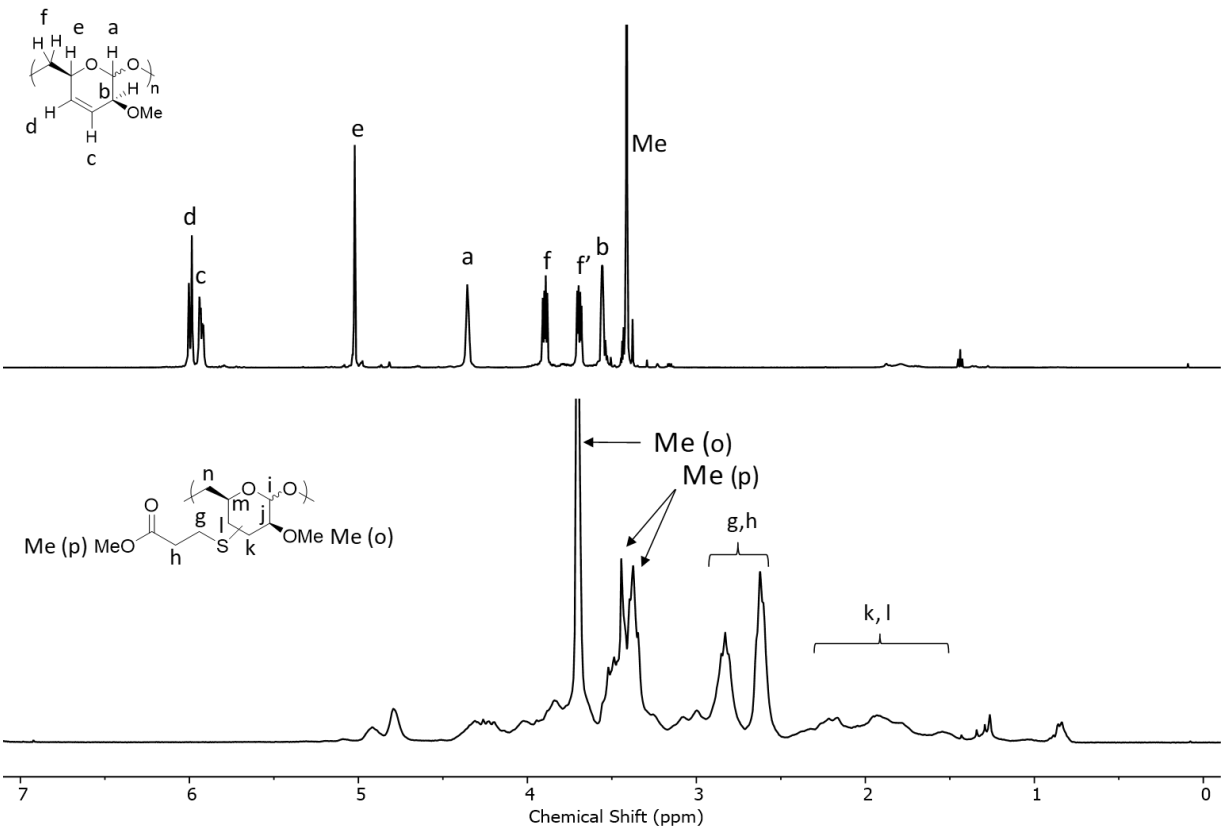

Figure 59. ^{1}H NMR spectra of polymer **7** (300 MHz, $CDCl_3$) obtained by thiol-ene click chemistry and of the precursor polymer **6** (600 MHz, $CDCl_3$).

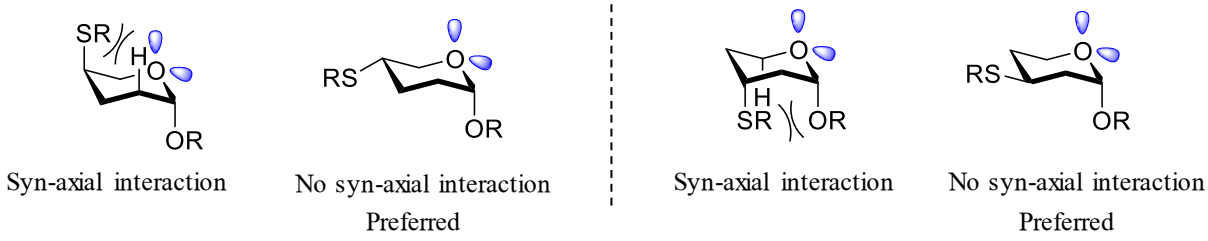

Syn-axial interaction | No syn-axial interaction Preferred | Syn-axial interaction | No syn-axial interaction Preferred

Figure 60. Exemplary pictorial representation of four different possible adducts and the thermodynamically preferred adduct.

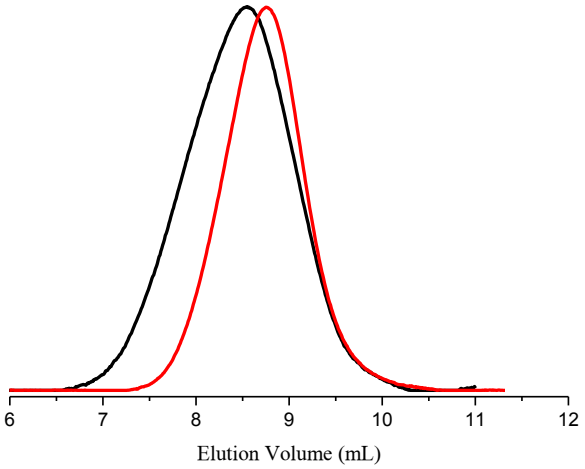

Figure 61. SEC-RI traces (eluent: THF) of polymer **6** (red, M_n^{app} = 19.7 kg/mol, $Đ$ = 1.3) and polymer **7** (black, M_n^{app} = 26.7 kg/mol, $Đ$ = 1.5) obtained by thiol-ene click chemistry.

3.3.6.2 Hydrogenation

Hydrogenation eliminates the double bond and thus makes the polymer inert towards the reaction of olefinic reactions such as cross-linking. Therefore, polymer **6** was subjected to hydrogenation with a catalytic amount of Pd-C and H_2 at atmospheric pressure. The hydrogenation was near quantitative (93% conversion), determined by ^1H NMR spectroscopy (Figure 62). The SEC-RI traces show a decrease in hydrodynamic size (Figure 63).

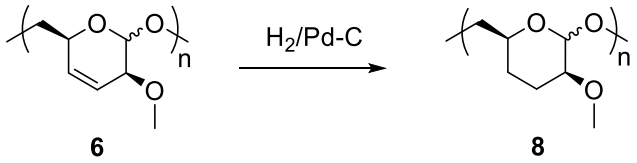

6 **8**

Scheme 17. Chemical modification of polymer **6** by hydrogenation.

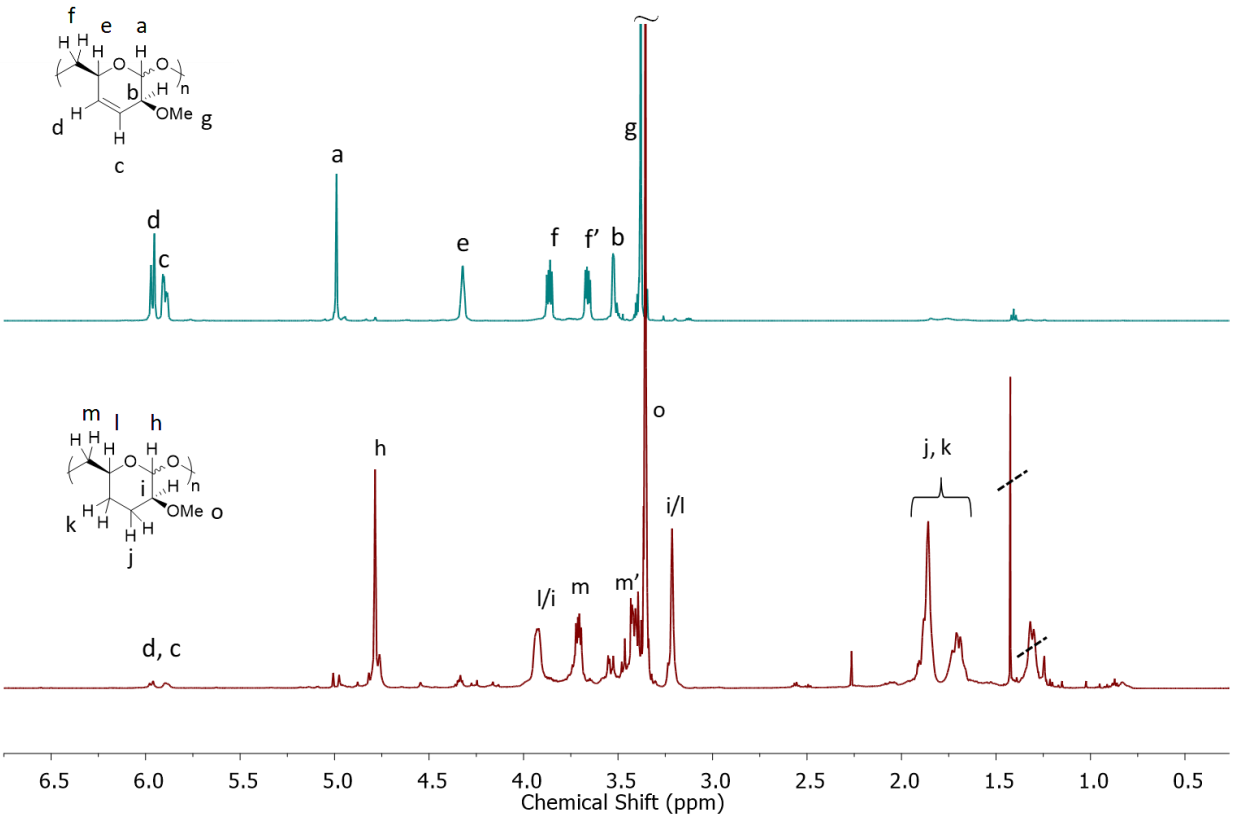

Figure 62. ^{1}H NMR spectra of the precursor polymer **6** (600 MHz, $CDCl_3$) (top) and the hydrogenated polymer **8** (300 MHz, $CDCl_3$) (bottom).

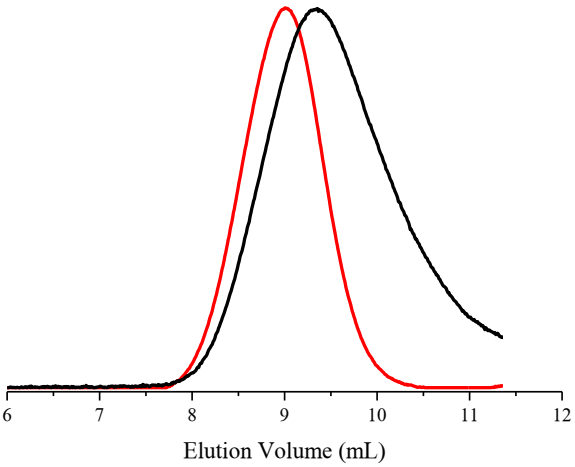

Figure 63. SEC-RI traces of polymer **6** (red) and polymer **8** (black) obtained by hydrogenation.

3.3.7 Degradation

The polymer **6** possesses acetal linkage in the main chain polymer. The acetal bonds are sensitive towards acid in presence of nucleophile (Scheme 18). In fact, cellulose, the most abundant naturally occurring polymer that bio-degrades, contains an acetal linkage in the main chain. To check the degradability, polymer **6** was dissolved in THF and treated with triflic acid and a few drops of methanol. After 10 hours of reaction, the polymer seemed to have completely degraded, as indicated by SEC measurements (Figure 64).

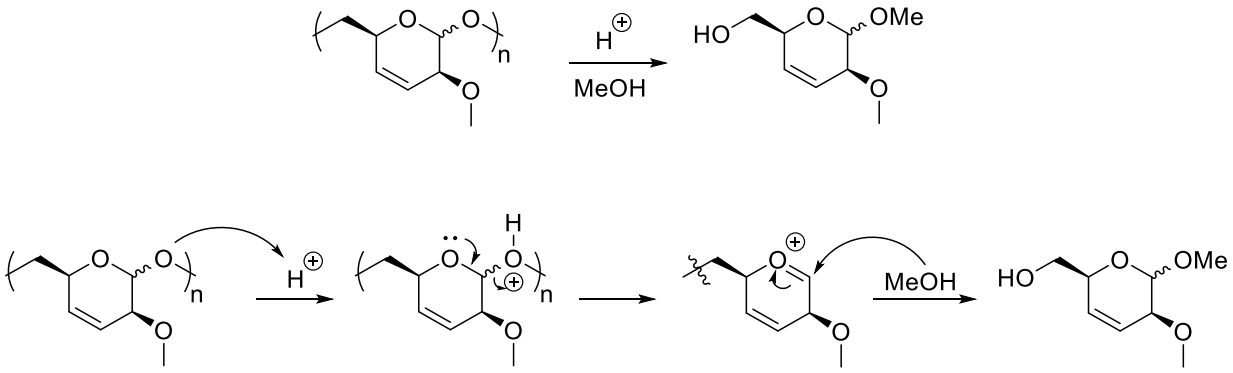

Scheme 18. Plausible mechanism acid-catalyzed degradation of polymer **6**.

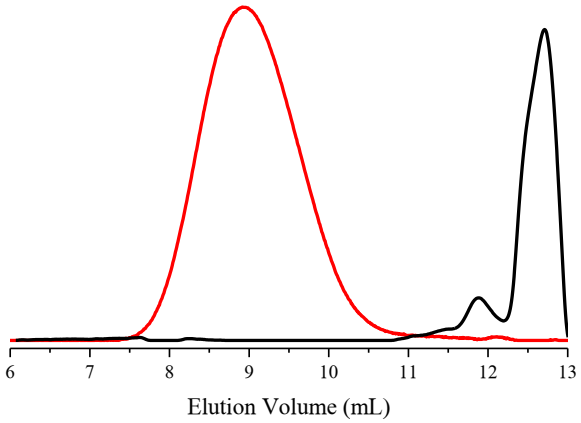

Figure 64. SEC-RI traces of polymer **6** (red) and degradation product (black).

3.3.8 Conclusion

In conclusion, the chiral monomer levoglucosenyl methyl ether was polymerized via cationic ring-opening polymerization with the near quantitative conversion of the monomer. The polymerizations were faster at a relatively higher temperature but produced polymers with higher molar mass at a relatively lower temperature. The obtained polymer contained only one structure due to the anomeric effect, although the possibility is to have two isomers during polymerization. The highest apparent number average molar mass of 36 kg/mol could be obtained with a relatively low dispersity of 1.5. The polymers are semi-crystalline in bulk, possessing a glass transition temperature ~35 ℃ and two melting transitions at ~42-50 ℃ and 70-100 ℃, as shown by differential scanning calorimetry. These polymers are thermally stable up to ~220 ℃, according to thermogravimetric analysis.

The kinetic study revealed that most of the monomer converted to polymer in a short period of about one hour. Additionally, the kinetic study shows the living nature of the polymerization until high conversion, where a sudden drop in molar mass of the polymers was observed with increasing monomer conversion. The dramatic drop in molar mass of the growing polymer chain could be due to chain transfer or backbiting reactions.

The obtained polymers could be purified by precipitation into methanol and storing them after drying leads to crosslinking of the polymer even at low temperature, a phenomenon that can be overcome by the addition of traces of radical inhibitor or by hydrogenation of the olefins. Such crosslinking can be due to the aerial oxidation of allylic units into peroxide radical, essentially leading to crosslinking through radical couplings of the olefin groups. The presence of functional olefins enables thiol-ene click chemistry under ultra-violate exposure conditions with a quantitative conversion.

4. Summary and outlook

Cellulose was converted into levoglucosenone by thermal pyrolysis. Levoglucosenone was reduced to produce levoglucosenol. Levoglucosenol was polymerized by ring-opening metathesis polymerization (ROMP) in 1,4-dioxane with a maximum weight-average molar mass of 150 kg/mol and $Đ$ ~2 (Scheme 19). The poly(levoglucosenol) is thermally stable (5% weight loss) up to ~220 °C and is amorphous in nature having relatively high glass transition temperature (T_g) ~100 °C. The amorphous nature is possibly due to the formation of isomeric structures in the polymeric chain owing to the addition of each new monomer in different orientations to the growing polymer chain. This was resolved by various NMR analyses. The polymer is only soluble in polar organic solvents such as 1,4-dioxane, dimethylformamide, dimethyl sulfoxide, and sulfolane and is insoluble in water, dichloromethane, ethyl acetate, alcohols, tetrahydrofuran, and toluene. 1,4-dioxane was chosen for easier removal of the solvent after polymerization. The polymerization was non-living in nature, following pseudo-first-order kinetics with the highest monomer conversion up to 78% at a relatively lower temperature. The rather small strain in the molecule gave little thermodynamic advantage in polymerization and hence, a lower temperature is needed in order to achieve enthalpy gain in the polymerization. The cyclic acetal group of the poly(levoglucosenol) backbone enables the slow degradation of the polymer when exposed to a moist acidic environment. The presence of the hydroxyl group in the main chain brings the potential for polymer modifications.

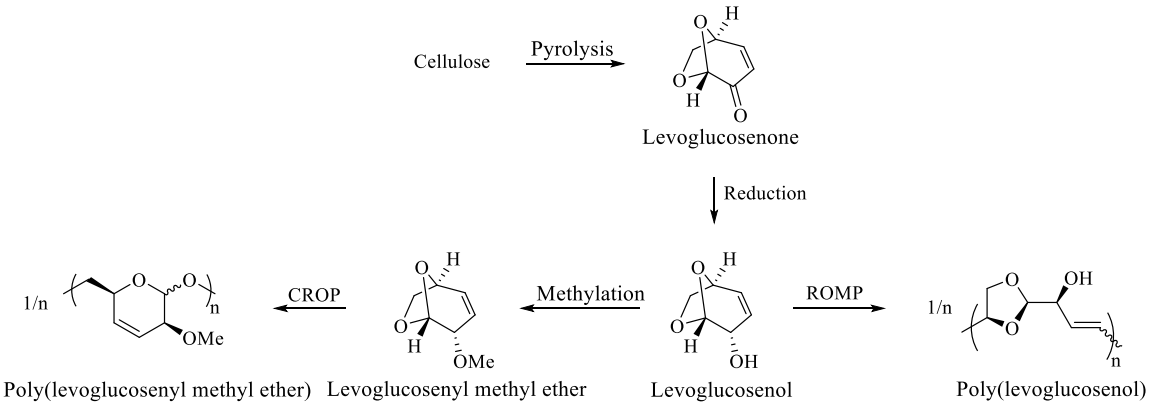

Scheme 19. Schematic illustration of the work.

This is, to our best knowledge, the first example of ROMP for a carbohydrate derivative. This opens an opportunity for novel functional carbohydrate polymer synthesis, however, the polymerization needs further optimization to achieve higher conversion. Further optimization to achieve living polymerization could also open new opportunities for the synthesis of block copolymers. The presence of olefin functionality widens the scope for functionalization that is still unexplored. Furthermore, the investigation of bio-degradation would be interesting as a goal to obtain biodegradable polymer obtained from a renewable resource.

Levoglucosenol can also be more useful by converting it to levoglucosenyl methyl ether. It was done with an isolated yield of 90%. Levoglucosenyl methyl ether was polymerized by cationic ring-opening polymerization (CROP) (Scheme 19). Although triflic acid was found to be a superior catalyst for the polymerization, boron trifluoride etherate is realized to be more convenient to use. Polymers were obtained up to an apparent number-average molar mass of ~36 kg/mol and relatively low dispersity $Đ$ ~1.4. These polymers were semi-crystalline exhibiting a glass transition temperature at ~35 °C and two melting transitions 42-50 °C, and 70-100 °C. Unlike poly(levoglucosenol), poly(levoglucosenyl methyl ether) is soluble in common organic solvents such as dichloromethane, chloroform, acetonitrile, and tetrahydrofuran. The polymerization is believed to proceed through an oxonium ion by a chain-growth mechanism. The polymerization was living in nature until high conversion, where a decrease in molar masses was observed, possibly due to back-biting or chain transfer reactions. The highest monomer conversion was found to be 97% at relatively high monomer-to-initiator loading (30 mol%). A complete structural characterization of the polymers was carried out by means of analytics such as NMR, SEC, ESI-MS, and DSC. The presence of functional groups in the polymer allowed thiol-ene addition and hydrogenation reactions with quantitative and near quantitative conversions respectively. The polymers underwent cross-linking even when stored at –20 °C. This can be overcome by hydrogenation of the olefin groups or by the addition of traces of radical inhibitors, such as BHT, to the polymer. This leads to the conclusion that crosslinking phenomena is proceeding through the double bonds, and is initiated by peroxide radicals, formed from aerial oxidation of allylic ether present in the polymer. Even though the polymers degrade in an acidic environment, future work should involve investigation towards biodegradation.

Overall, levoglucosenol and levoglucosenyl methyl ether are introduced as new monomer derived from cellulose in two and three simple steps, respectively. The monomers produced functionalize polymers. The former monomer was polymerized by ROMP and the latter by CROP (as well as by ROMP). These polymers can be utilized for the production of block copolymers, that may find use in self-assembly or other fields and also open opportunities for the synthesis of complex microstructure or functionalizable biomaterial. Also, the polymers may serve as novel sustainable thermoplastics.

5. Experimentals

5.1 Chemicals

Levoglucosenone (CAS number 37112-31-5) was synthesized according to the procedure mentioned below and was also purchased (99.3% purity) from Circa Group Ltd, Australia. Cellulose (microcrystalline) and dimethyl carbonate (analytical grade) were purchased from Alfa Aesar. Vinyl ether (99%), sodium borohydride ($NaBH_4$, 98%), NaH (60% dispersion in mineral oil), phosphoric acid (H_3PO_4, 98%), *p*-toluenesulfonic acid, 1,4-dioxane (99.98%), D_2O (99.9%) were purchased from Acros Chemicals. Ruthenium catalysts, benzophenone (99.9%), 10% Pd-C, *sec*-butyl lithium (1.4 M in hexane), *N,N*-dimethylformamide (DMF, 99.99%), CD_2Cl_2 (99.9%), $CDCl_3$ (99.8%), DMSO-d_6 (99.8%), lithium bromide (99%), and Dowex® 1×4 chloride resin were purchased from Sigma-Aldrich. Triflic acid (synthesis grade) and $BF_3{\cdot}OEt_2$ were purchased from Merck and Aldrich, respectively. Analytical grade methanol, ethanol, isopropanol, dichloromethane (DCM), tetrahydrofuran (THF), and toluene were purchased from Fischer Scientific. Sulfolane (99.9%) was purchased from Merck. Azobisisobutyronitrile (AIBN, 98%) were purchased from Fluka and recrystallized from isopropanol. *N*-Methyl-2-pyrrolidone (NMP, 99.97%) was purchased from Roth.

5.2 Analytical instrumentation and methods

5.2.1 Nuclear magnetic resonance spectroscopy

Nuclear Magnetic Resonance (NMR) spectra were recorded on Bruker Avance 300 MHz, 500 MHz, or Bruker Avance III 600 MHz spectrometers at room temperature or 293K. The signals were referenced to the solvent peak at δ (^{1}H) 2.50 ppm and (^{13}C) 39.52 ppm for DMSO-d_6, δ (^{1}H) 5.32 ppm and (^{13}C) 53.84 ppm for CD_2Cl_2, and δ (^{1}H) 7.26 ppm and (^{13}C) 77.16 ppm for $CDCl_3$.

5.2.2 Electrospray ionization time-of-flight mass spectrometry

Electrospray ionization time-of-flight (ESI-ToF) mass spectrometry was measured in positive ionization mode on a Micromass Q-TOF Micro (Waters Inc.). The sample was dissolved in methanol.

5.2.3 Size exclusion chromatography

Size Exclusion Chromatography (SEC) with simultaneous UV and RI (differential refractive index) detection was performed with THF as the eluent (flow rate of 0.5 mL/min) at room temperature. The stationary phase was a 300 x 8 mm^2 PSS SDV linear M column (3 μm particle size, molar mass range 10^2-10^6 Da). Solutions containing ~0.15% (w) polymer were filtered through 0.45 μm PTFE filters; the injected volume was 100 μL. Polystyrene standards (PSS, Mainz, Germany) were used for calibration.

5.2.4 Polarized optical microscopy

Polarized optical microscopy (POM) was performed with an Olympus BX53M polarized optical microscope (crossed polarizers) equipped with an SC50 camera and a Mettler Toledo HS82 hot stage. A polymer film was drop casted on a glass slide and was heated to 120 °C at a heating rate of 20 K/min, kept at this temperature for 60 s, and then cooled slowly down to room temperature.

5.2.5 Thermogravimetric analysis

Thermogravimetric Analysis (TGA) was measured on a Mettler Toledo TGA/SDTA851 in a temperature range from 25 to 900 °C at a heating rate of 10 K/min under a continuous nitrogen flow of 20 mL/min.

5.2.6 Differential scanning calorimetry

Differential Scanning Calorimetry (DSC) was measured on a Mettler Toledo DSC822e in a temperature range from –50 to 170 °C under a continuous nitrogen flow. The heating/cooling rate was 10-30 °C min^{-1}

5.2.7 Melting point

Melting points were obtained by a MEL-TEMP II device (Laboratory Devices Inc., USA); measurements were conducted in open capillaries.

5.3 Synthetic procedures and characterization of materials

5.3.1 Levoglucosenone

(Method adapted from *Green Chem*. **2007**, 9 (10), 1137-1140 and *J. Org. Chem.* **1998**, 63, 8133–8144). 120 g of microcrystalline cellulose was suspended in 500 mL of methanol with 3.6 g of H3PO4. This suspension was stirred for 30 min and then the methanol was evaporated. The acid-pretreated cellulose (15 g per batch) was placed in a tube-shaped round bottom flask in a Kugelrohr distillation apparatus oven under reduced pressure (0.1 mbar) and heat-ed to 300 °C for ~20 min. The liquids from multiple batches were combined, passed through basic alumina (or treated with sodium bicarbonate solution), washed with DCM, concentrated, and distilled in the Kugelrohr distillation apparatus at 160 °C at reduced pressure (0.1 mbar) to obtain a yellowish oil (5.0 g, 4.2 w% from cellulose).

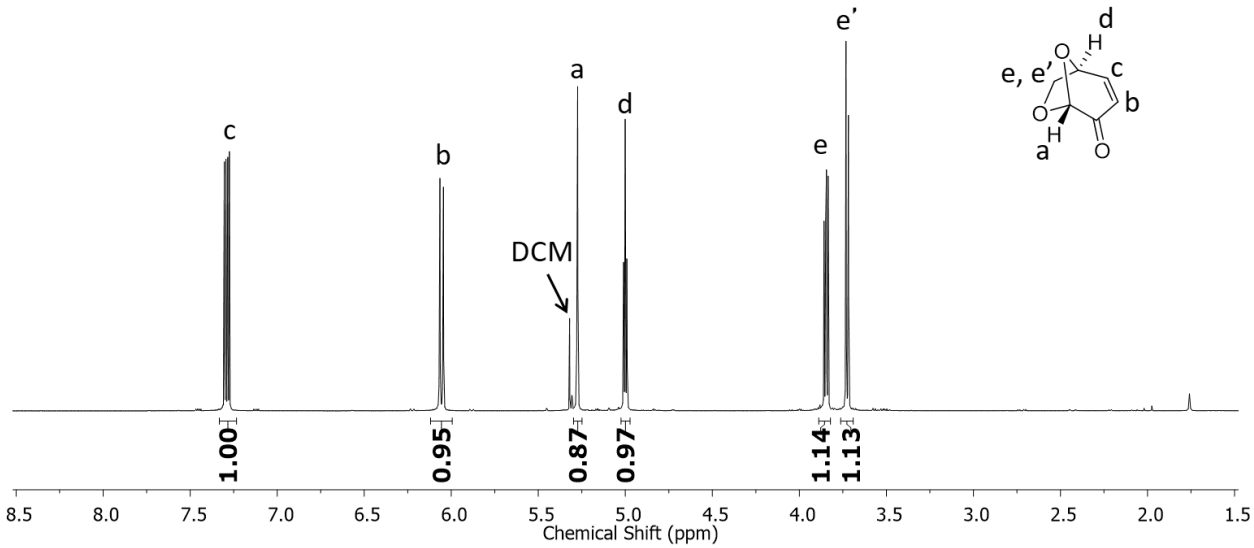

Figure S 1. ^{1}H NMR (500 MHz, CD_2Cl_2) spectrum of levoglucosenone (**1**); δ = 7.29 (dd, J = 10.0, 4.7 Hz, 1H), 6.06 (dd, J = 10.0, 1.7 Hz, 1H), 5.28 (d, J = 1.7 Hz, 1H), 5.00 (t, J = 5.0 Hz, 1H), 3.85 (dd, J = 6.9, 4.7 Hz, 1H), 3.73 (d, J = 6.9 Hz, 1H).

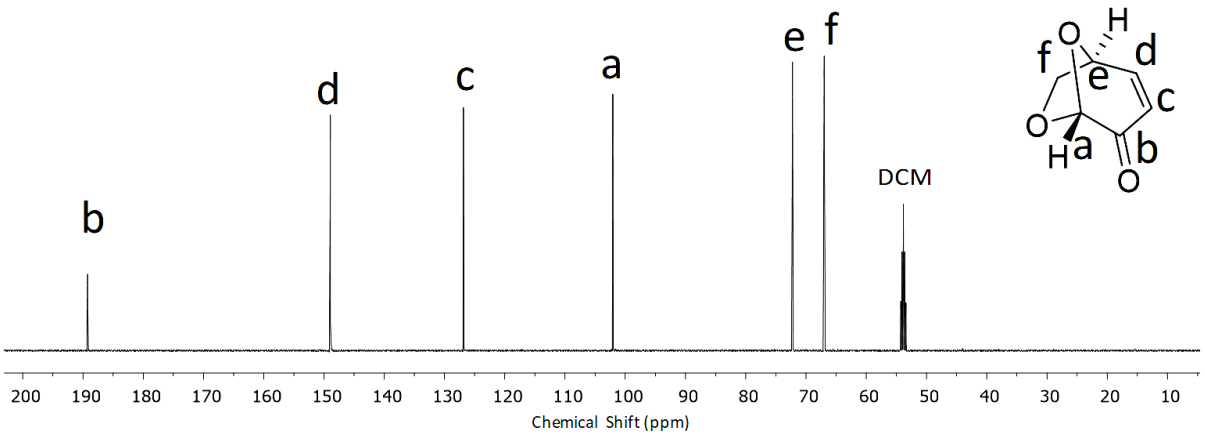

Figure S 2.[13]C NMR (125 MHz, CD_2Cl_2) spectrum of levoglucosenone (**1**); δ = 189.25, 148.95, 126.86, 102.06, 72.25, 66.99.

5.3.2 Levoglucosenol

(Method adapted from *J. Org. Chem.* **1998**, *6*3, 8133–8144). 5.0 g (39.7 mmol) of levoglucosenone (**1**) was dissolved 30 mL of water. A solution of $NaBH_4$ (2.4 g, 63.4 mmol in 10 mL water) was added and allowed to stir for 10 min. The reaction flask was then placed in an ice-cold water bath and 10 mL of acetone was added to quench the reaction (caution, very exothermic!). The aqueous solution was extracted extensively with ethyl acetate (7 × 20 mL). The organic phases were collected and concentrated. The crude levoglucosenol crystallized upon standing. It was further purified by sublimation at 40 °C under high vacuum (0.001 mbar) to yield 4.5 g (90 %) of levoglucosenol **2**; melting point, mp ~68 °C; specific rotation $[\alpha]_D^{25} = -58.0°$ (0.51% (w/v) 1,4-dioxane).

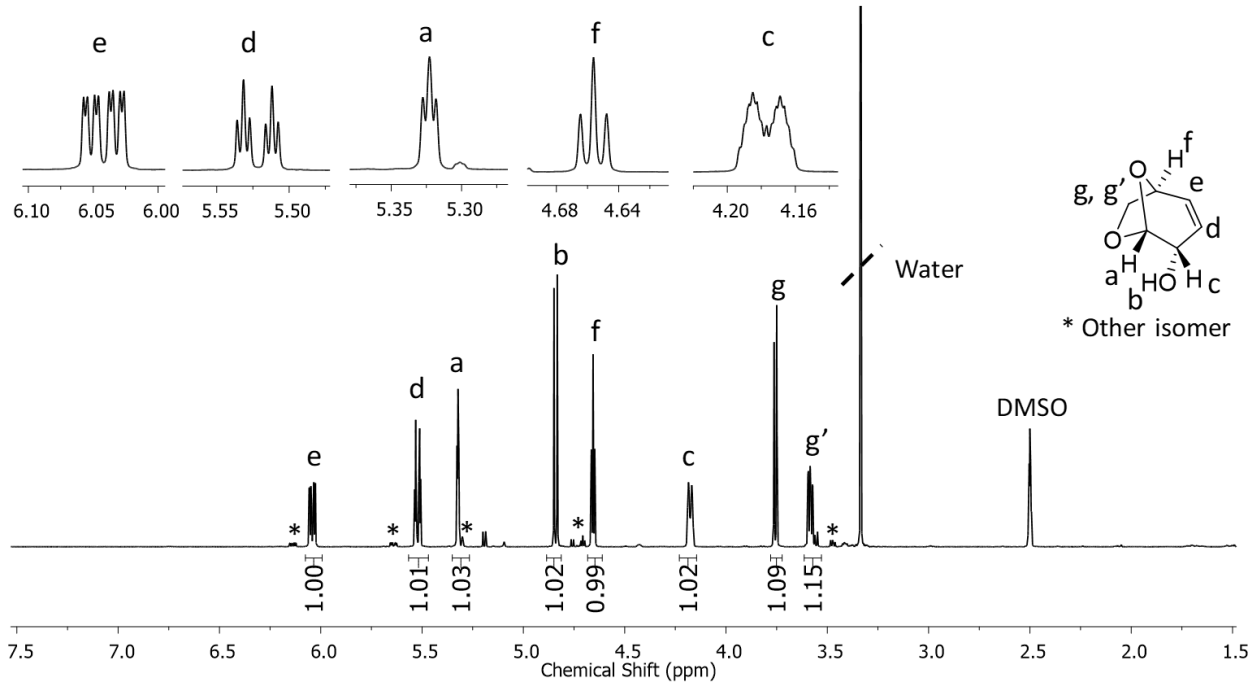

Figure S 3. ^{1}H NMR (500 MHz, DMSO-d_6) spectrum of levoglucosenol (**2**); δ = 6.04 (ddd, J = 9.9, 4.2, 1.5 Hz, 1H), 5.52 (dt, J = 9.9, 2.2 Hz, 1H), 5.32 (t, J = 2.3 Hz, 1H), 4.84 (d, J = 8.0 Hz, 1H), 4.66 (t, J = 4.2 Hz, 1H), 4.19-4.16 (m, 1H), 3.76 (d, J = 6.6 Hz, 1H), 3.61-3.57 (m, 1H).

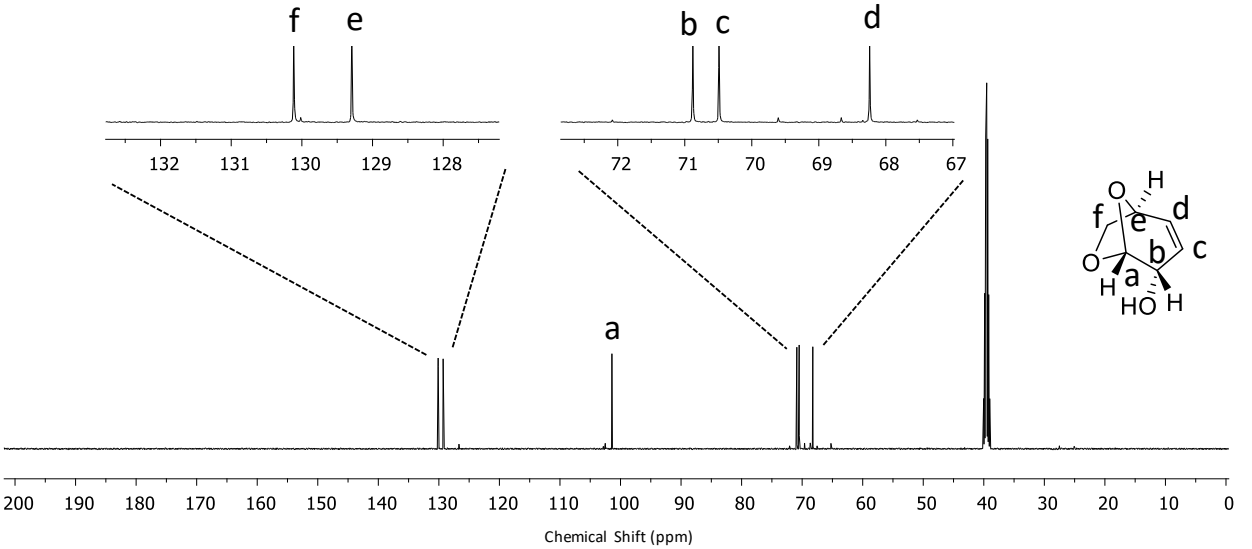

Figure S 4. ^{13}C NMR (125 MHz, DMSO-d_6) of levoglucosenol (**2**); δ = 130.1, 129.2, 101.4, 70.8, 70.4, 68.2.

5.3.3 Synthesis of levoglucosenyl methyl ether

NaH dispersed in mineral oil (450 mg considering 60 % NaH) was placed in a dry flask and washed 3 times with dry hexane. Dry THF (30 mL) was added and the dispersion was cooled in an ice bath while constantly stirring. To this, a solution of levoglucosenol (**2**), (10.24 g) in dry THF (30 mL) was slowly added (effervescence was observed). After the effervescence stopped, a solution of methyl iodide (8.8 ml) in dry THF (20 mL) was added and the mixture was allowed to stir at room temperature until thin layer chromatography (TLC) showed complete consumption of the starting material (after about a couple of hours). The crude material was poured into ice-cold water and extracted with DCM several times. The DCM portions were combined and evaporated in a rotary evaporator. The crude compounds were distilled in a Kugelrohr distillation apparatus at 140 °C under reduced pressure (0.1 mbar) to obtain levogluconsenyl methyl ether (**3**) as a colorless oil (overall yield 90 %). Compound **3** was characterized with the help of ^{1}H, ^{13}C, ^{1}H-^{1}H COSY, and ^{1}H-^{13}C HSQC NMR spectroscopy and by ESI MS.

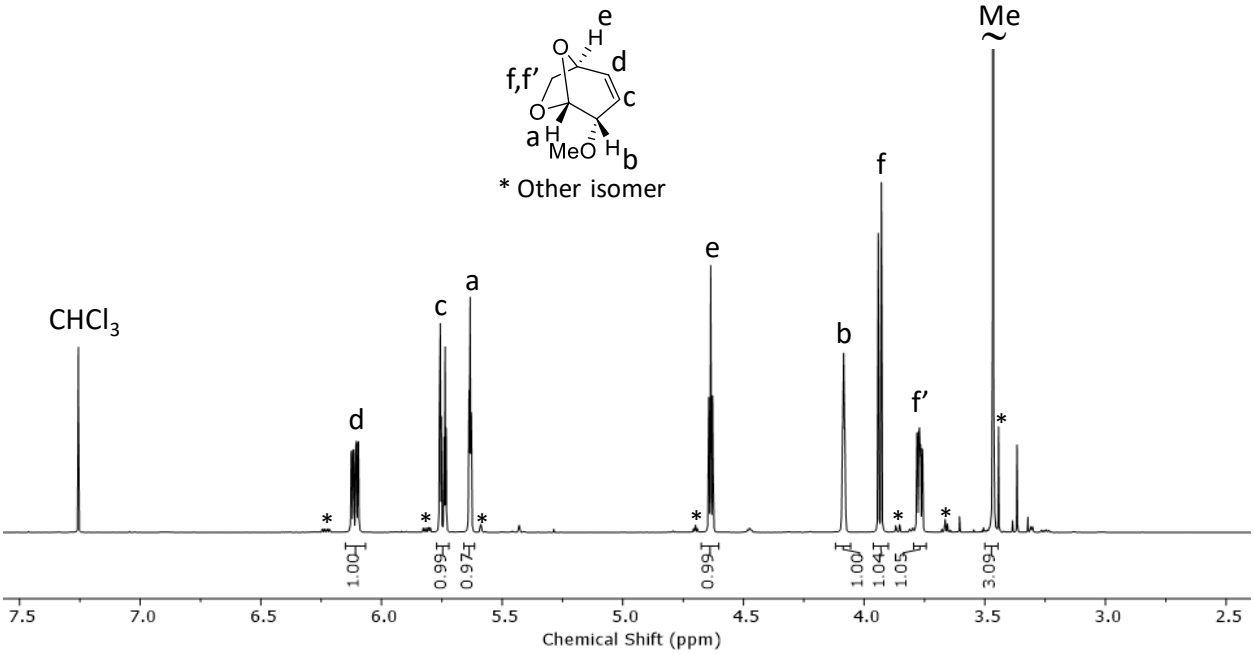

Figure S 5. ^{1}H NMR (500 MHz, $CDCl_3$) spectrum of **3**; δ = 6.14 (ddd, J = 9.9, 4.2, 1.2 Hz, 1H), 5.77 (dt, J = 10.0, 2.2 Hz, 1H), 5.66 (t, J = 2.3 Hz, 1H), 4.66 (t, J = 4.1 Hz, 1H), 4.12-4.10 (m, 1H), 3.96 (d, J = 6.6 Hz, 1H), 3.80 (ddd, J = 6.5, 4.1, 1.1 Hz, 1H), 3.49 (s, 3H).

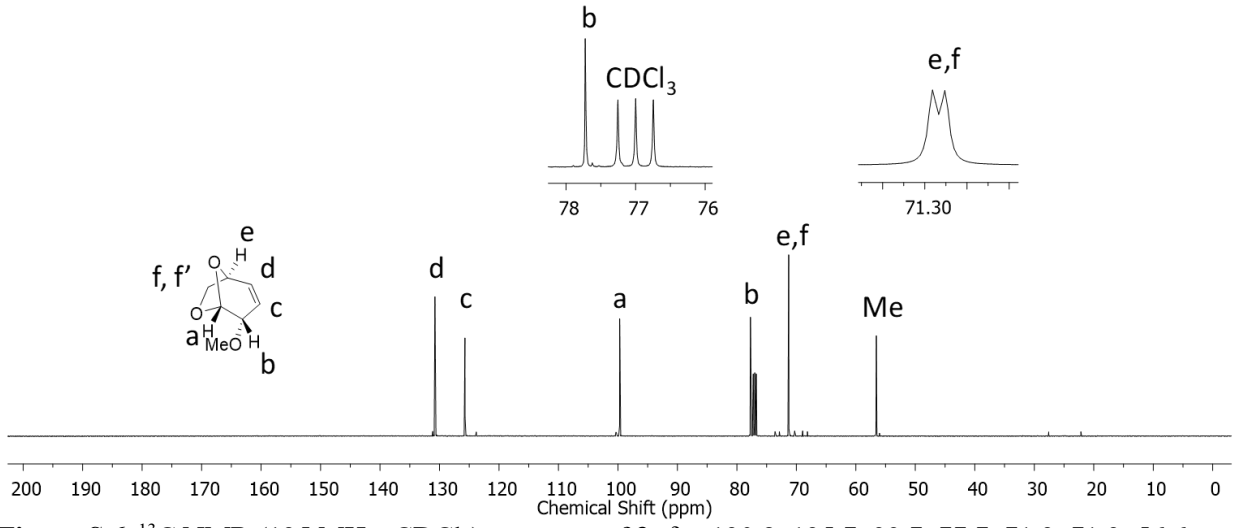

Figure S 6. ^{13}C NMR (125 MHz, $CDCl_3$) spectrum of **3**; δ = 130.8, 125.7, 99.7, 77.7, 71.3, 71.3, 56.6.

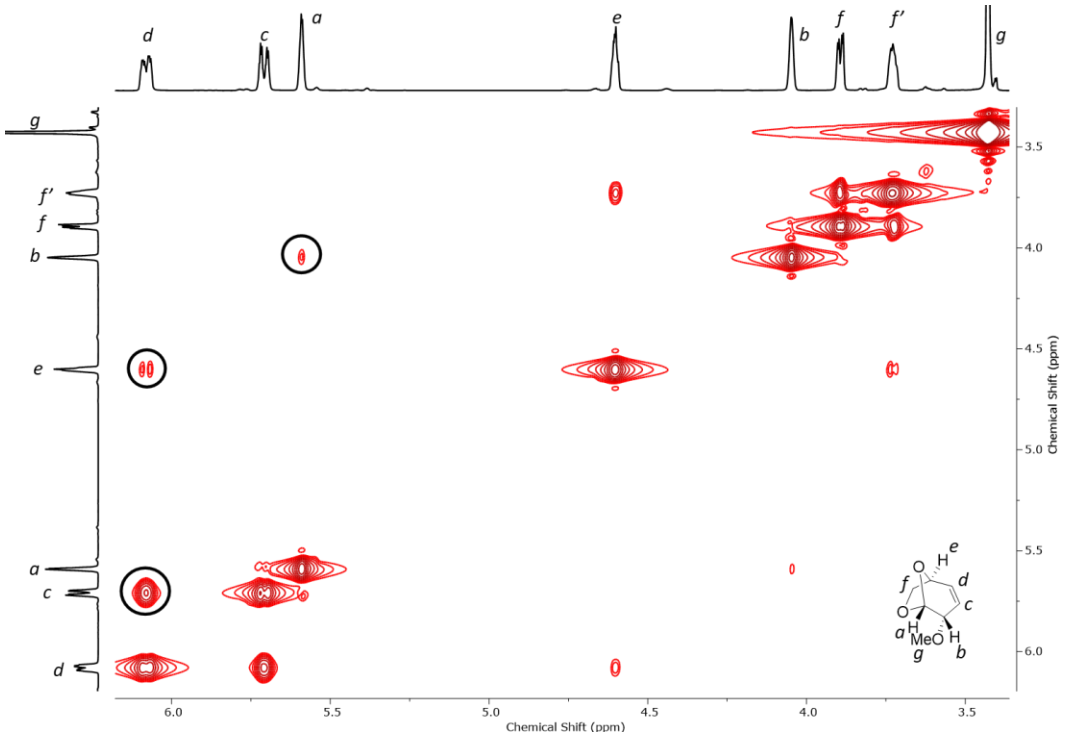

Figure S 7. ^{1}H-^{1}H COSY NMR (500 MHz, $CDCl_3$) spectrum of **3**.

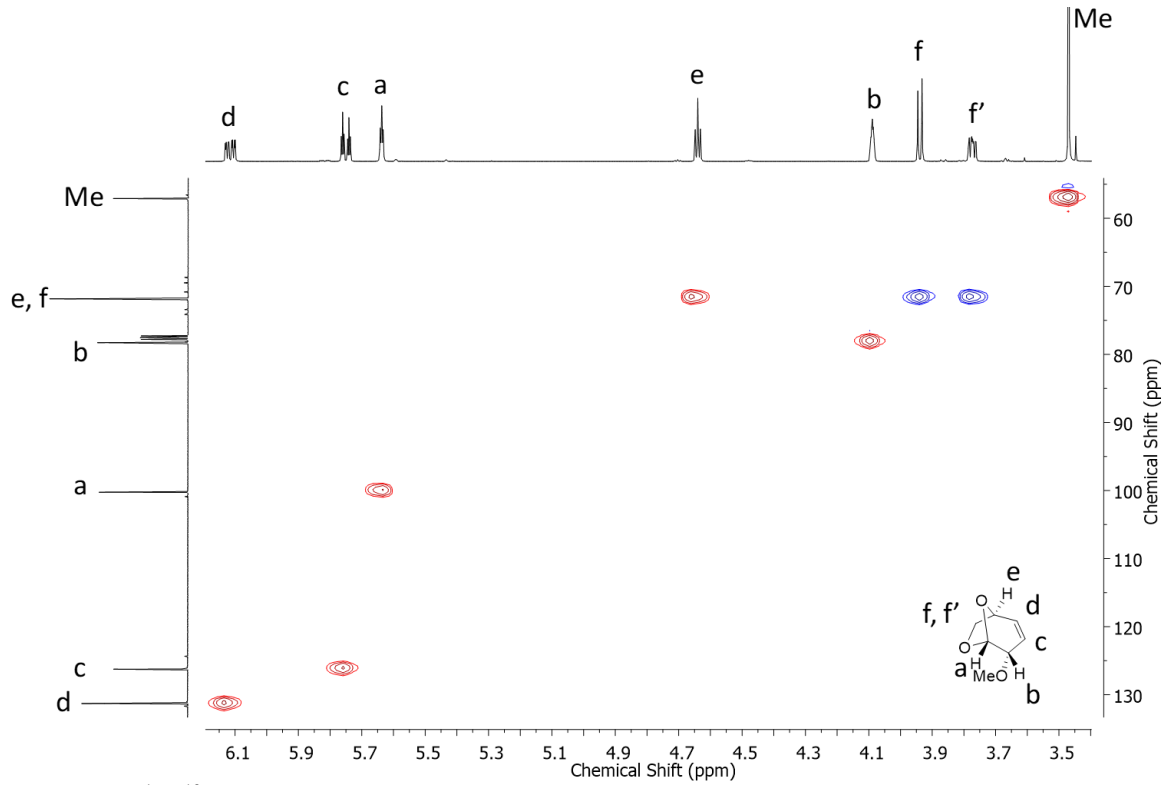

Figure S 8. ^{1}H-^{13}C HSQC NMR (500 MHz, 125 MHz, $CDCl_3$) spectrum of **3** (blue: negative contours, CH_2; red: positive contours, CH and CH_3).

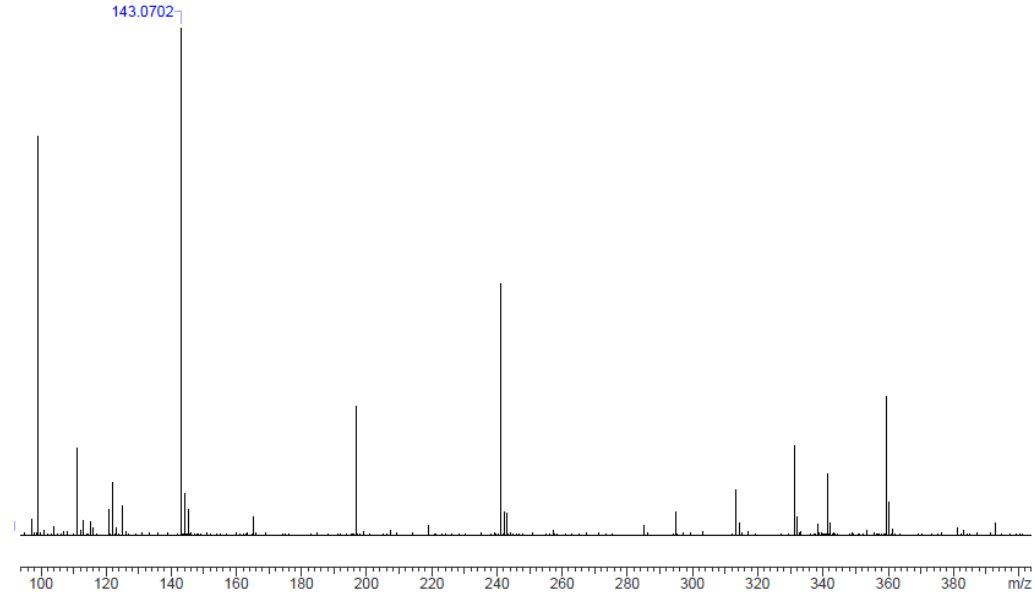

Figure S 9. ESI HRMS spectrum of **3**; *m/z* 143.070 (calculated: 143.070).

5.3.4 Polymerization

5.3.4.1 General procedure for ROMP (polylevoglucosenol).

To a dried 4 mL septum-sealed reaction vial, 128 mg (1 mmol) of levoglucosenol (**2**) and 0.15 mL of dry 1,4-dioxane were added. Upon dissolution of the levoglucosenol, a solution containing 7.92 mg of the Grubbs catalyst (**C6**) (dichloro[1,3-bis(2-methylphenyl)-2-imidazolidinylidene](2-isopropoxyphenylmethylene)ruthenium(II)) in 0.1 mL of dry 1,4-dioxane was added to the reaction vial at the desired temperature and stirred. For higher monomer to catalyst ratios, a stock solution of the catalyst in dry 1,4-dioxane was used. Upon completion of reaction time, a solution of ethyl vinyl ether in 1,4-dioxane was added to the reaction mixture and stirred for at least 30 min at 30 °C in the same septum sealed reaction vial. Polymers with high molar mass required prolonged time at 60 °C to dissolve completely. The polymers were precipitated into DCM, centrifuged and the solvent was separated followed by drying in vacuum at 60 °C. It is interesting to note that the unreacted monomer can be recovered almost quantitatively in pure form by sublimation of the reaction mixture.

5.3.4.1.1 Procedure for the preparation of polymer film

A solution of polymer **4** in 1,4-dioxane was dropped slowly (drop-casting method) in centrifuge tube (PTFE) partially filled with methanol, centrifuged and the solvent was removed following drying in a vacuum oven at 40 °C overnight. The film was produced at the inner side of the centrifuge tube and was removed carefully.

5.3.4.2 General procedure for CROP

In a typical experiment, 2 mmol of **3** was dissolved in a certain amount of dry DCM (depending on targeted concentration) and kept in a temperature bath (depending on the desired temperature). A required amount of stock solution of the acid initiator/catalyst (TfOH or $BF_3 \cdot OEt_2$) in dry DCM was added and the mixture was stirred for a pre-determined time. The reaction was quenched with

an excess of triethylamine followed by precipitation of the polymer **4** into methanol. The polymer was centrifuged and dried in a vacuum oven at 40 °C.

5.3.4.3 Thiol-ene addition

1) Initiation by UV: 50 mg of the polymer **4** and 64 mg of benzophenone were placed in a 9 ml septum sealed the transparent vial. Then, 420 mg of methyl 3-mercaptopropionate and 1 mL of dry THF were added. After three freeze-pump-thaw cycles, the mixture was irradiated with a 150 W Hg-medium pressure UV lamp for 18 h. The polymer **5** was then precipitated into methanol, centrifuged, and dried in a vacuum oven at 40 °C overnight.

2) Initiation by AIBN: 50 mg of the polymer **4** and 164 mg of AIBN were placed in a 9 ml septum sealed the transparent vial. Then, 420 mg of methyl 3-mercaptopropionate. After three freeze-pump-thaw cycles, the mixture was heated at 80 °C for 18 h. The polymer **5** was then precipitated into methanol, centrifuged, and dried in a vacuum oven at 40 °C overnight.

5.3.5 Hydrogenation

5.3.5.1 Hydrogenation of polylevoglucosenol 4

50 mg of polymer **4** was dissolved in 5 mL of THF and 1 mL of hexane, and 5 mg of Pd-C (10 wt%) was added. The mixture was subjected to H_2 gas at atmospheric pressure for 7 days. The polymer **6** was precipitated into methanol, centrifuged, and dried in a vacuum oven at 40 °C.

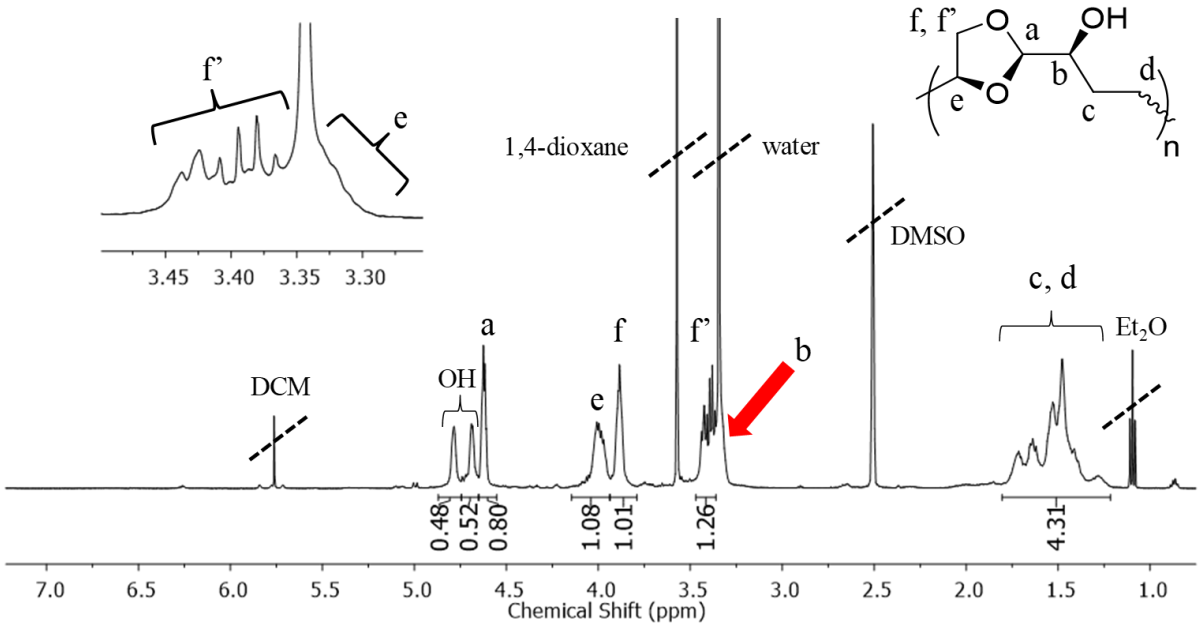

Figure S 10. ^{1}H NMR (500 MHz, DMSO) spectrum of polyacetal **8**. δ = 4.80-4.65 (bs, ~0.5H), 4.64-4.59 (bs, ~0.5H), 4.09-3.93 (m, 1H), 3.92-3.84 (m, 1H), 3.44-3.35 (m, 1H), 3.33-3.28 (m, 1H), 1.78-1.33 (m, 4 H).

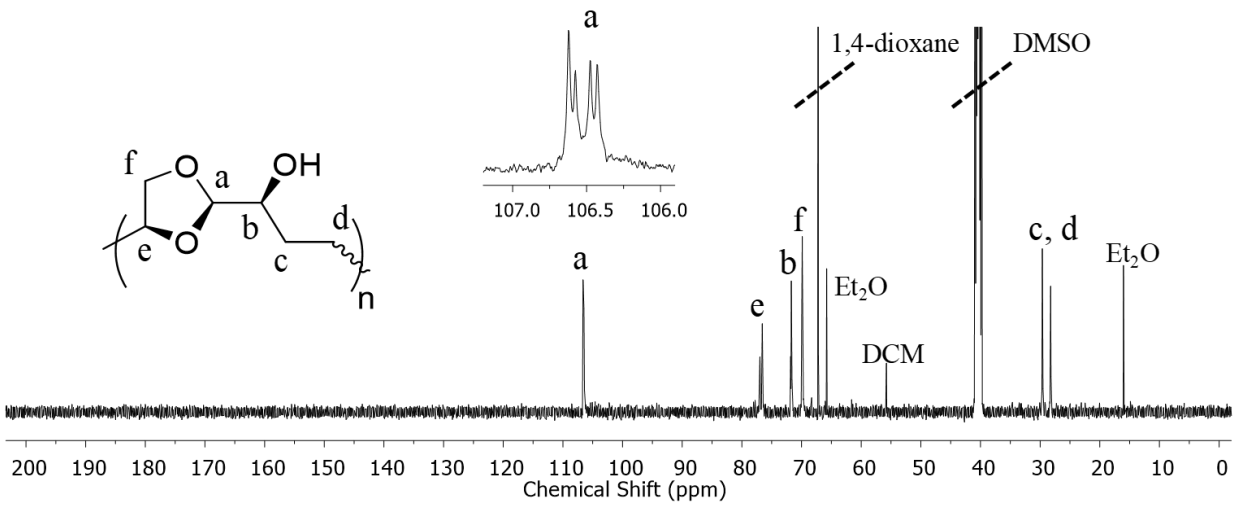

Figure S 11. ^{13}C NMR (125 MHz, DMSO-d_6) spectrum of polyacetal **8**. δ = 106.5, 76.8, 71.8, 69.9, 29.6, 28.2.

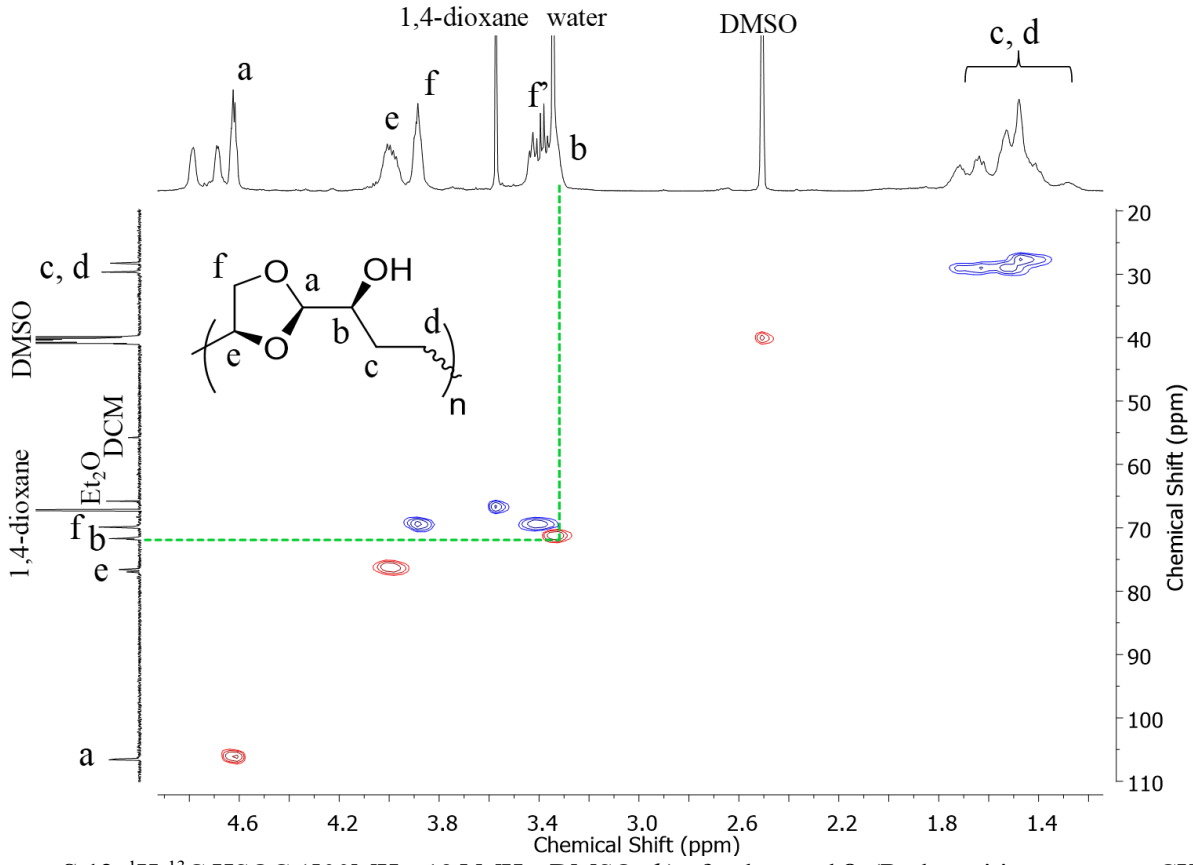

Figure S 12. ^{1}H-^{13}C HSQC (500MHz, 125 MHz, DMSO-d_6) of polyacetal **8**. (Red: positive contours: CH3, CH, blue: negative contours: CH2)

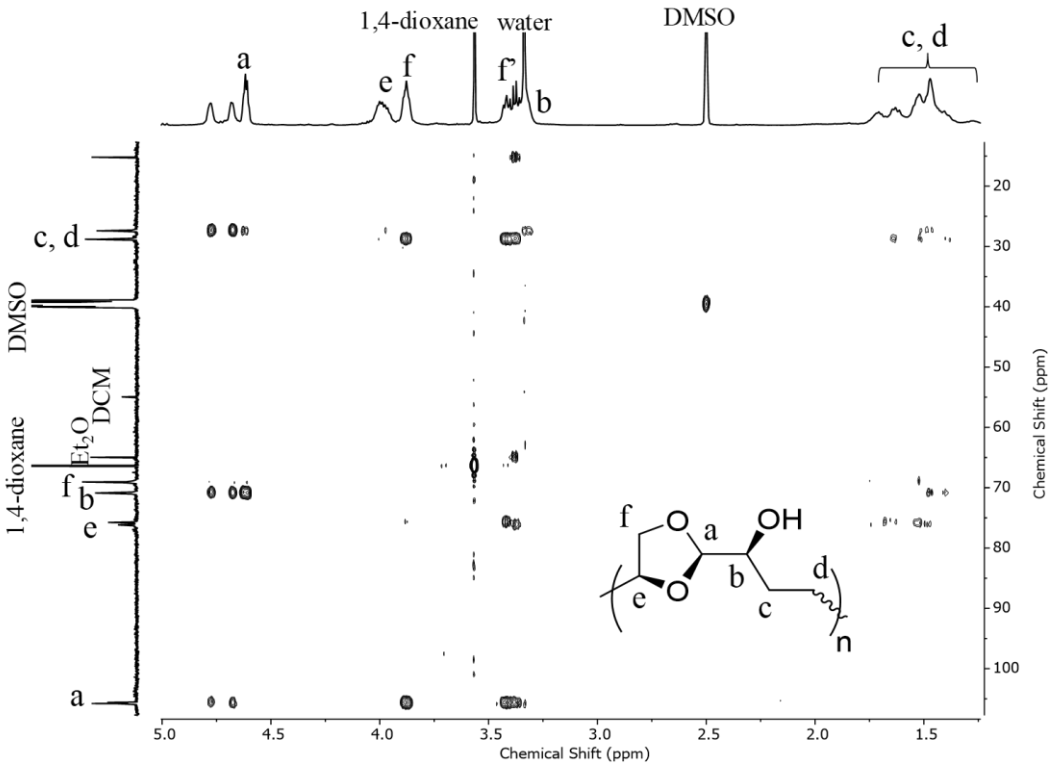

Figure S 13. ^{1}H-^{13}C HMBC (500MHz, 125 MHz, DMSO-d_6) of polyacetal **8**.

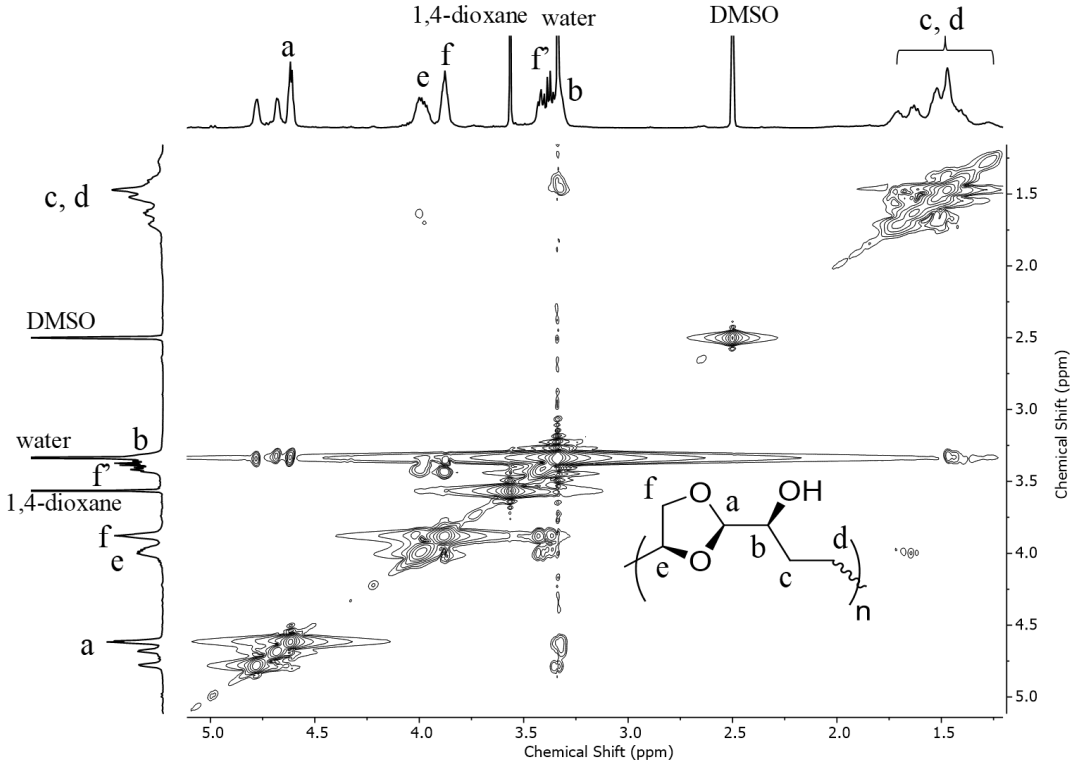

Figure S 14. ^{1}H-^{1}H COSY (500MHz, DMSO-d_6) of polyacetal **8**.

5.3.5.2 Hydrogenation of polymer 6

50 mg of polymer **5** was dissolved in 5 mL of THF and 1 mL of hexane, and 5 mg of Pd-C (10 wt%) was added. The mixture was subjected to H_2 gas at atmospheric pressure for 7 days. The polymer **6** was precipitated into methanol, centrifuged, and dried in a vacuum oven at 40 °C.

6. References

[1] Zhang, J.; Li, F.; Yang, D. DNA: From Carrier of Genetic Information to Polymeric Materials. *Trans. Tianjin Univ.* **2019**, *25* (4), 301–311. https://doi.org/10.1007/s12209-019-00188-w.

[2] Asif, M. Sustainability of Timber, Wood and Bamboo in Construction. In *Sustainability of Construction Materials*; Khatib, J. M., Ed.; Woodhead Publishing Series in Civil and Structural Engineering; Elsevier, 2009; pp 31–54. https://doi.org/10.1533/9781845695842.31.

[3] Thompson, R. C.; Swan, S. H.; Moore, C. J.; vom Saal, F. S. Our Plastic Age. *Philos. Trans. R. Soc. B Biol. Sci.* **2009**, *364* (1526), 1973–1976. https://doi.org/10.1098/rstb.2009.0054.

[4] Ramakrishna, S. , Mayer, J., W. Biomedical Applications of Polymer-Composite Materilas: A Review. **2003**, *61*, 861–865. https://doi.org/10.1109/isemc.2002.1032709.

[5] Sockalingam, S.; Chowdhury, S. C.; Gillespie, J. W.; Keefe, M. Recent Advances in Modeling and Experiments of Kevlar Ballistic Fibrils, Fibers, Yarns and Flexible Woven Textile Fabrics – a Review. *Text. Res. J.* **2016**, *87* (8), 984–1010. https://doi.org/10.1177/0040517516646039.

[6] Robeson, L. M. Applications of Polymer Blends: Emphasis on Recent Advances. *Polym. Eng. Sci.* **1984**, *24* (8), 587–597. https://doi.org/10.1002/pen.760240810.

[7] Perera, F. Pollution from Fossil-Fuel Combustion Is the Leading Environmental Threat to Global Pediatric Health and Equity: Solutions Exist. *Int. J. Env. Res. Pub. He.* 2018. https://doi.org/10.3390/ijerph15010016.

[8] Galloway, J. N. Acid Deposition: Perspectives in Time and Space. *Water. Air. Soil Pollut.* **1995**, *85* (1), 15–24. https://doi.org/10.1007/BF00483685.

[9] Lvovsky, Kseniya; Hughes, Gordon; Maddison, David; Ostro, Bart; Pearce, D. Environmental Costs of Fossil Fuels : A Rapid Assessment Method with Application to Six Cities. *World Bank, Washington, DC. © World Bank* **2000**. https://doi.org/https://openknowledge.worldbank.org/handle/10986/28300.

[10] Kubo, K.; Ogawa, J.; Kobuke, A.; Takami, K.; Tango, Y.; Egusa, G.; Kawase, T.; Yamamoto, S.; Hara, H.; Nishimoto, Y. Characterization of the Lag Phase of Insulin Action on Glucose Transport in Rat Isolated Adipocytes. *Hiroshima J. Med. Sci.* **1984**, *33* (1), 65–71.

[11] Wright, R. F.; Schindler, D. W. Interaction of Acid Rain and Global Changes: Effects on

Terrestrial and Aquatic Ecosystems. *Water. Air. Soil Pollut.* **1995**, *85* (1), 89–99. https://doi.org/10.1007/BF00483691.

[12] Kim, K.-H.; Kabir, E.; Kabir, S. A Review on the Human Health Impact of Airborne Particulate Matter. *Environ. Int.* **2015**, *74*, 136–143. https://doi.org/10.1016/j.envint.2014.10.005.

[13] Taub, D. R.; Miller, B.; Allen, H. Effects of Elevated CO2 on the Protein Concentration of Food Crops: A Meta-Analysis. *Glob. Chang. Biol.* **2008**, *14* (3), 565–575. https://doi.org/10.1111/j.1365-2486.2007.01511.x.

[14] Brussaard, C. P. D.; Peperzak, L.; Beggah, S.; Wick, L. Y.; Wuerz, B.; Weber, J.; Samuel Arey, J.; van der Burg, B.; Jonas, A.; Huisman, J.; et al. Immediate Ecotoxicological Effects of Short-Lived Oil Spills on Marine Biota. *Nat. Commun.* **2016**, *7*, 11206.

[15] World, O.; Day, E.; Communications, N. The Future of Plastic. *Nat. Commun.* **2018**, *9* (1), 2157. https://doi.org/10.1038/s41467-018-04565-2.

[16] Ostle, C.; Thompson, R. C.; Broughton, D.; Gregory, L.; Wootton, M.; Johns, D. G. The Rise in Ocean Plastics Evidenced from a 60-Year Time Series. *Nat. Commun.* **2019**, *10* (1), 1622. https://doi.org/10.1038/s41467-019-09506-1.

[17] Lebreton, L. C. M.; van der Zwet, J.; Damsteeg, J.-W.; Slat, B.; Andrady, A.; Reisser, J. River Plastic Emissions to the World's Oceans. *Nat. Commun.* **2017**, *8* (1), 15611. https://doi.org/10.1038/ncomms15611.

[18] Rochman, C. M.; Hoh, E.; Kurobe, T.; Teh, S. J. Ingested Plastic Transfers Hazardous Chemicals to Fish and Induces Hepatic Stress. *Sci. Rep.* **2013**, *3*, 3263.

[19] Sangroniz, A.; Zhu, J.-B.; Tang, X.; Etxeberria, A.; Chen, E. Y.-X.; Sardon, H. Packaging Materials with Desired Mechanical and Barrier Properties and Full Chemical Recyclability. *Nat. Commun.* **2019**, *10* (1), 3559. https://doi.org/10.1038/s41467-019-11525-x.

[20] Zhu, Y.; Romain, C.; Williams, C. K. Sustainable Polymers from Renewable Resources. *Nature* **2016**, *540*, 354.

[21] Galbis, J. A.; García-Martín, M. de G.; de Paz, M. V.; Galbis, E. Synthetic Polymers from Sugar-Based Monomers. *Chem. Rev.* **2016**, *116* (3), 1600–1636. https://doi.org/10.1021/acs.chemrev.5b00242.

[22] Wang, Q.; Dordick, J. S.; Linhardt, R. J. Synthesis and Application of Carbohydrate-Containing Polymers. *Chem. Mater.* **2002**, *14* (8), 3232–3244.

https://doi.org/10.1021/cm0200137.

[23] Poirier, Y.; Nawrath, C.; Somerville, C. Production of Polyhydroxyalkanoates, a Family of Biodegradable Plastics and Elastomers, in Bacteria and Plants. *Bio/Technology* **1995**, *13* (2), 142–150. https://doi.org/10.1038/nbt0295-142.

[24] Li, Z.; Yang, J.; Loh, X. J. Polyhydroxyalkanoates: Opening Doors for a Sustainable Future. *Npg Asia Mater.* **2016**, *8*, e265.

[25] Zheng, J.; Suh, S. Strategies to Reduce the Global Carbon Footprint of Plastics. *Nat. Clim. Chang.* **2019**, *9* (5), 374–378. https://doi.org/10.1038/s41558-019-0459-z.

[26] Tomei, J.; Helliwell, R. Food versus Fuel? Going beyond Biofuels. *Land use policy* **2016**, *56*, 320–326. https://doi.org/https://doi.org/10.1016/j.landusepol.2015.11.015.

[27] Brigham, C. Chapter 3.22 - Biopolymers: Biodegradable Alternatives to Traditional Plastics; Török, B., Dransfield, T. B. T.-G. C., Eds.; Elsevier, 2018; pp 753–770. https://doi.org/https://doi.org/10.1016/B978-0-12-809270-5.00027-3.

[28] Esposito, D.; Antonietti, M. Redefining Biorefinery: The Search for Unconventional Building Blocks for Materials. *Chem. Soc. Rev.* **2015**, *44* (16), 5821–5835. https://doi.org/10.1039/C4CS00368C.

[29] Mohan, D.; Pittman, C. U.; Steele, P. H. Pyrolysis of Wood/Biomass for Bio-Oil: A Critical Review. *Energy & Fuels* **2006**, *20* (3), 848–889. https://doi.org/10.1021/ef0502397.

[30] Bennett, N. M.; Helle, S. S.; Duff, S. J. B. Extraction and Hydrolysis of Levoglucosan from Pyrolysis Oil. *Bioresour. Technol.* **2009**, *100* (23), 6059–6063. https://doi.org/https://doi.org/10.1016/j.biortech.2009.06.067.

[31] Houminer, Y.; Patai, S. Thermal Polymerization of Levoglucosan. *J. Polym. Sci. Part A-1 Polym. Chem.* **1969**, *7* (10), 3005–3014. https://doi.org/10.1002/pol.1969.150071020.

[32] Sherwood, J.; De bruyn, M.; Constantinou, A.; Moity, L.; McElroy, C. R.; Farmer, T. J.; Duncan, T.; Raverty, W.; Hunt, A. J.; Clark, J. H. Dihydrolevoglucosenone (Cyrene) as a Bio-Based Alternative for Dipolar Aprotic Solvents. *Chem. Commun.* **2014**, *50* (68), 9650–9652. https://doi.org/10.1039/C4CC04133J.

[33] New Solvent Seeks to Replace NMP. *C&EN Glob. Enterp.* **2019**, *97* (22), 14. https://doi.org/10.1021/cen-09722-buscon1.

[34] Miftakhov, M. S.; Valeev, F. A.; Gaisina, I. N. Levoglucosenone: The Properties, Reactions, and Use in Fine Organic Synthesis. *Russ. Chem. Rev.* **1994**, *63* (10), 869–882.

https://doi.org/10.1070/rc1994v063n10abeh000123.

[35] Nishikawa, T.; Araki, H.; Isobe, M. Novel Stereoselective Reaction of Levoglucosenone with Furfural. *Biosci. Biotechnol. Biochem.* **1998**, *62* (1), 190–192. https://doi.org/10.1271/bbb.62.190.

[36] Sarotti, A. M.; Spanevello, M. M. Z. and R. A. Recent Applications of Levoglucosenone as Chiral Synthon. *Current Organic Synthesis*. 2012, pp 439–459. https://doi.org/http://dx.doi.org/10.2174/157017912802651401.

[37] Cao, F.; Schwartz, T. J.; McClelland, D. J.; Krishna, S. H.; Dumesic, J. A.; Huber, G. W. Dehydration of Cellulose to Levoglucosenone Using Polar Aprotic Solvents. *Energy Environ. Sci.* **2015**, *8* (6), 1808–1815. https://doi.org/10.1039/C5EE00353A.

[38] Astruc, D. The Metathesis Reactions: From a Historical Perspective to Recent Developments. *New J. Chem.* **2005**, *29* (1), 42–56. https://doi.org/10.1039/B412198H.

[39] Hérisson, P. J.; Chauvin, Y. Catalyse de Transformation Des Oléfines Par Les Complexes Du Tungstène. II. Télomérisation Des Oléfines Cycliques En Présence d'oléfines Acycliques. *Die Makromol. Chemie* **1970**, *141* (3487), 161–176. https://doi.org/10.1002/macp.1971.021410112.

[40] Calderon, N.; Chen, H. Y.; Scott, K. W. Olefin Metathesis - A Novel Reaction for Skeletal Transformations of Unsaturated Hydrocarbons. *Tetrahedron Lett.* **1967**, *8* (34), 3327–3329. https://doi.org/https://doi.org/10.1016/S0040-4039(01)89881-6.

[41] Toreki, R.; Schrock, R. R. A Well-Defined Rhenium(VII) Olefin Metathesis Catalyst. *J. Am. Chem. Soc.* **1990**, *112* (6), 2448–2449. https://doi.org/10.1021/ja00162a071.

[42] Nguyen, S. B. T.; Johnson, L. K.; Grubbs, R. H.; Ziller, J. W. Ring-Opening Metathesis Polymerization (ROMP) of Norbornene by a Group VIII Carbene Complex in Protic Media. *J. Am. Chem. Soc.* **1992**, *114* (10), 3974–3975. https://doi.org/10.1021/ja00036a053.

[43] Samojłowicz, C.; Bieniek, M.; Grela, K. Ruthenium-Based Olefin Metathesis Catalysts Bearing N-Heterocyclic Carbene Ligands. *Chem. Rev.* **2009**, *109* (8), 3708–3742. https://doi.org/10.1021/cr800524f.

[44] Sutthasupa, S.; Shiotsuki, M.; Sanda, F. Recent Advances in Ring-Opening Metathesis Polymerization, and Application to Synthesis of Functional Materials. *Polym. J.* **2010**, *42* (12), 905–915. https://doi.org/10.1038/pj.2010.94.

[45] Hoogenboom, R. Poly(2-Oxazoline)s: A Polymer Class with Numerous Potential

Applications. *Angew. Chem. Int. Ed.* **2009**, *48* (43), 7978–7994. https://doi.org/10.1002/anie.200901607.

[46] Hufendiek, A.; Lingier, S.; Du Prez, F. E. Thermoplastic Polyacetals: Chemistry from the Past for a Sustainable Future? *Polym. Chem.* **2019**, *10* (1), 9–33. https://doi.org/10.1039/C8PY01219A.

[47] Nuyken, O.; Pask, S. D. Ring-Opening Polymerization-An Introductory Review. *Polymers (Basel).* **2013**, *5* (2), 361–403. https://doi.org/10.3390/polym5020361.

[48] Shibasaki, Y.; Sanada, H.; Yokoi, M.; Sanda, F.; Endo, T. Activated Monomer Cationic Polymerization of Lactones and the Application to Well-Defined Block Copolymer Synthesis with Seven-Membered Cyclic Carbonate. *Macromolecules* **2000**, *33* (12), 4316–4320. https://doi.org/10.1021/ma992138b.

[49] Hoogenboom, R.; Wiesbrock, F.; Huang, H.; Leenen, M. A. M.; Thijs, H. M. L.; van Nispen, S. F. G. M.; van der Loop, M.; Fustin, C.-A.; Jonas, A. M.; Gohy, J.-F.; et al. Microwave-Assisted Cationic Ring-Opening Polymerization of 2-Oxazolines: A Powerful Method for the Synthesis of Amphiphilic Triblock Copolymers. *Macromolecules* **2006**, *39* (14), 4719–4725. https://doi.org/10.1021/ma060952a.

[50] Leiske, M. N.; Hartlieb, M.; Sobotta, F. H.; Paulus, R. M.; Görls, H.; Bellstedt, P.; Schubert, U. S. Cationic Ring-Opening Polymerization of Protected Oxazolidine Imines Resulting in Gradient Copolymers of Poly(2-Oxazoline) and Poly(Urea). *Polym. Chem.* **2016**, *7* (30), 4924–4936. https://doi.org/10.1039/C6PY00785F.

[51] Nuyken, O.; Pask, S. D. Ring-Opening Polymerization—An Introductory Review. *Polymers (Basel).* **2013**, *5* (2), 361–403. https://doi.org/10.3390/polym5020361.

[52] Penczek, S. Cationic Ring-Opening Polymerization (CROP) Major Mechanistic Phenomena. *J. Polym. Sci. Part A Polym. Chem.* **2000**, *38* (11), 1919–1933. https://doi.org/10.1002/(SICI)1099-0518(20000601)38:11<1919::AID-POLA10>3.0.CO;2-W.

[53] Xiao, R.; Grinstaff, M. W. Chemical Synthesis of Polysaccharides and Polysaccharide Mimetics. *Prog. Polym. Sci.* **2017**, *74*, 78–116. https://doi.org/https://doi.org/10.1016/j.progpolymsci.2017.07.009.

[54] Satoh, T.; Imai, T.; Ishihara, H.; Maeda, T.; Kitajyo, Y.; Sakai, Y.; Kaga, H.; Kaneko, N.; Ishii, F.; Kakuchi, T. Synthesis, Branched Structure, and Solution Property of

Hyperbranched d-Glucan and d-Galactan. *Macromolecules* **2005**, *38* (10), 4202–4210. https://doi.org/10.1021/ma0475479.

[55] Uryu, T.; Yamaguchi, C.; Morikawa, K.; Terui, K.; Kanai, T.; Matsuzaki, K. Ring-Opening Polymerization of 1,4-Anhydro-2,3,6-Tri-0-Benzyl-.Alpha.-D-Glucopyranose and 1,4-Anhydro-2,3,6-Tri-0-Benzyl-.Beta.-D-Galactopyranose. *Macromolecules* **1985**, *18* (4), 599–605. https://doi.org/10.1021/ma00146a003.

[56] Hatanaka, K.; Kanazawa, S.; Uryu, T.; Matsuzaki, K. Ring-Opening Polymerization of Anhydro-Deoxy-Sugar Derivative and Chemical Synthesis of Stereoregular 2-Deoxy-(1 → 6)-α-D-Arabino-Hexopyranan. *J. Polym. Sci. Polym. Chem. Ed.* **1984**, *22* (9), 1987–1996. https://doi.org/10.1002/pol.1984.170220904.

[57] Hattori, K.; Yoshida, T.; Uryu, T. Ring-Opening Polymerization and Copolymerization of a New Benzylated 1,6-Anhydro-3-Azido-3-Deoxy-β-D-Allopyranose and Synthesis of Amino-Polysaccharides with 1,6-α-Allopyranosidic Structure. *Macromol. Chem. Phys.* **1997**, *198* (1), 29–39. https://doi.org/10.1002/macp.1997.021980103.

[58] Zachoval, J.; Schuerch, C. The Catalyzed Polymerization of 1,2-Anhydro-3,4,6-Tri-O-Acetyl-α-D-Glucopyranose. *J. Polym. Sci. Part C Polym. Symp.* **1969**, *28* (1), 187–195. https://doi.org/10.1002/polc.5070280116.

[59] Uryu, T.; Kitano, K.; Tachikawa, H.; Ito, K.; Matsuzaki, K. Polymerization of Anhydro Sugar Derivatives. Cationic Polymerization of 5,6-Anhydro-1,2-O-Isopropylidene-α-D-Glucofuranose and Structure of the Polymer. *Die Makromol. Chemie* **1978**, *179* (7), 1773–1782. https://doi.org/10.1002/macp.1978.021790712.

[60] Ohnishi, A.; Kato, K.; Takagi, E. Curie-Point Pyrolysis of Cellulose. *Polym. J.* **1975**, *7* (4), 431–437. https://doi.org/10.1295/polymj.7.431.

[61] Yoshida, D.; Yoshida, T. Elucidation of High Ring-Opening Polymerizability of Methylated 1,6-Anhydro Glucose. *J. Polym. Sci. Part A Polym. Chem.* **2009**, *47* (4), 1013–1022. https://doi.org/10.1002/pola.23178.

[62] Sui, X.; Wang, Z.; Liao, B.; Zhang, Y.; Guo, Q. Preparation of Levoglucosenone through Sulfuric Acid Promoted Pyrolysis of Bagasse at Low Temperature. *Bioresour. Technol.* **2012**, *103* (1), 466–469. https://doi.org/https://doi.org/10.1016/j.biortech.2011.10.010.

[63] Shibagaki, M.; Takahashi, K.; Kuno, H.; Honda, I.; Matsushita, H. Synthesis of Levoglucosenone. *Chem. Lett.* **1990**, *19* (2), 307–310. https://doi.org/10.1246/cl.1990.307.

[64] Kadota, K.; Kurusu, T.; Taniguchi, T.; Ogasawara, K. Lipase-Mediated Synthesis of Both Enantiomers of Levoglucosenone from Acrolein Dimer. *Adv. Synth. Catal.* **2001**, *343* (6-7), 618–623. https://doi.org/10.1002/1615-4169(200108)343:6/7<618::AID-ADSC618>3.0.CO;2-E.

[65] Jung, M. E.; Kiankarimi, M. Synthesis of Methylene-Expanded 2‘,3‘-Dideoxyribonucleosides. *J. Org. Chem.* **1998**, *63* (23), 8133–8144. https://doi.org/10.1021/jo980436l.

[66] Sarotti, A. M.; Spanevello, R. A.; Suárez, A. G. An Efficient Microwave-Assisted Green Transformation of Cellulose into Levoglucosenone. Advantages of the Use of an Experimental Design Approach. *Green Chem.* **2007**, *9* (10), 1137. https://doi.org/10.1039/b703690f.

[67] Giordano, E. D. V; Frinchaboy, A.; Suárez, A. G.; Spanevello, R. A. Synthesis of Tri-O-Acetyl-d-Allal from Levoglucosenone. *Org. Lett.* **2012**, *14* (17), 4602–4605. https://doi.org/10.1021/ol302061a.

[68] Ma, X.; Anderson, N.; White, L. V; Bae, S.; Raverty, W.; Willis, A. C.; Banwell, M. G. The Conversion of Levoglucosenone into Isolevoglucosenone. *Aust. J. Chem.* **2015**, *68* (4), 593–599.

[69] Ma, X.; Liu, X.; Yates, P.; Raverty, W.; Banwell, M. G.; Ma, C.; Willis, A. C.; Carr, P. D. Manipulating the Enone Moiety of Levoglucosenone: 1,3-Transposition Reactions Including Ones Leading to Isolevoglucosenone. *Tetrahedron* **2018**, *74* (38), 5000–5011. https://doi.org/10.1016/j.tet.2018.03.023.

[70] Behrendt, F. N.; Schlaad, H. Metathesis Polymerization of Cystine-Based Macrocycles. *Polym. Chem.* **2017**, *8* (2), 366–369. https://doi.org/10.1039/C6PY01864E.

[71] Peng, Y.; Decatur, J.; Meier, M. A. R.; Gross, R. A. Ring-Opening Metathesis Polymerization of a Naturally Derived Macrocyclic Glycolipid. *Macromolecules* **2013**, *46* (9), 3293–3300. https://doi.org/10.1021/ma400291c.

[72] Fomine, S.; Tlenkopatchev, M. A. Ring-Opening of Cyclohexene via Metathesis by Ruthenium Carbene Complexes. A Computational Study. *Organometallics* **2007**, *26* (18), 4491–4497. https://doi.org/10.1021/om700425d.

[73] Bhaumik, A.; Peterson, G. I.; Kang, C.; Choi, T.-L. Controlled Living Cascade Polymerization To Make Fully Degradable Sugar-Based Polymers from d-Glucose and d-

Galactose. *J. Am. Chem. Soc.* **2019**, *141* (31), 12207–12211. https://doi.org/10.1021/jacs.9b05822.

[74] Hamasaki, A.; Maruta, S.; Nakamura, A.; Tokunaga, M. Palladium-Catalyzed 1,4-Addition of Carboxylic Acids to Butadiene Monoxide. *Adv. Synth. Catal.* **2012**, *354* (11-12), 2129–2134. https://doi.org/10.1002/adsc.201200059.

[75] Ruckel, E. R.; Schuerch, C. Chemical Synthesis of a Stereoregular Linear Polysaccharide. *J. Am. Chem. Soc.* **1966**, *88* (11), 2605–2606. https://doi.org/10.1021/ja00963a052.

[76] Liang, Y.; Franz, A. H.; Newbury, C.; Lebrilla, C. B.; Patten, T. E. Synthesis and End Group Structure of 2-Deoxydextrans Prepared via the Cationic Ring-Opening Polymerization of an Anhydro Sugar. *Macromolecules* **2002**, *35* (9), 3402–3412. https://doi.org/10.1021/ma012033k.

[77] Collins, G. L.; Greene, R. K.; Berardinelli, F. M.; Garruto, W. V. Observations on the Initiation of Trioxane with Boron Trifluoride Dibutyl Etherate. *J. Polym. Sci. Polym. Lett. Ed.* **1979**, *17* (10), 667–671. https://doi.org/10.1002/pol.1979.130171008.

[78] Yağci, Y.; Ledwith, A. Mechanistic and Kinetic Studies on the Photoinitiated Polymerization of Tetrahydrofuran. *J. Polym. Sci. Part A Polym. Chem.* **1988**, *26* (7), 1911–1918. https://doi.org/10.1002/pola.1988.080260717.

[79] Jackson, H. L.; McCormack, W. B.; Rondestvedt, C. S.; Smeltz, K. C.; Viele, I. E. Control of Peroxidizable Compounds. *J. Chem. Educ.* **1970**, *47* (3), A175. https://doi.org/10.1021/ed047pA175.

7. Appendix

7.1 Attempt for the polymerization of levoglucosenone

1 mmol of Levoglucosenone (**1**) (126 mg), 32 mg AIBN was taken in septum sealed vial. It was then subjected to three freeze-thaw-pump cycles and heated to 80°C for 22 hours. The samples is then brought to room temperature and used for SEC (THF) measurements.

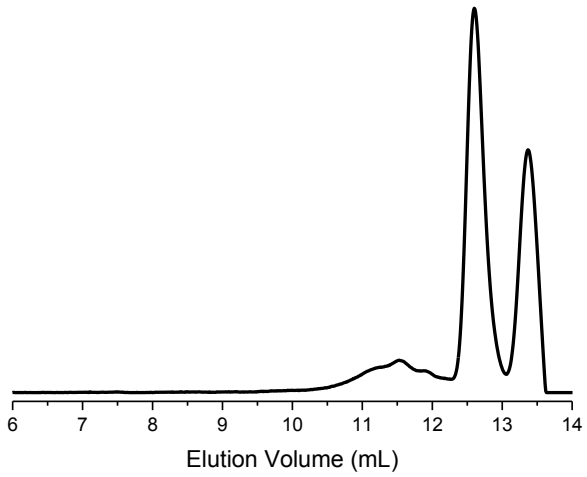

Figure S 15. Polymerization attempt of **1**, with AIBN. The peak between 10-12 is due to the oligomeric material with molar mass or 560 g/mol (polystyrene standars calibration.)

7.2 NMR spectra

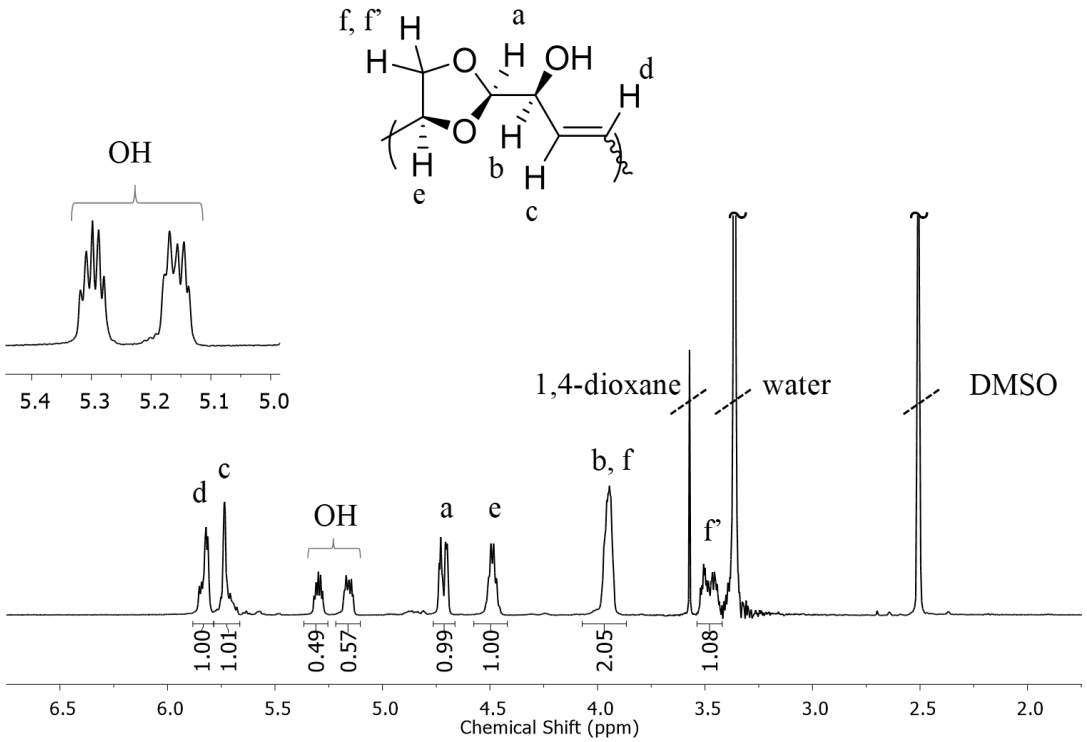

Figure S 16. ^{1}H NMR (500 MHz) spectrum of polyacetal **4** (run 2) in DMSO-d_6; δ = 5.90-5.79 (m, 1H), 5.79-5.65 (m, 1H), 5.37-5.10 (m, 1H), 4.78-4.64 (m, 1H), 4.58–4.42 (m, 1H), 4.05-3.87 (m, 2H), 3.54-3.42 (m, 1H).

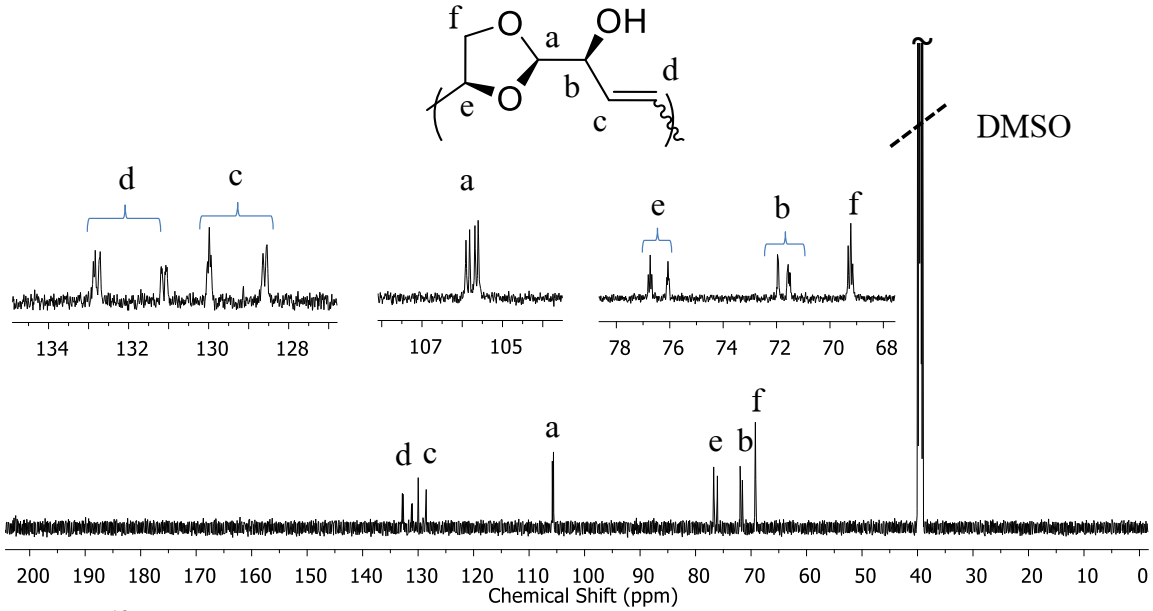

Figure S 17. ^{13}C NMR (150 MHz) spectrum of polyacetal **4** (run 2) in DMSO-d6; δ = 132.7, 131.1, 129.9, 128.5, 105.7, 76.4, 71.5, 69.2

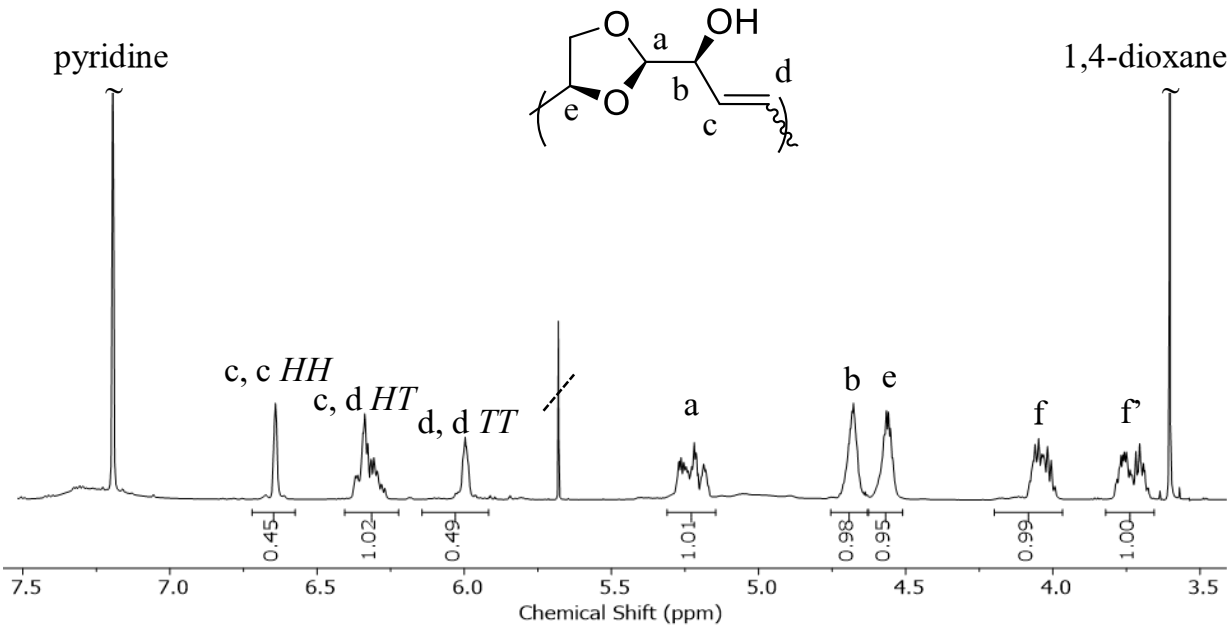

Figure S 18. ^{1}H NMR (600 MHz, pyridine-d_5) spectrum of polyacetal **4**. δ = 6.66-6.63 (m, 0.5H), 6.40-6.25 (m, 1H), 6.14-5.89 (m, 0.5H), 5.31-5.14 (m, 1H), 4.75-4.63 (m, 1H), 4.62-4.50 (m, 1H), 4.20-3.96 (m, 1H), 3.82-3.66 (m, 1H).

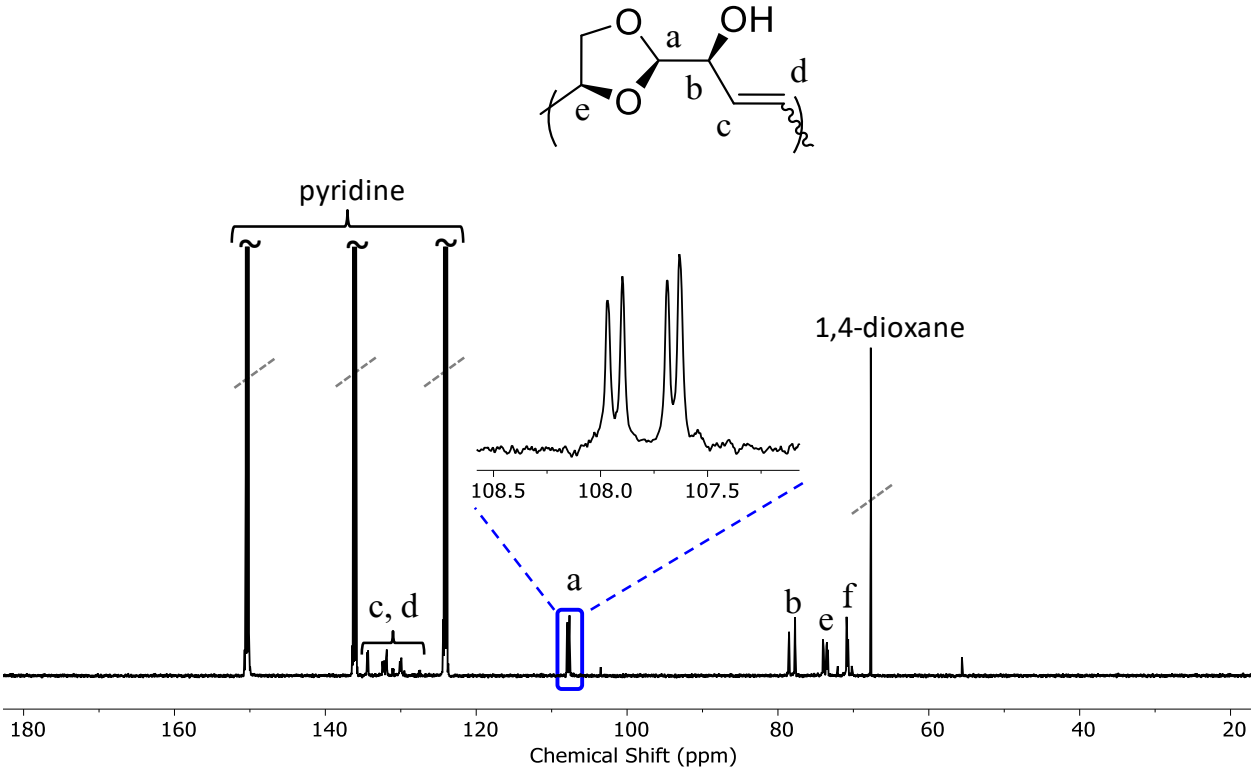

Figure S 19. ^{13}C NMR (150 MHz, pyridine-d_5) δ = 134.4, 134.4, 134.4, 134.3, 132.4, 132.3, 132.2, 132.1, 131.9, 131.8, 130.1, 130.1, 130.1, 130.0, 129.9, 129.9, 107.9, 107.9, 107.6, 107.6, 78.5, 78.5, 78.4, 77.7, 77.7, 77.7, 74.0, 73.9, 73.5, 73.5, 73.4, 73.3, 70.9, 70.8, 70.7, 70.7

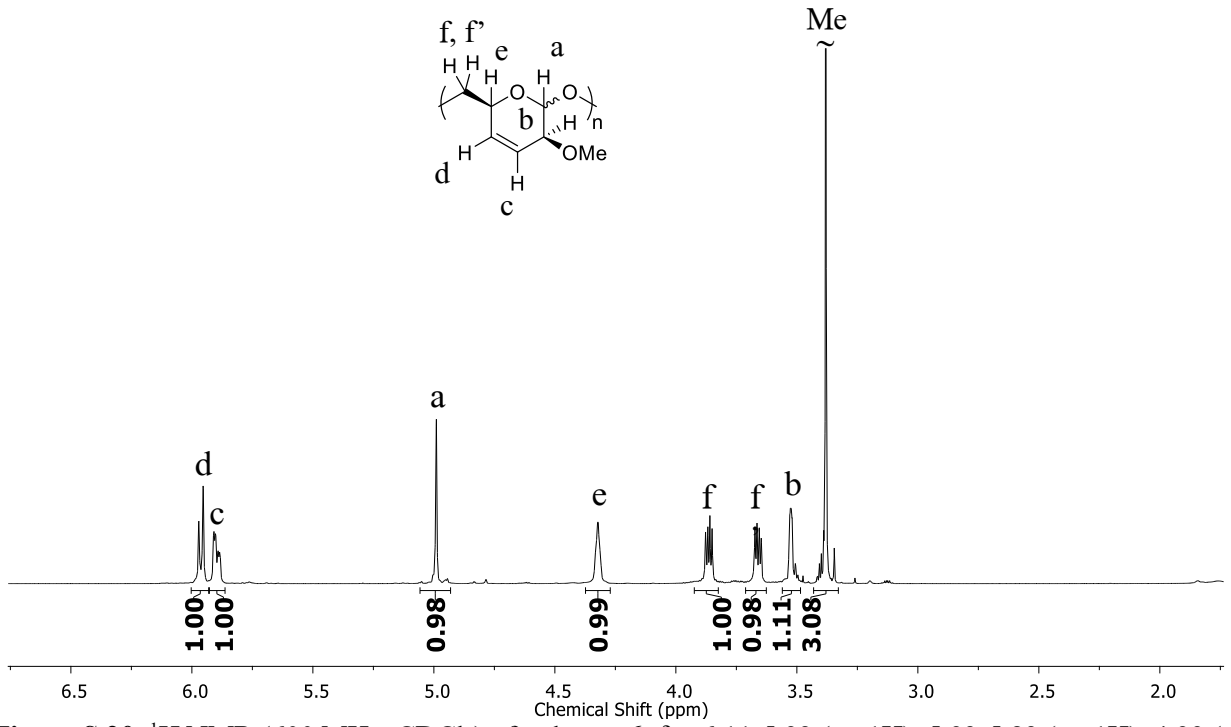

Figure S 20. ^{1}H NMR (600 MHz, $CDCl_3$) of polymer **6.** δ = 6.11-5.92 (m, 1H), 5.93-5.83 (m, 1H), 4.99 (s, 1H), 4.36-4.27 (m, 1H), 3.92-3.82 (s, 1H), 3.67 (dd, J = 10.7, 5.0 Hz, 1H), 3.61-3.50 (m, 1H), 3.38 (s, 3H).

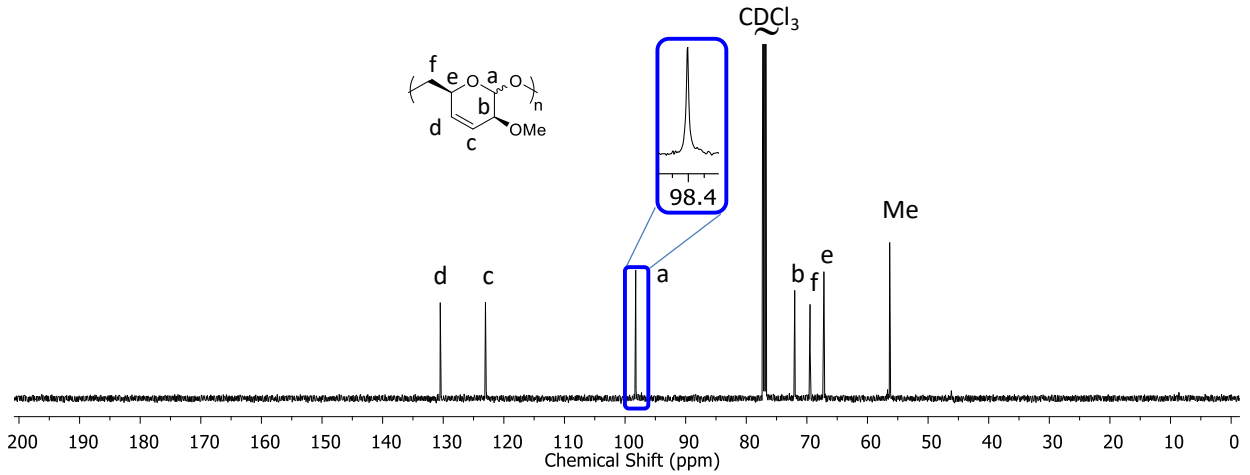

Figure S 21. ^{13}C NMR (150 MHz, CDCl3) spectrum of polymer **6** (run 11 in Table S2); δ = 130.5, 123.0, 98.3, 72.0, 69.5, 67.2, 56.3

7.3 Size exclusion chromatograms

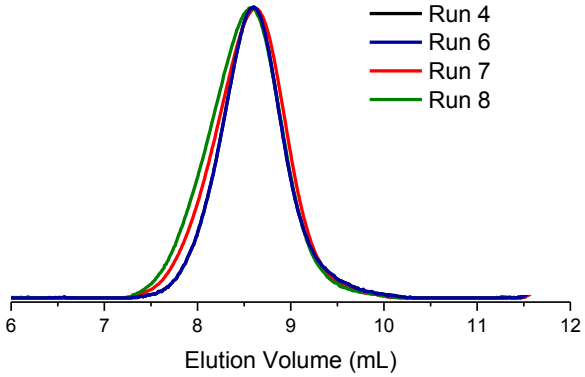

Figure S 22. SEC elugrams of polymer **6**, entries of **Table 5**.

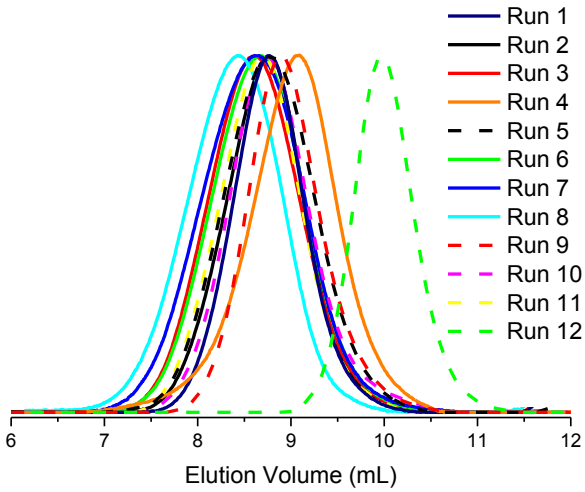

Figure S 23. SEC elugrams of polymer **6**, entries of **Table 6**.